EFFICIENT SOLUTION TECHNIQUES FOR AXISYMMETRIC PROBLEMS

By

MINAH OH

A DISSERTATION PRESENTED TO THE GRADUATE SCHOOL
OF THE UNIVERSITY OF FLORIDA IN PARTIAL FULFILLMENT
OF THE REQUIREMENTS FOR THE DEGREE OF
DOCTOR OF PHILOSOPHY

UNIVERSITY OF FLORIDA

2010

© 2010 Minah Oh

Dedicated to my parents, Kwang Seong Oh and Seong Hye Oh; my sister, Minjeong Oh; and my significant other, Joshua Ducey

ACKNOWLEDGMENTS

I first want to thank my Ph.D. dissertation advisor, Dr. Jay Gopalakrishnan for guiding me to become a true mathematician. You gave me invaluable support since day one of graduate school, and I always felt so lucky for having you as my advisor. I also want to thank Dr. Paul Robinson for teaching me differential geometry and for giving me sincere advice whenever I had any problems. I send my gratitude to Dr. Henry Zmuda for helping me find great applications for my dissertation, and to Dr. Patrick De Leenheer and Dr. William Hager for their constant advice in graduate school and in the job market. I am grateful to have all of the above mentioned professors in my committee, and I very much appreciate their contribution to this dissertation. Lastly but not the least, I want to thank Dr. Paul Humke for helping me come to graduate school and for giving me continuous encouragement since then.

TABLE OF CONTENTS

page

ACKNOWLEDGMENTS 4

LIST OF TABLES 7

LIST OF FIGURES 8

ABSTRACT 9

CHAPTER

1 INTRODUCTION 10

1.1 The Time Harmonic Maxwell Equations 10
1.2 The Maxwell Equations under Axial Symmetry 13

2 PRELIMINARIES ON FUNCTION SPACES 15

2.1 Distributions 15
2.2 Standard Sobolev Spaces 16
2.3 Weighted Sobolev Spaces 19

3 PRELIMINARIES ON ALGORITHMS 25

3.1 Finite Element Methods 25
3.2 Multigrid Solver 28

4 COMMUTING PROJECTORS IN WEIGHTED SPACES 32

4.1 A Global Projector in Weighted Spaces 32
4.2 Commuting Smoothed Projectors in Weighted Spaces 39
4.2.1 Definitions 40
4.2.2 Construction 46

5 ANALYSIS OF A DUAL MIXED PROBLEM IN WEIGHTED SPACES 57

5.1 Problem Statement and Analysis 57
5.2 Numerical Results 65

6 FINITE ELEMENT ANALYSIS FOR THE MERIDIAN PROBLEM 67

6.1 The Edge Finite Element Method 67
6.2 Proof of the Quasi-Optimality Result 69
6.3 Numerical Results 74

7 MULTIGRID ANALYSIS FOR THE MERIDIAN PROBLEM 76

7.1 Multigrid Analysis for the Related Positive Definite Problem 77
7.1.1 The Multigrid Algorithm 77

7.1.2 Multigrid Analysis 81
7.1.3 Numerical Results 90
7.2 Multigrid Analysis for the Indefinite Problem 91
7.2.1 The Multigrid Algorithm 92
7.2.2 Multigrid Analysis 99
7.2.3 Numerical Results 105

8 A BIOMEDICAL APPLICATION OF THE MERIDIAN PROBLEM 108

APPENDIX

A PROOF OF THE EXACT SEQUENCE PROPERTY 112

B PROOF OF PROPOSITION 4.2.1 114

REFERENCES 119

BIOGRAPHICAL SKETCH 122

LIST OF TABLES

Table page

5-1 Mixed problem convergence rates 66

6-1 FEM convergence rates 75

7-1 V-cycle convergence rates 91

7-2 Backslash-cycle convergence rates: $\kappa = 1$ 106

7-3 Backslash-cycle convergence rates: $\kappa = 10$ 106

LIST OF FIGURES

Figure page

4-1 Domain D_a corresponding to point a 41

7-1 Domains 91

7-2 Wavenumber vs coarsest meshsize 107

8-1 Coaxial-based double slot choked probe 109

8-2 Distribution of the electromagnetic power 110

Abstract of Dissertation Presented to the Graduate School
of the University of Florida in Partial Fulfillment of the
Requirements for the Degree of Doctor of Philosophy

EFFICIENT SOLUTION TECHNIQUES FOR AXISYMMETRIC PROBLEMS

By

Minah Oh

May 2010

Chair: Jay Gopalakrishnan
Major: Mathematics

Consider a three-dimensional ($3D$) problem defined on a domain symmetric by rotation around an axis with data independent of the angular component. By using cylindrical coordinates, we can then reduce this axisymmetric $3D$ problem into a two-dimensional ($2D$) one. The advantage of such dimension reduction is that the discretization of the $3D$ problem results in a linear system of the same size as the $2D$ one saving computational time significantly. Due to the Jacobian arising from change of variables, however, we must work in weighted Sobolev spaces, where the weight function is the radial component r, once this dimension reduction is done. In this dissertation, we analyze the time harmonic Maxwell equations under axial symmetry. In particular, we provide an edge finite element analysis and a multigrid analysis of the so-called “meridian” problem, a problem arising from the axisymmetric Maxwell equations. New commuting projectors in weighted spaces are introduced, and a dual mixed problem in weighted spaces, which is interesting in its own right, is analyzed. These will provide the main ingredients for the analysis of the meridian problem.

CHAPTER 1
INTRODUCTION

The problem to be analyzed in this dissertation is the time harmonic Maxwell equations under axial symmetry. It is well-known that the time harmonic Maxwell equations decouples into two $2D$ problems under axial symmetry: one called the azimuthal problem and the other called the meridian problem [2, 9, 21]. This chapter consists of two sections. The first section describes how the Maxwell equations get reduced to its time harmonic form. The second chapter presents the decoupling of the time harmonic Maxwell equations under axial symmetry.

1.1 The Time Harmonic Maxwell Equations

In this section, we describe in detail how the Maxwell equations get reduced to its time harmonic form by assuming propagation at a single frequency. We closely follow the argument in [31, Chapter 1]. The Maxwell equations can be stated as follows:

$$\begin{aligned} \frac{\partial \mathcal{B}}{\partial t} + \mathbf{curl}\,\mathcal{E} &= 0, \\ \operatorname{div}\mathcal{D} &= \rho, \\ \frac{\partial \mathcal{D}}{\partial t} - \mathbf{curl}\,\mathcal{H} &= -\mathcal{J}, \\ \operatorname{div}\mathcal{B} &= 0, \end{aligned} \tag{1–1}$$

where $\mathcal{D}$ is the electric displacement, $\mathcal{B}$ is the magnetic induction, $\mathcal{E}$ is the electric field, $\mathcal{H}$ is the magnetic field, ρ is the charge density function, and $\mathcal{J}$ is the current density function. Then either by Fourier transform in time or to analyze electromagnetic

propagation at a single frequency, we can write

$$\mathcal{E} = R(e^{-i\omega t}\hat{\mathbf{E}}(\mathbf{x})),$$
$$\mathcal{D} = R(e^{-i\omega t}\hat{\mathbf{D}}(\mathbf{x})),$$
$$\mathcal{H} = R(e^{-i\omega t}\hat{\mathbf{H}}(\mathbf{x})),$$
$$\mathcal{B} = R(e^{-i\omega t}\hat{\mathbf{B}}(\mathbf{x})),$$
$$\mathcal{J} = R(e^{-i\omega t}\hat{\mathbf{J}}(\mathbf{x})),$$
$$\rho = R(e^{-i\omega t}\hat{\rho}(\mathbf{x})),$$

where $R(e^{-i\omega t}\hat{\mathbf{E}}(\mathbf{x}))$ denotes the real part of $e^{-i\omega t}\hat{\mathbf{E}}(\mathbf{x})$, etc., and ω denotes the angular frequency, i.e., $\omega = 2\pi f$, where f is the frequency. By substituting these into (1–1), we reach the time harmonic Maxwell equations:

$$\begin{aligned} -i\omega\hat{\mathbf{B}} + \mathbf{curl}\,\hat{\mathbf{E}} &= 0, \\ \operatorname{div}\hat{\mathbf{D}} &= \hat{\rho}, \\ -i\omega\hat{\mathbf{D}} - \mathbf{curl}\,\hat{\mathbf{H}} &= -\hat{\mathbf{J}}, \\ \operatorname{div}\hat{\mathbf{B}} &= 0. \end{aligned} \tag{1–2}$$

In vacuum or free space, the fields are related by the equation

$$\hat{\mathbf{D}} = \epsilon_0\hat{\mathbf{E}} \text{ and } \hat{\mathbf{B}} = \mu_0\hat{\mathbf{H}},$$

where $\epsilon_0 \approx 8.854 \times 10^{-12} Fm^{-1}$ is called the electric permittivity, and $\mu_0 = 4\pi \times 10^{-7} Hm^{-1}$ is called the magnetic permeability. Furthermore, the speed of light in vacuum is given by $c = \sqrt{\epsilon_0\mu_0}^{-1} (\approx 2.998 \times 10^8 ms^{-1})$.

In the case when various different materials occupy the domain of the electromagnetic field, and if the material properties do not depend on the direction of the field and the material is linear (*inhomogeneous, isotropic materials)*, then we have the relation

$$\hat{\mathbf{D}} = \epsilon\hat{\mathbf{E}} \text{ and } \hat{\mathbf{B}} = \mu\hat{\mathbf{H}}, \tag{1–3}$$

where ϵ and μ are positive, bounded, scalar functions of position which depend on the material. Additionally, in a conducting material, the electromagnetic field itself gives rise to currents. By assuming that the Ohms law holds, we have that

$$\hat{\mathbf{J}} = \sigma\hat{\mathbf{E}} + \hat{\mathbf{J}}_a, \tag{1–4}$$

where $\sigma \geq 0$ is called the conductivity, and $\hat{\mathbf{J}}_a$ is the applied current density. Regions where $\sigma > 0$ are called conductors. $\sigma = 0, \epsilon = \epsilon_0$, and $\mu = \mu_0$ in vacuum.

Thus, in inhomogeneous, isotropic materials, by substituting (1–3) and (1–4) into (1–2) and simplifying, we obtain the final version of the first-order Maxwell system:

$$\begin{aligned} -i\kappa\mu_r\mathbf{H} + \mathbf{curl}\,\mathbf{E} &= 0 \\ i\kappa\epsilon_r\mathbf{E} + \mathbf{curl}\,\mathbf{H} &= \frac{1}{i\kappa}\mathbf{F}, \end{aligned} \tag{1–5}$$

where $\kappa = \omega\sqrt{\epsilon_0\mu_0}$ is the wavenumber, $\mathbf{E} = \sqrt{\epsilon_0}\hat{\mathbf{E}}$, $\mathbf{H} = \sqrt{\mu_0}\hat{\mathbf{H}}$, and $\mathbf{F} = i\kappa\sqrt{\mu_0}\hat{\mathbf{J}}_a$. ϵ_r and μ_r are called the relative permittivity and relative permeability respectively, and it is defined by

$$\epsilon_r = \frac{1}{\epsilon_0}(\epsilon + \frac{i\sigma}{\omega}) \text{ and } \mu_r = \frac{\mu}{\mu_0}$$

($\epsilon_r = 1 = \mu_r$ in vacuum).

Remark 1.1.1. The wavenumber κ is related to the wavelengh $\lambda = \frac{c}{f}$ in the following way:

$$\kappa = \omega\sqrt{\epsilon_0\mu_0} = 2\pi f c^{-1} = \frac{2\pi}{cf^{-1}} = \frac{2\pi}{\lambda}.$$

Finally, in (1–5), by writing $\mathbf{H}$ in terms of $\mathbf{E}$ using the first equation, and substituting into the second equation, we obtain the second-order Maxwell system:

$$\mathbf{curl}(\frac{1}{\mu_r}\,\mathbf{curl}\,\mathbf{E}) - \kappa^2\epsilon_r\mathbf{E} = \mathbf{F}. \tag{1–6}$$

1.2 The Maxwell Equations under Axial Symmetry

Throughout this dissertation, we assume that we are solving the time harmonic Maxwell equations on an axisymmetric $3D$-domain with axisymmetric data $\mathbf{F}$. Vector valued functions are called axisymmetric when each of their components with respect to the $\mathbf{e}_r, \mathbf{e}_\theta, \mathbf{e}_z$ basis are independent of the θ-variable. Then the corresponding solution $\mathbf{E}$ in this case will also be axisymmetric [6].

Let us write $\mathbf{E} = E_r\mathbf{e}_r + E_\theta\mathbf{e}_\theta + E_z\mathbf{e}_z$. Then in cylindrical coordinates, under axial symmetry ($\partial_\theta = 0$), the **curl** operators reads:

$$\mathbf{curl}\,\mathbf{E} = -\partial_z E_\theta \mathbf{e}_r + (\partial_z E_r - \partial_r E_z)\mathbf{e}_\theta + \frac{1}{r}\partial_r(rE_\theta)\mathbf{e}_z.$$

We will use the following notation in relation with the above formula for $\mathbf{curl}\,\mathbf{E}$:

$$\begin{aligned} \mathrm{curl}_{rz}(E_r, E_z) &= \partial_z E_r - \partial_r E_z, \\ \mathbf{curl}_{rz} E_\theta &= (-\partial_z E_\theta, \frac{1}{r}\partial_r(rE_\theta)). \end{aligned} \tag{1–7}$$

Notice that E_r and E_z only affects the θ-component of $\mathbf{curl}\,\mathbf{E}$ while E_θ only affects the r and z components of $\mathbf{curl}\,\mathbf{E}$. Therefore, (1–6) decouples into two $2D$ problems by writing $\mathbf{E} = (E_r, 0, E_z) + (0, E_\theta, 0)$. One is called the meridian problem and the other is called the azimuthal problem:

Meridian Problem:

$$\mathbf{curl}_{rz}(\frac{1}{\mu_r}\mathrm{curl}_{rz}\mathbf{E}_{rz}) - \kappa^2\epsilon_r\mathbf{E}_{rz} = \mathbf{F}_{rz} \tag{1–8}$$

Azimuthal Problem:

$$\mathrm{curl}_{rz}(\frac{1}{\mu_r}\mathbf{curl}_{rz}E_\theta) - \kappa^2\epsilon_r E_\theta = F_\theta, \tag{1–9}$$

where $\mathbf{E}_{rz}$ denotes (E_r, E_z), and similar notation holds for $\mathbf{F}$. Therefore, by solving the meridian problem we obtain the rz-component of $\mathbf{E}$ and by solving the azimuthal problem we get the θ-component of $\mathbf{E}$. In other words, by solving two 2D problems, we find the solution for the 3D Maxwell equations (1–6).

In this dissertation, we will analyze the meridian problem. In particular, the main result of this dissertation is the finite element analysis and the multigrid analysis of the meridian problem.

CHAPTER 2
PRELIMINARIES ON FUNCTION SPACES

Our purpose here is to define some standard and weighted Sobolev spaces and to recall their properties. To simplify the discussion, we shall work from now on with real-valued functions, but the results stated here can be extended to complex-valued functions as well. Note that we use the notation $\mathbb{R}$ to denote the real number field and $\mathbb{N}$ to denote the set of non-negative integers.

2.1 Distributions

Let Ω be an open subset of $\mathbb{R}^n$, and define $\mathcal{D}(\Omega)$ to be the linear space of infinitely differentiable functions that have compact support in Ω. We often call this space the test function space. Next, let $\mathcal{D}'(\Omega)$ denote the dual space of $\mathcal{D}(\Omega)$ in the sense that a linear functional $T : \mathcal{D}(\Omega) \to \mathbb{R}$ is contained in $\mathcal{D}'(\Omega)$, provided that for every compact set $K \subset \Omega$ there exist constants C and k such that

$$|T(\phi)| \leq C \sum_{|\alpha| \leq k} sup_K |\partial^\alpha \phi|,$$

for all $\phi \in \mathcal{D}(\Omega)$, where we used the standard multi-index notation for derivatives: $\alpha = (\alpha_1, \alpha_2, \cdots, \alpha_n) \in \mathbb{N}^n$, $|\alpha| = \sum_{i=1}^n \alpha_i$, and $\partial^\alpha \phi = \dfrac{\partial^{|\alpha|}\phi}{\partial x_1^{\alpha_1} \cdots \partial x_n^{\alpha_n}}$.

This space is called the space of distributions, and if $f \in \mathcal{D}'(\Omega)$ is locally integrable, then

$$< f, \phi > = \int_\Omega f \phi dV \qquad \text{for all } \phi \in \mathcal{D}(\Omega),$$

where $< \cdot, \cdot >$ denotes the duality pairing. Therefore, $L^1_{loc}(\Omega) \subset \mathcal{D}'(\Omega)$, where $L^1_{loc}(\Omega)$ denotes the space of locally integrable functions defined on Ω.

If $f \in L^1_{loc}(\mathbb{R})$, the derivative of f exists, and it is also locally integrable, then for all $\phi \in \mathcal{D}(\mathbb{R})$,

$$< f', \phi >= \int_{-\infty}^{\infty} f'(x)\phi(x)dx = -\int_{-\infty}^{\infty} f(x)\phi'(x)dx = - < f, \phi' >,$$

by the integration by parts formula and by the fact that all $\phi \in \mathcal{D}(\mathbb{R})$ have compact support in $\mathbb{R}$. We adopt this rule for all $\mathcal{D}'(\Omega)$ in general and define the derivative of distributions in the following way.

For $f \in \mathcal{D}'(\Omega)$, define $\partial^\alpha f \in \mathcal{D}'(\Omega)$ by

$$< \partial^\alpha f, \phi >= (-1)^{|\alpha|} < f, \partial^\alpha \phi > \qquad \text{for all } \phi \in \mathcal{D}(\Omega).$$

Note that the above definition makes sense, since functions in $\mathcal{D}(\Omega)$ are infinitely differentiable. For a more detailed discussion of distributions see [36].

Additionally, we will later use the notation $\mathcal{D}(\overline{\Omega})$ to denote the linear space of restrictions of functions in $\mathcal{D}(\mathbb{R}^n)$ to $\overline{\Omega}$. Note that functions in $\mathcal{D}(\Omega)$ vanish on the boundary of Ω due to its compact support on Ω, but functions in $\mathcal{D}(\overline{\Omega})$ may not vanish on the boundary.

2.2 Standard Sobolev Spaces

Now with this notion of taking derivatives in the sense of distribution, we can define some basic Sobolev spaces in our interest. Recall that

$$L^2(\Omega) = \left\{ u : \int_\Omega |u|^2 dV < \infty \right\}$$

is a Hilbert space with the inner product being

$$(u, v) = \int_\Omega uv dV.$$

We will denote $\|\cdot\|$ for the L^2-norm. Since $L^2(\Omega) \subset L^1_{loc}(\Omega) \subset \mathcal{D}'(\Omega)$, we can define

$$H^1(\Omega) = \left\{ u \in L^2(\Omega) : \mathbf{grad}\, u \in L^2(\Omega)^n \right\},$$

where we are taking the gradient of $u \in L^2(\Omega)$ in the sense of distribution. The semi-norm, norm and inner product associated to this Hilbert space are

$$|u|_{H^1(\Omega)} = (\int_\Omega |\,\mathbf{grad}\, u|^2 dV)^{\frac{1}{2}},$$
$$\|u\|_{H^1(\Omega)} = (\|u\|^2 + |u|^2_{H^1(\Omega)})^{\frac{1}{2}},$$
$$(u, v)_{H^1(\Omega)} = \int_\Omega uv + \mathbf{grad}\, u \cdot \mathbf{grad}\, v dV.$$

Remark 2.2.1. For any integer $m \geq 0$, we can define

$$H^m(\Omega) = \left\{u \in L^2(\Omega) : \partial^\alpha u \in L^2(\Omega) \text{ for all } |\alpha| \leq m\right\}$$

with the inner product

$$(u, v)_{H^m(\Omega)} = (u, v) + \sum_{|\alpha|=m} (\partial^\alpha u, \partial^\alpha v).$$

For any positive real number s, $H^s(\Omega)$ is defined by means of interpolation [4].

For the remainder of this section, we assume that $\Omega \subset \mathbb{R}^3$, and we define two Sobolev spaces of vector valued functions, i.e.,

$$\mathbf{H}(\mathbf{curl}, \Omega) = \left\{\mathbf{u} \in L^2(\Omega)^3 : \mathbf{curl}\,\mathbf{u} \in L^2(\Omega)^3\right\},$$
$$\mathbf{H}(\mathrm{div}, \Omega) = \left\{\mathbf{u} \in L^2(\Omega)^3 : \mathrm{div}\,\mathbf{u} \in L^2(\Omega)\right\}.$$

These are Hilbert spaces with the inner product

$$(\mathbf{u}, \mathbf{v})_{\mathrm{H(curl},\Omega)} = (\mathbf{u}, \mathbf{v}) + (\mathbf{curl}\,\mathbf{u}, \mathbf{curl}\,\mathbf{v}),$$
$$(\mathbf{u}, \mathbf{v})_{\mathrm{H(div},\Omega)} = (\mathbf{u}, \mathbf{v}) + (\mathrm{div}\,\mathbf{u}, \mathrm{div}\,\mathbf{v}).$$

These are spaces of equivalence classes of functions defined upto measure zero. Therefore, we must define appropriate trace maps in order to talk about the boundary (set of measure zero) value of functions in these Sobolev spaces. Details on these trace

maps can be founded in [24, Chapter 1], but a brief description of them will be given here.

In the remainder of this chapter, for simplicity, we assume that $\Omega \subset \mathbb{R}^3$ is simply connected, bounded, and Lipschitz-continuous with connected boundary. Let $C^\infty(\overline{\Omega})$ denote the space of infinitely differentiable functions defined on $\overline{\Omega}$, and let $tr : C^\infty(\overline{\Omega}) \to C^\infty(\partial\Omega)$ be the restriction map, where $\partial\Omega$ denotes the boundary of Ω. Since $C^\infty(\overline{\Omega})$ is dense in $H^1(\Omega)$, and this map is continuous with respect to the H^1-norm, there exists a unique continuous extension of the map tr to $H^1(\Omega)$. We shall still denote this extension by tr. In fact, tr maps into $H^{\frac{1}{2}}(\partial\Omega)$ in this case, i.e., $tr : H^1(\Omega) \to H^{\frac{1}{2}}(\partial\Omega)$ is continuous. Similarly, we can define the trace on $\mathbf{H}(\mathbf{curl}, \Omega)$ and $\mathbf{H}(\mathrm{div}, \Omega)$ via continuous trace maps. In particular, $\mathbf{u} \mapsto \mathbf{u} \times \mathbf{n}|_{\partial\Omega}$ and $\mathbf{u} \mapsto \mathbf{u} \cdot \mathbf{n}|_{\partial\Omega}$ are the continuous trace maps $\mathbf{H}(\mathbf{curl}, \Omega) \to H^{-\frac{1}{2}}(\partial\Omega)^3$ and $\mathbf{H}(\mathrm{div}, \Omega) \to H^{-\frac{1}{2}}(\partial\Omega)$ respectively, where $\mathbf{n}$ denotes the unit outward normal of the boundary, and $H^{-\frac{1}{2}}(\partial\Omega)$ denotes the dual space of $H^{\frac{1}{2}}(\partial\Omega)$. These results are proved in [24, Chapter 1.2].

By using these trace maps, we can define closed subspaces of $H^1(\Omega)$, $\mathbf{H}(\mathbf{curl}, \Omega)$ and $\mathbf{H}(\mathrm{div}, \Omega)$ respectively:

$$\begin{aligned} H_0^1(\Omega) &= \left\{ u \in H^1(\Omega) : u|_{\partial\Omega} = 0 \right\}, \\ \mathbf{H}_0(\mathbf{curl}, \Omega) &= \left\{ \mathbf{u} \in \mathbf{H}(\mathbf{curl}, \Omega) : \mathbf{u} \times \mathbf{n}|_{\partial\Omega} = 0 \right\}, \\ \mathbf{H}_0(\mathrm{div}, \Omega) &= \left\{ \mathbf{u} \in \mathbf{H}(\mathrm{div}, \Omega) : \mathbf{u} \cdot \mathbf{n}|_{\partial\Omega} = 0 \right\}. \end{aligned} \tag{2–1}$$

Equivalently, we may define $H_0^1(\Omega)$, $\mathbf{H}_0(\mathbf{curl}, \Omega)$, and $\mathbf{H}_0(\mathrm{div}, \Omega)$ as the closure of $\mathcal{D}(\Omega)$ with respect to the norm on $H^1(\Omega)$, $\mathbf{H}(\mathbf{curl}, \Omega)$, and $\mathbf{H}(\mathrm{div}, \Omega)$ respectively. These subspaces are important theoretically and practically. For example, as we shall see in later chapters, if we consider the Maxwell equations with perfectly conducting boundary conditions, the electric field lies in the space $\mathbf{H}_0(\mathbf{curl}, \Omega)$. The next continuous embedding result is stated and proved in [24, Chapter 1.3].

Theorem 2.2.1. *If Ω is convex, then the spaces $\mathbf{H}_0(\mathbf{curl},\Omega)\cap\mathbf{H}(\mathrm{div},\Omega)$ and $\mathbf{H}(\mathbf{curl},\Omega)\cap\mathbf{H}_0(\mathrm{div},\Omega)$ are both continuously embedded in $H^1(\Omega)^3$. Thus,*

$$\|\mathbf{u}\|_{H^1(\Omega)^3}\leq C(\|\mathbf{u}\|+\|\mathbf{curl}\,\mathbf{u}\|+\|\mathrm{div}\,\mathbf{u}\|),$$

if $\mathbf{u}\in\mathbf{H}_0(\mathbf{curl},\Omega)\cap\mathbf{H}(\mathrm{div},\Omega)$ or $\mathbf{u}\in\mathbf{H}(\mathbf{curl},\Omega)\cap\mathbf{H}_0(\mathrm{div},\Omega)$.

The following more general result is proved in [22].

Theorem 2.2.2. *If Ω is a bounded Lipschitz domain, then the spaces $\mathbf{H}_0(\mathbf{curl},\Omega)\cap\mathbf{H}(\mathrm{div},\Omega)$ and $\mathbf{H}(\mathbf{curl},\Omega)\cap\mathbf{H}_0(\mathrm{div},\Omega)$ are both continuously embedded in $H^{\frac{1}{2}}(\Omega)^3$. Thus,*

$$\|\mathbf{u}\|_{H^{\frac{1}{2}}(\Omega)^3}\leq C(\|\mathbf{u}\|+\|\mathbf{curl}\,\mathbf{u}\|+\|\mathrm{div}\,\mathbf{u}\|),$$

if $\mathbf{u}\in\mathbf{H}_0(\mathbf{curl},\Omega)\cap\mathbf{H}(\mathrm{div},\Omega)$ or $\mathbf{u}\in\mathbf{H}(\mathbf{curl},\Omega)\cap\mathbf{H}_0(\mathrm{div},\Omega)$.

Above, and in the rest of the dissertation, we use C to denote a generic constant independent of the functions involved in norm estimates, which may take different values at different occurrences.

We end this section by stating two integration by parts formulas [24, Chapter 1.2]. Notice that for the closed subspaces (2–1), the formulas could be written in a simpler form due to zero boundary conditions.

Theorem 2.2.3. *(Green's Formula)*

$$(\mathbf{v},\mathbf{grad}\,\phi)+(\mathrm{div}\,\mathbf{v},\phi)=<\mathbf{v}\cdot\mathbf{n},\phi>_{\partial\Omega}\qquad \textit{for all } \mathbf{v}\in\mathbf{H}(\mathrm{div},\Omega),\phi\in H^1(\Omega),$$

$$(\mathbf{curl}\,\mathbf{u},\boldsymbol{\phi})-(\mathbf{u},\mathbf{curl}\,\boldsymbol{\phi})=<\mathbf{u}\times\mathbf{n},\boldsymbol{\phi}>_{\partial\Omega}\qquad \textit{for all } \mathbf{u}\in\mathbf{H}(\mathbf{curl},\Omega),\boldsymbol{\phi}\in H^1(\Omega)^3,$$

where $<\cdot,\cdot>_{\partial\Omega}$ denotes the duality pairing between either $H^{-\frac{1}{2}}(\partial\Omega)$ and $H^{\frac{1}{2}}(\partial\Omega)$ or $H^{-\frac{1}{2}}(\partial\Omega)^3$ and $H^{\frac{1}{2}}(\partial\Omega)^3$.

2.3 Weighted Sobolev Spaces

In this section, we introduce some important weighted Sobolev spaces that will be the function spaces in our main interest. If we have a $3D$ problem defined on an axisymmetric domain, and if the given data is also axisymmetric, then this $3D$ problem

can be reduced to a $2D$ one via cylindrical coordinates (r, θ, z). This is a remarkable feature, as it reduces computational time significantly, but due to the Jacobian arising from change of variables, we are now in weighted Sobolev spaces where the weight function is the radial component r.

In particular, suppose $\Omega \subset \mathbb{R}^3$ is symmetric with respect to the z-axis, and D is the restriction of Ω to the rz-plane where $r \geq 0$ (often called the meridian half-plane which will be denoted by $\mathbb{R}^2_+$). Therefore, Ω is obtained by rotating D around the z-axis. Here and throughout this dissertation except in Chapter 3, $\Omega \subset \mathbb{R}^3$ and $D \subset \mathbb{R}^2_+$ will always indicate domains related in such kind of way.

Let $\breve{L}^2(\Omega)$ denote the subspace of $L^2(\Omega)$ that consists of functions that are invariant under rotation. We adopt this notation $\breve{X}(\Omega)$ in general for any Sobolev space $X(\Omega)$. Vector-valued functions are called axisymmetric if each of its components are invariant under rotation. We will use f_D to denote the restriction of f defined on Ω onto D, i.e., $f_D(r, z) = f(r, 0, z)$. Similar notation follows for vector-valued functions as well. Then, for $f \in \breve{L}^2(\Omega)$,

$$\begin{aligned}\int_D |f_D(r,z)|^2 r dr dz &= \frac{1}{2\pi}\int_\Omega |f(r,\theta,z)|^2 r dr d\theta dz,\\ &= \frac{1}{2\pi}\int_\Omega |f(x,y,z)|^2 dx dy dz,\\ &< \infty.\end{aligned}$$

Therefore, it is clear that

$$f \in \breve{L}^2(\Omega) \text{ if and only if } f_D \in L^2_r(D), \tag{2–2}$$

where

$$L^2_r(D) = \left\{ u : \int_D |u(r,z)|^2 r dr dz < \infty \right\}.$$

This is a Hilbert space with the inner product

$$(u, v)_r = \int_D uvrdrdz,$$

and the induced norm will be denoted by $||\cdot||_r$.

Remark 2.3.1. If $D \subset \mathbb{R}^2_+$ intersects the axis of symmetry ($r = 0$) then $L^2(D)$ is strictly included in $L^2_r(D)$. For example, if D is the unit square in $\mathbb{R}^2_+$ and $f(r, z) = \frac{1}{\sqrt{r}}$ then $f(r, z) \notin L^2(D)$ but $f(r, z) \in L^2_r(D)$. In the finite element analysis and the multigrid analysis, we often use specific members in weighted Sobolev spaces. Therefore, extending the results known for the standard Sobolev spaces to weighted Sobolev spaces requires attention, and that is the focus of this dissertation.

Note that in cylindrical coordinates, under axial symmetry ($\partial_\theta = 0$), we have

$$\mathbf{grad}\,\phi = \partial_r\phi\mathbf{e}_r + \partial_z\phi\mathbf{e}_z, \tag{2–3}$$

$$\operatorname{div}\mathbf{v} = \frac{1}{r}\partial_r(rv_r) + \partial_z v_z, \tag{2–4}$$

$$\mathbf{curl}\,\mathbf{u} = -\partial_z u_\theta\mathbf{e}_r + (\partial_z u_r - \partial_r u_z)\mathbf{e}_\theta + \frac{1}{r}\partial_r(ru_\theta)\mathbf{e}_z. \tag{2–5}$$

We define two **curl** values in $2D$ in the following way.

$$\begin{aligned} \operatorname{curl}_{rz}(u_r, u_z) &= \partial_z u_r - \partial_r u_z, \\ \mathbf{curl}_{rz}\phi &= (-\partial_z\phi, \frac{1}{r}\partial_r(r\phi)). \end{aligned} \tag{2–6}$$

Notice that curl_{rz} takes a vector valued function and returns a scalar valued function, while $\mathbf{curl}_{rz}$ does vice versa. curl_{rz} and $\mathbf{curl}_{rz}$ are then related through the $3D$-curl under axial symmetry by (2–5), i.e., $\operatorname{curl}_{rz}(u_r, u_z)$ and $\mathbf{curl}_{rz}u_\theta$ return the θ-component and the rz-component of $\mathbf{curl}\,\mathbf{u}$ respectively under axial symmetry. Therefore, if $\mathbf{u} = (u_r, 0, u_z) \in \breve{\mathbf{H}}(\mathbf{curl}, \Omega)$ then we have that

$$(u_r, u_z)_D \in L^2_r(D)^2 \qquad \text{by (2–2)},$$

$$\operatorname{curl}_{rz}(u_r, u_z)_D \in L^2_r(D) \qquad \text{by (2–5)}.$$

We give a name to such weighted Sobolev space:

$$\mathbf{H}_r(\text{curl}, D) = \left\{\mathbf{w} \in L^2_r(D)^2 : \text{curl}_{rz}\mathbf{w} \in L^2_r(D)\right\}.$$

The inner product associated with this Hilbert space is

$$\Lambda(\mathbf{u}, \mathbf{v}) = (\mathbf{u}, \mathbf{v})_r + (\text{curl}_{rz}\mathbf{u}, \text{curl}_{rz}\mathbf{v})_r,$$

and the induced norm will be denoted by $||\cdot||_\Lambda$.

Similarly, by using (2–3), we have that if $\phi \in \breve{H}^1(\Omega)$, then $\phi_D \in H^1_r(D)$, where

$$H^1_r(D) = \left\{\phi \in L^2_r(D) : \mathbf{grad}_{rz}\phi \in L^2_r(D)^2\right\},$$

and $\mathbf{grad}_{rz}\phi = (\partial_r\phi, \partial_z\phi)$. In general, $H^k_r(D)$ is defined to be functions in $L^2_r(D)$ whose distributional derivatives up to order $k \geq 1$ is also in $L^2_r(D)$. Furthermore, for any positive real number s, $H^s_r(D)$ is defined as the Hilbert interpolation space $[H^{[s]+1}_r(D), H^{[s]}_r(D)]_{[s]+1-s}$ of index $[s]+1-s$ between the spaces $H^{[s]+1}_r(D)$ and $H^{[s]}_r(D)$, where $[s]$ stands for the integer part of s [6]. The norm and semi-norm of $H^s_r(D)$ is defined in the usual way, and they will be denoted by $||\cdot||_{H^s_r(D)}$ and $|\cdot|_{H^s_r(D)}$ respectively.

We define additional weighted function spaces here for the convenience of the reader. Let $\widetilde{H}^1_r(D) = L^2_{1/r}(D) \cap H^1_r(D)$, where

$$L^2_{1/r}(D) = \{u \in L^2(D) : \|u\|^2_{L^2_{1/r}(D)} = \int_D \frac{1}{r}\,|u|^2\,dr\,dz < \infty\}.$$

Then

$$\|v\|_{\widetilde{H}^1_r(D)} = (\|v\|^2_{H^1_r(D)} + \|v\|^2_{L^2_{1/r}(D)})^{\frac{1}{2}}$$

defines a norm on $\widetilde{H}^1_r(D)$. Furthermore, the semi-norm and norm

$$|v|_{\widetilde{H}^2_r(D)} = \left(\left|\frac{1}{r}\partial_r(rv)\right|^2_{H^1_r(D)} + |\partial_z v|^2_{H^1_r(D)}\right)^{\frac{1}{2}},$$

$$\|v\|_{\widetilde{H}^2_r(D)} = (|v|^2_{\widetilde{H}^2_r(D)} + \|v\|^2_{\widetilde{H}^1_r(D)} + \|\partial_z v\|^2_{L^2_{1/r}(D)})^{\frac{1}{2}},$$

define the Hilbert space

$$\widetilde{H}^2_r(D) = \{v \in \widetilde{H}^1_r(D) : \|v\|_{\widetilde{H}^2_r(D)} < \infty\}.$$

We summarize the isomorphisms between these weighted Sobolev spaces and standard Sobolev spaces under axial symmetry. The following results can be found in [2, Section 3.2].

Theorem 2.3.1. *The following isomorphism theorems hold:*

1. *The trace mapping $f \to f_D$ is an isometry (up to a factor $\frac{1}{\sqrt{2\pi}}$) from $\breve{L}^2(\Omega)$ to $L^2_r(D)$. The same holds for the reciprocal lifting, $L^2_r(D) \to \breve{L}^2(\Omega)$.*

2. *For $s \in (0, 2]$, the trace operator is an isomorphism from $\breve{H}^s(\Omega)$ to $H^s_+(D)$, where*

$$\begin{aligned} H^s_+(D) &= H^s_r(D) && \text{if } s \neq 2, \\ H^2_+(D) &= \left\{w \in H^2_r(D) : \partial_{rr} w \in L^2_{1/r}(D)\right\}. \end{aligned}$$

3. *For $s \in (0, 2]$, the trace operator is an isomorphism from $\breve{H}^s(\Omega)^3$ to $H^s_-(D) \times H^s_-(D) \times H^s_+(D)$, where*

$$\begin{aligned} H^s_-(D) &= H^s_r(D) \quad \text{if } s \neq 1, \\ H^1_-(D) &= \widetilde{H}^1_r(D). \end{aligned}$$

4. *The range of the trace operator from $\breve{\mathbf{H}}(\mathbf{curl}, \Omega)$ is*

$$\left\{(w_r, w_\theta, w_z) : (w_r, w_z) \in L^2_r(D)^2, \mathrm{curl}_{rz}(w_r, w_z) \in L^2_r(D), rw_\theta \in H^1_{1/r}(D)\right\}.$$

Furthermore, let us observe how the boundary conditions of the $3D$ problem transfer into boundary conditions of the $2D$ problem. Let $\partial D = \Gamma_0 \cup \Gamma_1$ where Γ_0 is the part of the boundary that is on the axis of symmetry ($r = 0$), and Γ_1 denotes the remainder of the boundary. Functions in $\widetilde{H}^1_r(D)$ are well known to have zero trace on Γ_0 [2, 25]. It is also known that functions in $H^1_r(D)$ have traces in $L^2_r(\Gamma_1)$, i.e., for ϕ in $H^1_r(D)$, the trace $\phi|_{\Gamma_1}$ makes sense as a function in $L^2_r(\Gamma_1)$, but trace on Γ_0 is not defined

in general [28]. We can define the tangential trace operator $\gamma_t : \mathcal{D}(\overline{D})^2 \mapsto \widetilde{H}^1_r(D)'$ by

$$\langle \gamma_t(\mathbf{v}), \phi \rangle = \int_{\Gamma_1} r\, \mathbf{v} \cdot \mathbf{t}\, \phi \;\, ds \qquad \text{for all } \phi \in \widetilde{H}^1_r(D), \tag{2–7}$$

where $\langle \cdot, \cdot \rangle$ denotes duality pairing in $\widetilde{H}^1_r(D)$, and $\mathbf{t}$ is the unit tangent vector on ∂D, oriented counterclockwise. In [21, Proposition 2.2], it is shown that γ_t extends to a continuous linear map from $\mathbf{H}_r(\mathrm{curl}, D)$ to $\widetilde{H}^1_r(D)'$. Moreover, the integration by parts formula

$$\langle \gamma_t(\mathbf{v}), \phi \rangle = (\mathbf{v}, \mathbf{curl}_{rz}\phi)_r - (\mathrm{curl}_{rz}\mathbf{v}, \phi)_r \tag{2–8}$$

holds for all $\mathbf{v}$ in $\mathbf{H}_r(\mathrm{curl}, D)$ and ϕ in $\widetilde{H}^1_r(D)$.

Naturally, the boundary conditions for the 3D problem give rise to boundary conditions on Γ_1. We consider perfectly conducting boundary conditions on $\partial\Omega$ in the Maxwell Equations, which asserts that the 3D electric field has zero tangential component on $\partial\Omega$. In the axisymmetric case, this boundary condition, loosely speaking, translates into an essential boundary condition of the form $\mathbf{E}_{rz} \cdot \mathbf{t} = 0$ on Γ_1. Therefore, if $\mathbf{E} \in \mathbf{H}_0(\mathbf{curl}, \Omega)$ then $(E_r, E_z)_D \in \mathbf{H}_{r,\diamond}(\mathrm{curl}, D)$, where $\mathbf{H}_{r,\diamond}(\mathrm{curl}, D)$ is a closed subspace of $\mathbf{H}_r(\mathrm{curl}, D)$ defined as:

$$\mathbf{H}_{r,\diamond}(\mathrm{curl}, D) = \{\mathbf{v} \in \mathbf{H}_r(\mathrm{curl}, D) : \gamma_t(\mathbf{v}) = 0\}\,.$$

Similarly, define

$$H^1_{r,\diamond}(D) = \left\{\phi \in H^1_r(D) : \phi|_{\Gamma_1} = 0\right\},$$

and notice that if $f \in \breve{H}^1_0(\Omega)$ then $f_D \in H^1_{r,\diamond}(D)$. The finite element analysis and the multigrid algorithm we shall give in later chapters are for an equation posed in $\mathbf{H}_{r,\diamond}(\mathrm{curl}, D)$.

CHAPTER 3
PRELIMINARIES ON ALGORITHMS

Finite Element Method is a method of finding an approximation of the exact solution to a partial differential equation (PDE). It is a method that changes a PDE system defined on some infinite dimensional space into a matrix system, i.e., a finite dimensional problem. Multigrid is an efficient way to solve the matrix system obtained by the finite element method. Both finite element method and multigrid are well-known not only for its efficiency but also for its well-established mathematical theory behind it. In this chapter, we give a brief introduction to the finite element method and the multigrid V-cycle algorithm.

3.1 Finite Element Methods

Let $\Omega \subset \mathbb{R}^2$ and $f \in L^2(\Omega)$. Suppose we want to solve the following Poisson equation:

Find $u \in H^1(\Omega)$ such that

$$\begin{aligned} -\triangle u &= f \quad \text{on } \Omega, \\ u &= 0 \quad \text{on } \partial\Omega. \end{aligned} \tag{3–1}$$

By multiplying an arbitrary $v \in H^1(\Omega)$ with homogeneous Dirichlet boundary conditions ($v \in H_0^1(\Omega)$) on both side of the equation, and by applying Theorem 2.2.3 in the $2D$ case, we get the weak formulation of (3–1):

Find $u \in H_0^1(\Omega)$ such that

$$\int_\Omega \mathbf{grad}\, u \cdot \mathbf{grad}\, v dV = \int_\Omega f v dV \text{ for all } v \in H_0^1(\Omega). \tag{3–2}$$

Note that (3–2) has a unique solution by the Lax-Milgram Lemma.

The finite element method wants to change this problem (3–2) into a finite dimensional problem. Therefore, the next step is to construct a finite dimensional subspace $M_h \subset H_0^1(\Omega)$.

We first divide the domain into finitely many triangles satisfying some assumptions. In particular, we assume that the finite element triangulation $\mathscr{T}_h$ of Ω satisfies the usual geometrical conformity conditions [18] with a representative meshsize h, which is the following.

Suppose $\Omega \subset \mathbb{R}^n$ is a polyhedral domain subdivided into n-simplices K collected into $\mathscr{T}_h$. We say that $\mathscr{T}_h$ is a finite element mesh if it satisfies the following conditions:

1. The interior of K_i and K_j are disjoint whenever $i \neq j$ for all $K_i, K_j \in \mathscr{T}_h$.
2. $\bigcup_{K \in \mathscr{T}_h} K = \bar{\Omega}$.
3. Any face of any $K \in \mathscr{T}_h$ is either a subset of $\partial\Omega$ or a face of another $K' \in \mathscr{T}_h$.

Here and throughtout the paper, we assume that the mesh $\mathscr{T}_h$ is quasiuniform. A mesh is quasiuniform if it satisfies the next two conditions:

1. shape regularity: There exists $\alpha > 0$ such that $\dfrac{h_k}{\rho_k} \leq \alpha$ for all $k \in \mathscr{T}_h$, where h_k is the diameter of the triangle K, and ρ_k is maximum radius of the inscribed circles in K.
2. There exists $\beta > 0$ such that $\beta h \leq h_k$ for all $K \in \mathscr{T}_h$, where $h = \max_K h_k$.

Next, we construct a finite dimensional subspace of $H_0^1(\Omega)$ in the following way:

$$M_h = \left\{ v \in H_0^1(\Omega) : v|_K = a_K x + b_K y + c_K \text{ for some } a_K, b_K, c_K \in \mathbb{R} \text{ for all } K \in \mathscr{T}_h \right\}.$$

Then instead of solving (3–2) we solve the finite dimensional problem that looks just like (3–2) but with the infinite dimensional space $H_0^1(\Omega)$ replaced by the finite dimensional subspace M_h:

Find $u_h \in M_h$ such that

$$\int_\Omega \mathbf{grad}\, u_h \cdot \mathbf{grad}\, v_h dV = \int_\Omega f v_h dV \text{ for all } v_h \in M_h. \tag{3–3}$$

We will discuss how this problem can be changed into a matrix system, but let us first see how well the finite element approximation u_h of (3–3) approximates the exact solution u of (3–2). The following results are proved in [18].

Theorem 3.1.1. *Let $u \in H_0^1(\Omega)$ and $u_h \in M_h$ be the unique solution of (3–2) and (3–3) respectively. Then*

1. *(Quasi-Optimality Result)*

$$||u - u_h||_{H^1(\Omega)} \leq C \inf_{v_h \in M_h} ||u - v_h||_{H^1(\Omega)}.$$

2. *(Error Estimate)*

$$||u - u_h||_{H^1(\Omega)} \leq Ch|u|_{H^2(\Omega)}$$

3. *(Regularity Result) If Ω is convex then*

$$||u||_{H^2(\Omega)} \leq C||f||.$$

The quasi-optimality result follows directly from the Cea's Lemma, and this tells us that the error between u and u_h is bounded by a constant multiple of the best approximation of u in M_h. We obtain item 2 by using item 1 and the error estimate $||u - \Pi u|| \leq Ch|u|_{H^2(\Omega)}$, where $\Pi : H_0^1(\Omega) \to M_h$ is the canonical projection operator. Item 2 is meaningful only when $u \in H^2(\Omega)$, which item 3 implies under the convexity assumption of Ω. In the case when Ω is non-convex, u has less regularity, but similar results as item 2 continue to hold with a weaker norm and a lower degree of h on the right hand side. Item 2 implies that $||u - u_h||_{H^1(\Omega)}$ approaches zero as the meshsize h approaches zero, i.e., the discrete solution converges to the exact solution as we continue to refine the mesh.

Since M_h is a finite dimensional subspace, we use basis functions $\{\phi_i\}_{i=1}^N$ to solve (3–3). Let $\mathfrak{V}_h$ denote the set of interior nodes of $\mathscr{T}_h$. For each $\mathfrak{v}_i \in \mathfrak{V}_h$, let ϕ_i be the unique function in M_h that satisfies $\phi_i(\mathfrak{v}_j) = \delta_{ij}$, where δ is the Kronecker delta here. These functions are often called hat functions, and it is easy to see that these hat functions form a basis in M_h. Thus we can write the discrete solution of (3–3) as $u_h = \sum_{i=1}^N u_i\phi_i$, where N is the number of interior nodes, and since (3–3) holds for all

$v_h \in M_h$, it must hold for all $\{\phi_i\}_{i=1}^N$ in particular. Therefore,

$$\int_\Omega \mathbf{grad}(\sum_{i=1}^N u_i\phi_i) \cdot \mathbf{grad}\,\phi_j dV = \int_\Omega f\phi_j dV \text{ for all } j = 1 \cdots N,$$
$$\sum_{i=1}^N (\int_\Omega \mathbf{grad}\,\phi_i \cdot \mathbf{grad}\,\phi_j dV) u_i = \int_\Omega f\phi_j dV \text{ for all } j = 1 \cdots N.$$

Hence

$$\widehat{A}\vec{u} = \vec{b},$$

where $\widehat{A}$ is the $N \times N$ matrix such that $\widehat{A}_{ji} = \int_\Omega \mathbf{grad}\,\phi_i \cdot \mathbf{grad}\,\phi_j dV$, and $\vec{b}$ is the length N vector whose j-th component is $\int_\Omega f\phi_j dV$. Not only is the matrix $\widehat{A}$ invertible, it is also symmetric positive definite. By solving this matrix system (by finding $\vec{u}$) we find the coefficients $\{u_i\}_{i=1}^N$, and so we obtain the approximation u_h by using $u_h = \sum_{i=1}^N u_i\phi_i$.

As seen above, the size of the matrix system obtained by the finite element method corresponds to the dimension of the finite element subspace, Thus, as the mesh gets finer the corresponding matrix problem that needs to be solved gets larger. The finer the mesh is, however, the closer the approximation solution is to the exact one, so we are now interested in solving this large sparse matrix system efficiently.

3.2 Multigrid Solver

We have seen in the previous section that, by using finite element methods, we can change a continuous PDE system into a matrix system. Now we are interested in solving this matrix system in an efficient way. Multigrid techniques give iterative methods for solving matrix systems obtained by the finite element method, by using a sequence of meshes. It is very powerful, since often the convergence is uniform with respect to the mesh size. In other words, the number of iterations to convergence stays nearly constant no matter how large the matrix becomes. We refer to [11, 14] for details on multigrid theory.

Suppose A is an operator that satisfies $(Au, v)_q = a(u, v)$ for some bilinear form $a(\cdot, \cdot)$ and some innerproduct $(\cdot, \cdot)_q$ on some function space M. Consider a sequence of

nested finite element subspaces of M, i.e.,

$$M_1 \subset M_2 \subset \cdots \subset M_J.$$

In particular, $\{\mathscr{T}_i\}_{i=1}^J$ is a sequence of meshes such that $\mathscr{T}_{i+1}$ is a refinement of $\mathscr{T}_i$ for all $1 \leq i \leq J-1$, and M_i is the finite element subspace with respect to the mesh $\mathscr{T}_i$ for all $1 \leq i \leq J$. Define $A_k : M_k \to M_k$ by

$$(A_k u_k, v_k)_q = a(u_k, v_k) \text{ for all } u_k, v_k \in M_k.$$

We want to construct an efficient multigrid iteration to solve equations of the form $A_J x = f$ on M_J.

Let $R_k : M_k \to M_k$ be a smoother, and define $Q_k : M_{k+1} \to M_k$ by

$$(Q_k u_{k+1}, v_k)_q = (u_{k+1}, v_k)_q \text{ for all } v_k \in M_k.$$

In other words, Q_k is the $(\cdot,\cdot)_q$-orthogonal projection from M_{k+1} onto M_k. Then the standard V-cycle multigrid algorithm is as follows:

Algorithm 3.2.1 (V-cycle). Given u and f in M_k, define the output $MG_k(u, f)$ in M_k by the following recursive procedure:

1. Set $MG_1(u, f) = A_1^{-1} f$.
2. For $k > 1$, define $MG_k(u, f)$ recursively:
   (a) $v^{(1)} = u + R_k(f - A_k u)$. (Presmoothing)
   (b) $v^{(2)} = v^{(1)} + MG_{k-1}(0, Q_{k-1}(f - A_k v^{(1)}))$. (Correction using coarse meshes)
   (c) $v^{(3)} = v^{(2)} + R_k^t(f - A_k v^{(2)})$. (Postsmoothing)
   (d) Set $MG_k(u, f) = v^{(3)}$.

The following Theorem gives conditions on the smoother R_k which assures the uniform convergence of the multigrid V-cycle [10, 11, 14].

Theorem 3.2.1. *(Uniform V-cycle Convergence)*

Let $\mathcal{E}_k : M_k \to M_k$ be the error reduction operator of MG_k, and let P_{k-1} be the $a(\cdot,\cdot)$-orthogonal projection from M_k to M_{k-1}. Suppose there exists a constant C independent of k such that

$$\|(I - P_{k-1})K_k u\|_a^2 \leq C(\|u\|_a^2 - \|K_k u\|_a^2) \text{ for all } u \in M_k \tag{3–4}$$

where $K_k = I - R_k A_k$. Then,

$$0 \leq a(\mathcal{E}_k u, u) \leq \delta a(u, u) \text{ for all } u \in M_k$$

with $\delta = \frac{C}{1+C}$.

In the remainder of this section, we explain why the conclusion of Theorem 3.2.1 implies the uniform convergence of the multigrid V-cycle. Recall that the error reduction operator, by definition, satisfies

$$x - x_n = \mathcal{E}_k(x - x_{n-1}),$$

where x is the exact solution and x_n is the result of the n-th iteration of the multigrid solver. Hence,

$$\|x - x_n\|_a \leq \|\mathcal{E}_k\|_a^n \|x - x_0\|_a$$

on M_k. Theroem 3.2.1 implies that

$$\begin{aligned}
\|\mathcal{E}_k\|_a^2 &= \sup_{v \neq 0} \frac{a(\mathcal{E}_k v, \mathcal{E}_k v)}{a(v, v)}, \\
&\leq \lambda_{max}(\mathcal{E}_k)^2, \\
&\leq \delta^2,
\end{aligned}$$

where $\lambda_{max}(\mathcal{E}_k)$ denotes the maximum eigenvalue of $\mathcal{E}_k$. Therefore,

$$\|\mathcal{E}_k\|_a \leq \delta,$$

so that

$$\|x - x_n\|_a \leq \delta^n \|x - x_0\|_a .$$

Since δ is independent of the meshsize, this shows that the multigrid algorithm converges at a uniform rate independent of the meshsize.

CHAPTER 4
COMMUTING PROJECTORS IN WEIGHTED SPACES

In this chapter, we will construct projectors in weighted spaces with commuting properties and approximation properties. These projectors will play an essential role in Chapters 5, 6, and 7. We construct two different type of projectors on $\mathbf{H}_{r,\diamond}(\mathrm{curl}, D)$, which will be presented in two separate sections. Here and in the remaining of this dissertation, we will assume that the rotational domain $\Omega \subset \mathbb{R}^3$ is a simply connected, bounded Lipschitz domain with connected boundary. Additionally, we will assume that D is simply connected and Γ_1 is connected in order to use the exact sequence property (4–3).

4.1 A Global Projector in Weighted Spaces

The purpose of this section is to exhibit a projector Π_h^W into the Nédélec finite element [32] subspace of $\mathbf{H}_{r,\diamond}(\mathrm{curl}, D)$ that has a commutativity property involving the $L_r^2(D)$-orthogonal projection Π_h^S into a space of piecewise constant functions. The results in this section are contained in [20].

First, let us define the finite element subspaces onto which the projections map. Let

$$\mathbf{N}_1 = \{(a - bz, c + br) : a, b, c \in \mathbb{R}\},$$

$$P_1 = \{c_0 + c_1 r + c_2 z : c_i \in \mathbb{R} \text{ for } i = 0, 1, 2\}.$$

The finite element spaces we shall use are

$$V_h = \left\{u \in H_r^1(D) : u|_K \in P_1 \text{ for all } K \in \mathscr{T}_h\right\},$$

$$\mathbf{W}_h = \{\mathbf{v} \in \mathbf{H}_r(\mathrm{curl}, D) : \mathbf{v}|_K \in \mathbf{N}_1 \text{ for all } K \in \mathscr{T}_h\},$$

$$V_{h,\diamond} = \{v \in V_h : v|_{\Gamma_1} = 0\},$$

$$\mathbf{W}_{h,\diamond} = \{\mathbf{v} \in \mathbf{W}_h : \gamma_t(\mathbf{v}) = 0\},$$

$$S_h = \left\{u \in L_r^2(D) : u|_K \text{ is constant for all } K \in \mathscr{T}_h\right\},$$

where we assume that D is meshed by a finite element triangulation $\mathscr{T}_h$ satisfying the usual geometrical conformity conditions (see Chapter 3 section 3.1) with a representative meshsize h. Projectors into these finite element spaces with commutativity properties have been constructed previously. Indeed, in [21], we find projectors $\widehat{\Pi}_h^V$, $\widehat{\Pi}_h^W$, and $\widehat{\Pi}_h^S$ onto $V_{h,\diamond}$, $\mathbf{W}_{h,\diamond}$, and S_h respectively. In particular, it is proved in [21] that they satisfy

$$\mathrm{curl}_{rz}\widehat{\Pi}_h^W\mathbf{v} = \widehat{\Pi}_h^S\mathrm{curl}_{rz}\mathbf{v} \tag{4–1}$$

$$\|\widehat{\Pi}_h^W\mathbf{v} - \mathbf{v}\|_r \leq Ch|\mathbf{v}|_{H_r^1(D)^2} \tag{4–2}$$

for all $\mathbf{v}$ in $H_r^1(D)^2$ (see [21, Lemma 5.1] for (4–1) and [21, Lemma 5.3] for (4–2)). The projection $\widehat{\Pi}_h^S\phi$ equals the $L_r^2(K)$-orthogonal projection of ϕ for all K intersecting Γ_0, while for the remaining elements K', it equals the (unweighted) $L^2(K')$-orthogonal projection of ϕ.

Unfortunately, these projectors are inadequate for our purposes in Chapter 5. Let Π_h^S denote the $L_r^2(D)$-orthogonal projection into S_h. For our analysis later, we need a projector Π_h^W that satisfies the commutativity property in (4–1) with Π_h^S. The projector $\widehat{\Pi}_h^S$ of [21] is not equal to Π_h^S. Therefore, the remainder of this section is devoted to the construction of the projector Π_h^W with the properties we need, as listed in the following theorem.

Theorem 4.1.1. *Let $\Pi_h^S : L_r^2(D) \to S_h$ be the $L_r^2(D)$-orthogonal projection. There is a projector $\Pi_h^W : \mathbf{H}_{r,\diamond}(\mathrm{curl}, D) \to \mathbf{W}_{h,\diamond}$ such that*

1. *Π_h^W is well defined and continuous on $\mathbf{H}_{r,\diamond}(\mathrm{curl}, D)$,*
2. *the commutativity property*

$$\Pi_h^S\mathrm{curl}_{rz}\mathbf{u} = \mathrm{curl}_{rz}\Pi_h^W\mathbf{u},$$

holds for all $\mathbf{u}$ in $\mathbf{H}_{r,\diamond}(\mathrm{curl}, D)$,

3. the approximation property

$$\left\|\mathbf{u} - \Pi_h^W \mathbf{u}\right\|_\Lambda \leq C \inf_{\mathbf{u}_h \in \mathbf{W}_{h,\diamond}} \|\mathbf{u} - \mathbf{u}_h\|_\Lambda$$

holds for all $\mathbf{u}$ *in* $\mathbf{H}_{r,\diamond}(\mathrm{curl}, D)$*.*

We remark that the projector Π_h^W is continuous on $\mathbf{H}_{r,\diamond}(\mathrm{curl}, D)$, whereas typical projectors into the Nédélec space, such as Nédélec's original projector [32], as well as the projector $\widehat{\Pi}_h^W$, require more regularity due to edge-based degrees of freedom. This is achieved by a global definition of Π_h^W without local degrees of freedom, given in the proof of this theorem below.

For the proof and subsequent analysis, we will need an "exact sequence property" and the so-called "discrete Helmholtz decomposition," but adapted to our weighted inner product setting. Because we have assumed that Γ_1 is connected and D is simply connected, it follows that the sequence

$$0 \longrightarrow V_{h,\diamond} \xrightarrow{\mathrm{grad}_{rz}} \mathbf{W}_{h,\diamond} \xrightarrow{\mathrm{curl}_{rz}} S_h \longrightarrow 0 \tag{4–3}$$

is exact, as proved in Appendix A. This means that the map $\mathrm{curl}_{rz} : \mathbf{W}_{h,\diamond} \mapsto S_h$ is surjective and its null space coincides with the $\mathbf{grad}_{rz}(V_{h,\diamond})$. Such results are standard in the case of no boundary conditions or when boundary conditions hold on the entire boundary. In our application, a boundary condition is prescribed only on part of ∂D, namely Γ_1. Since we have not been able to locate a reference for the proof of exactness in this case, we include a short proof in Appendix A.

Next, let us adapt the well-known discrete Helmholtz decomposition to our weighted norms. Given a $\mathbf{v}_h$ in $\mathbf{W}_{h,\diamond}$, there is a unique ϕ_h in $V_{h,\diamond}$ satisfying

$$(\mathbf{grad}_{rz}\phi_h, \mathbf{grad}_{rz}\psi_h)_r = (\mathbf{v}_h, \mathbf{grad}_{rz}\psi_h)_r \quad \text{for all } \psi_h \text{ in } V_{h,\diamond}.$$

The unique existence of ϕ_h is guaranteed by the Lax-Milgram lemma, which may be invoked for this variational problem thanks to [25, Proposition 2.1]. It is trivial to verify

the stability estimate

$$\|\mathbf{grad}_{rz}\phi_h\|_r \leq \|\mathbf{v}_h\|_r. \tag{4–4}$$

Let $\mathbf{r}_h = \mathbf{v}_h - \mathbf{grad}_{rz}\phi_h$. Then the weighted discrete Helmholtz decomposition is

$$\mathbf{v}_h = \mathbf{grad}_{rz}\phi_h + \mathbf{r}_h.$$

Note that the components of the decomposition are orthogonal with respect to the weighted inner products of both $L^2_r(D)^2$ and $\mathbf{H}_r(\mathrm{curl}, D)$.

To characterize $\mathbf{r}_h$ further, let $\mathrm{curl}'_{rz} : S_h \mapsto \mathbf{W}_{h,\diamond}$ be defined by

$$(\mathrm{curl}'_{rz} s_h, \mathbf{w}_h)_r = (s_h, \mathrm{curl}_{rz}\mathbf{w}_h)_r, \qquad \text{for all } s_h \text{ in } S_h \text{ and } \mathbf{w}_h \text{ in } \mathbf{W}_{h,\diamond},$$

i.e., curl'_{rz} is the adjoint of $\mathrm{curl}_{rz} : \mathbf{W}_{h,\diamond} \to S_h$, with respect to the weighted inner product $(\cdot,\cdot)_r$. By the exactness of (4–3),

$$\mathbf{grad}_{rz}(V_{h,\diamond}) = \ker(\mathrm{curl}_{rz})$$

where $\ker(\mathrm{curl}_{rz})$ denotes the null space of curl_{rz} in $\mathbf{W}_{h,\diamond}$. Hence the orthogonality of $\mathbf{r}_h$ with $\mathbf{grad}_{rz}(V_{h,\diamond})$ implies that $\mathbf{r}_h$ is in the range of the adjoint curl'_{rz}, i.e., there is an element a_h in S_h such that

$$\mathbf{r}_h = \mathrm{curl}'_{rz} a_h,$$

and moreover, a_h is unique due to the injectivity of curl'_{rz} (which follows from the surjectivity of curl_{rz} in the exact sequence (4–3)). In other words, an alternate way of stating the decomposition is that for all $\mathbf{v}_h$ in $\mathbf{W}_{h,\diamond}$, there is a unique a_h in S_h and a unique ϕ_h in $V_{h,\diamond}$ such that

$$\mathbf{v}_h = \mathbf{grad}_{rz}\phi_h + \mathrm{curl}'_{rz} a_h. \tag{4–5}$$

We shall now use this decomposition to prove Theorem 4.1.1.

Proof of Theorem 4.1.1. Define $\Pi_h^W : \mathbf{H}_{r,\diamond}(\mathrm{curl}, D) \to \mathbf{W}_{h,\diamond}$ by

$$(\Pi_h^W \mathbf{v}, \mathbf{grad}_{rz}\eta_h)_r = (\mathbf{v}, \mathbf{grad}_{rz}\eta_h)_r \qquad \text{for all } \eta_h \text{ in } V_{h,\diamond}, \tag{4–6a}$$

$$(\mathrm{curl}_{rz}\Pi_h^W \mathbf{v}, s_h)_r = (\mathrm{curl}_{rz}\mathbf{v}, s_h)_r \qquad \text{for all } s_h \text{ in } S_h. \tag{4–6b}$$

We will now verify that the asserted statements hold for this Π_h^W.

1. First of all, observe that (4–6) is a square system of equations. Indeed, due to the exactness of (4–3), the number of equations in (4–6) equal

$$\begin{aligned}\dim(V_{h,\diamond}) + \dim(S_h) &= \dim(\mathbf{grad}_{rz}(V_{h,\diamond})) + \dim(\mathrm{curl}_{rz}(\mathbf{W}_{h,\diamond})),\\ &= \dim(\ker(\mathrm{curl}_{rz})) + \dim(\mathrm{curl}_{rz}(\mathbf{W}_{h,\diamond})),\\ &= \dim(\mathbf{W}_{h,\diamond}),\end{aligned}$$

by the rank-nullity theorem. Thus, we only need to show that the kernel of the linear system (4–6) is trivial. If $\mathbf{v} = 0$, then the right hand side of (4–6) is zero, so

$$(\Pi_h^W \mathbf{v}, \mathbf{grad}_{rz}\eta_h + \mathrm{curl}'_{rz} s_h)_r = 0 \qquad \text{for all } \eta_h \text{ in } V_{h,\diamond} \text{ and } s_h \text{ in } S_h.$$

This implies that $\Pi_h^W \mathbf{v} = 0$, by the weighted discrete Helmholtz decomposition of $\mathbf{W}_{h,\diamond}$. Therefore, Π_h^W is well defined.

Before we proceed to prove the continuity of Π_h^W on $\mathbf{H}_{r,\diamond}(\mathrm{curl}, D)$, let us note that

$$\|s_h\|_r \le C\|\mathrm{curl}'_{rz} s_h\|_r \qquad \text{for all } s_h \in S_h. \tag{4–7}$$

This follows from [21, Theorem 6.1(2)], which asserts that

$$\|\mathbf{v}_h\|_r \le C\|\mathrm{curl}_{rz}\mathbf{v}_h\|_r \qquad \text{for all } \mathbf{v}_h \in \mathbf{R}_h^\perp \tag{4–8}$$

where $\mathbf{R}_h^\perp$ denotes the orthogonal complement of $\mathbf{grad}_{rz}(V_{h,\diamond})$ in $\mathbf{W}_{h,\diamond}$ in the weighted $L_r^2(D)$-norm. Indeed, (4–8) implies that

$$\|\mathrm{curl}'_{rz} a_h\|_r = \sup_{\mathrm{v}_h \in \mathrm{R}_h^\perp} \frac{(\mathrm{curl}'_{rz} a_h, \mathbf{v}_h)_r}{\|\mathbf{v}_h\|_r} \ge \sup_{\mathrm{v}_h \in \mathrm{R}_h^\perp} \frac{(a_h, \mathrm{curl}_{rz}\mathbf{v}_h)_r}{C\,\|\mathrm{curl}_{rz}\mathbf{v}_h\|_r} = \frac{1}{C}\,\|a_h\|_r\,,$$

which proves (4–7).

Now, to prove the continuity of Π_h^W, let us first use the weighted discrete Helmholtz decomposition (4–5) and write $\Pi_h^W \mathbf{v} = \mathbf{grad}_{rz}\phi_h + \mathrm{curl}'_{rz} a_h$, with ϕ_h in $V_{h,\diamond}$ and a_h in S_h. Setting $\eta_h = \phi_h$ in (4–6a) and $s_h = a_h$ in (4–6b) and applying Cauchy-Schwarz inequality,

$$\begin{aligned} \|\mathbf{grad}_{rz}\phi_h\|_r &\le \|\mathbf{v}\|_r, \qquad \text{and} \\ \|\mathrm{curl}'_{rz} a_h\|_r^2 &= (\mathrm{curl}_{rz}\mathbf{v}, a_h)_r \le \|\mathrm{curl}_{rz}\mathbf{v}\|_r \, \|a_h\|_r \\ &\le \|\mathrm{curl}_{rz}\mathbf{v}\|_r \, C \, \|\mathrm{curl}'_{rz} a_h\|_r \end{aligned}$$

by (4–7). Hence, the stated continuity of Π_h^W follows by the stability of the weighted discrete Helmholtz decomposition.

2. Commutativity is clear from (4–6b) and the definition of Π_h^S.

3. To prove the error estimate, consider an arbitrary $\mathbf{u}$ in $\mathbf{H}_{r,\diamond}(\mathrm{curl}, D)$ and $\mathbf{u}_h$ in $\mathbf{W}_{h,\diamond}$. Use the weighted discrete Helmholtz decomposition to split

$$\Pi_h^W \mathbf{u} - \mathbf{u}_h = \mathbf{grad}_{rz}\psi_h + \mathrm{curl}'_{rz} b_h,$$

with ψ_h in $V_{h,\diamond}$ and b_h in S_h. Then, by (4–6),

$$\begin{aligned} (\Pi_h^W \mathbf{u} - \mathbf{u}, \Pi_h^W \mathbf{u} - \mathbf{u}_h)_r &= (\Pi_h^W \mathbf{u} - \mathbf{u}, \mathbf{grad}_{rz}\psi_h + \mathrm{curl}'_{rz} b_h)_r, \\ &= (\Pi_h^W \mathbf{u} - \mathbf{u}, \mathrm{curl}'_{rz} b_h)_r, \\ &= (\mathrm{curl}_{rz}\Pi_h^W \mathbf{u}, b_h)_r - (\mathbf{u}_h, \mathrm{curl}'_{rz} b_h)_r - (\mathbf{u} - \mathbf{u}_h, \mathrm{curl}'_{rz} b_h)_r, \\ &= (\mathrm{curl}_{rz}\mathbf{u}, b_h)_r - (\mathrm{curl}_{rz}\mathbf{u}_h, b_h)_r - (\mathbf{u} - \mathbf{u}_h, \mathrm{curl}'_{rz} b_h)_r, \end{aligned}$$

and hence

$$\left\|\Pi_h^W \mathbf{u} - \mathbf{u}_h\right\|_r^2 = (\mathbf{u} - \mathbf{u}_h, \Pi_h^W \mathbf{u} - \mathbf{u}_h)_r + (\mathrm{curl}_{rz}(\mathbf{u} - \mathbf{u}_h), b_h)_r - (\mathbf{u} - \mathbf{u}_h, \mathrm{curl}'_{rz} b_h)_r.$$

Now, using the Cauchy-Schwarz inequality,

$$\begin{aligned}\left\|\Pi_h^W \mathbf{u} - \mathbf{u}_h\right\|_r^2 &\leq \|\mathbf{u} - \mathbf{u}_h\|_\Lambda \left(\|\Pi_h^W \mathbf{u} - \mathbf{u}_h\|_r + \|b_h\|_r + \|\mathrm{curl}'_{rz} b_h\|_r\right) \\ &\leq C\|\mathbf{u} - \mathbf{u}_h\|_\Lambda \, \|\Pi_h^W \mathbf{u} - \mathbf{u}_h\|_r,\end{aligned}$$

where we have applied (4–7) to b_h, and used the stability of the discrete Helmholtz decomposition. The triangle inequality now yields the estimate

$$\left\|\mathbf{u} - \Pi_h^W \mathbf{u}\right\|_r \leq C \, \|\mathbf{u} - \mathbf{u}_h\|_\Lambda \, .$$

Finally, since

$$\|\mathrm{curl}_{rz}(\mathbf{u} - \Pi_h^W \mathbf{u})\|_r = \|\mathrm{curl}_{rz}\mathbf{u} - \Pi_h^S \mathrm{curl}_{rz}\mathbf{u}\|_r \leq \|\mathrm{curl}_{rz}\mathbf{u} - \mathrm{curl}_{rz}\mathbf{u}_h\|_r,$$

we have

$$\|\mathbf{u} - \Pi_h^W \mathbf{u}\|_\Lambda \leq C\|\mathbf{u} - \mathbf{u}_h\|_\Lambda.$$

Since $\mathbf{u}_h$ in $\mathbf{W}_{h,\diamond}$ is arbitrary, this proves the stated approximation property. □

The following corollary gives more specific estimates in terms of the meshsize h, under certain conditions.

Corollary 4.1.1. *Let* $\mathbf{u}$ *be in* $H_r^s(D)^2$ *for any* $0 \leq s \leq 1$*. The approximation property*

$$\left\|\mathbf{u} - \Pi_h^W \mathbf{u}\right\|_\Lambda \leq Ch^s \left(\|\mathbf{u}\|_{H_r^s(D)^2} + \|\mathrm{curl}_{rz}\mathbf{u}\|_{H_r^s(D)}\right)$$

holds provided that $\mathrm{curl}_{rz}\mathbf{u}$ *is in* $H_r^s(D)$*, and*

$$\left\|\mathbf{u} - \Pi_h^W \mathbf{u}\right\|_r \leq Ch^s \, \|\mathbf{u}\|_{H_r^s(D)^2} \tag{4–9}$$

holds provided that $\mathrm{curl}_{rz}\mathbf{u}$ *is in* S_h*. If* $s = 1$ *the norms on the right hand side of both inequalities above can be replaced by semi-norms.*

Proof. In the case that $\mathrm{curl}_{rz}\mathbf{u}$ is in $H_r^s(D)$, the first estimate follows directly from Theorem 4.1.1 item 3 and Corollary 4.2.1, by taking $\mathbf{u}_h = \Pi_h^c \mathbf{u}$ (see section 4.2).

This projector will be constructed in the next section, but we use this result here for the completion of this proof.

Now suppose $\mathrm{curl}_{rz}\mathbf{u}$ is in S_h. Then the following estimate of Theorem 4.1.1 item 3

$$\|\mathbf{u} - \Pi_h^W \mathbf{u}\|_\wedge \leq C\|\mathbf{u} - \Pi_h^c \mathbf{u}\|_\wedge$$

reduces to simply

$$\|\mathbf{u} - \Pi_h^W \mathbf{u}\|_r \leq C\|\mathbf{u} - \Pi_h^c \mathbf{u}\|_r$$

because of the commutativity properties. Indeed, $\mathrm{curl}_{rz}\Pi_h^c\mathbf{u} = \Pi_h^o \mathrm{curl}_{rz}\mathbf{u} = \mathrm{curl}_{rz}\mathbf{u}$ and similarly $\mathrm{curl}_{rz}\Pi_h^W\mathbf{u} = \mathrm{curl}_{rz}\mathbf{u}$. Using Theorem 4.2.1, the estimate (4–9) then follows. □

4.2 Commuting Smoothed Projectors in Weighted Spaces

In this section, we construct the projector used in the proof of Corollary 4.1.1 in the previous section. In order to prove the edge finite element approximation for the reduced Maxwell system, when the original rotational domain is a bounded Lipschitz domain, we need commuting projectors in weighted spaces, that require lower-order regularity than those that are already known [20, 21]. A weighted Clément operator has been constructed [3] for its application to the axisymmetric Stokes problem, but this operator is insufficient for the analysis of the axisymmetric Maxwell equations.

In this section, we construct commuting projectors in weighted spaces that are defined on the weighted L^2-space. We modify the commuting quasi-interpolators by Schöberl [35] that was constructed in standard Sobolev spaces, so that they are appropriate for weighted Sobolev spaces. Additionally, in order to change these operators into projectors, we adapt the method used in [17] which introduces the inverse operator of the restriction of the quasi-interpolator to its projected space.

Note that throughout this section, we let $\mathrm{curl}_{rz}(v_r, v_z) = \partial_r v_z - \partial_z v_r$ which is a multiple of -1 to our original definition of curl_{rz} (see (2–6)). This is to avoid the use of extra negative($-$) symbols in the proofs in this section whenever we apply the integration by parts formula Theorem 2.2.3 in the $2D$-case [24, Theorem 2.11]. Of course, the

results proved here still hold true when we consider curl_{rz} according to our original definition.

4.2.1 Definitions

For smooth functions, classical nodal interpolation operators can be applied, and these operators I_h^g, I_h^c, and I_h^o make the following diagram commute:

$$\begin{array}{ccccc} H^1_{r,\diamond}(D) & \xrightarrow{\mathrm{grad}_{rz}} & \mathbf{H}_{r,\diamond}(\mathrm{curl}, D) & \xrightarrow{\mathrm{curl}_{rz}} & L^2_r(D) \\ \downarrow I_h^g & & \downarrow I_h^c & & \downarrow I_h^o \\ V_{h,\diamond} & \xrightarrow{\mathrm{grad}_{rz}} & \mathbf{W}_{h,\diamond} & \xrightarrow{\mathrm{curl}_{rz}} & S_h \end{array}$$

I_h^g and I_h^c cannot be applied, however, to all functions in $H^1_{r,\diamond}(D)$ and $\mathbf{H}_{r,\diamond}(\mathrm{curl}, D)$ respectively. They can only be applied to functions in these spaces with extra regularity due to the local degrees of freedom used in their constructions:

$$\begin{aligned} (I_h^g\omega)(\mathbf{x}) &= \sum_{\mathfrak{v}\in\mathcal{V}} \omega(\mathfrak{v})\phi_{\mathfrak{v}}(\mathbf{x}), \\ (I_h^c\mathbf{z})(\mathbf{x}) &= \sum_{\mathfrak{e}\in\mathcal{E}} (\int_{\mathfrak{e}} \mathbf{z}\cdot\mathbf{t}ds)\phi_{\mathfrak{e}}(\mathbf{x}), \\ (I_h^o s)(\mathbf{x}) &= \sum_{K\in\mathscr{T}_h} (\frac{1}{|K|}\int_K s d\mathbf{x})\phi_K, \end{aligned}$$

where $\mathscr{T}_h$ is a triangulation of D, $\mathcal{V}$ denotes the set of vertices in $\mathscr{T}_h$ not on Γ_1, $\mathcal{E}$ denotes the set of edges in $\mathscr{T}_h$ not on Γ_1, and $K \in \mathscr{T}_h$ denotes all triangles in $\mathscr{T}_h$.

Our goal is to construct commuting projectors that can be applied to all functions in $L^2_r(D)$ or $L^2_r(D)^2$. Therefore we will define mesh dependent smoothers for functions in $L^2_r(\mathbb{R}^2_+)$ so that we can apply the classical nodal interpolation operators after we apply these smoothers to L^2_r-functions. Before defining these smoothers, we first state a proposition that will be used in their definitions. The proof of Proposition 4.2.1 is given in Appendix B.

Proposition 4.2.1. *Let* $\mathbf{a} = (a_r, a_z)$ *be a point in* $\mathbb{R}^2_+$ *and let* D_{a} *be the domain associated to* $\mathbf{a}$ *as in one of the cases in Figure 4-1.*

In all three cases, for any $k \geq 0$*, there exists a function* $\eta_{\mathrm{a}}(r, z) \in P_k$ *such that*

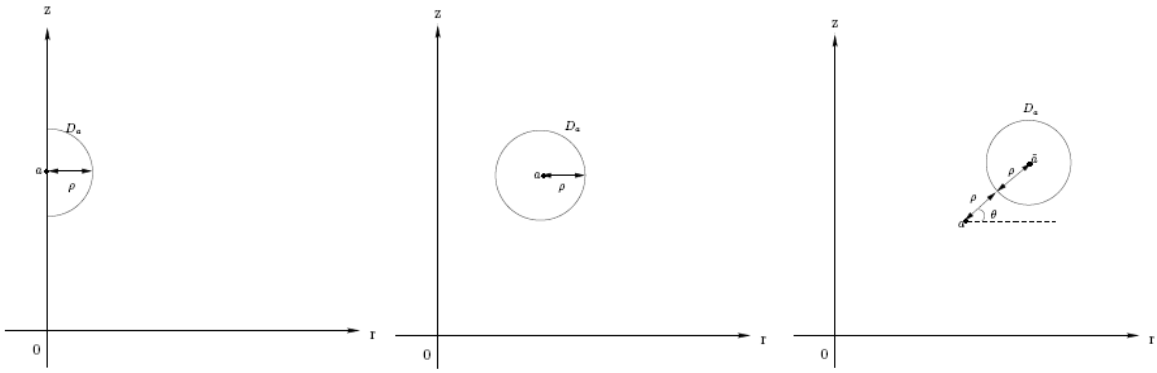

A Case 1 B Case 2 C Case 3

Figure 4-1. Domain D_a corresponding to point a

1. $(\eta_{\mathrm{a}}, p)_{r,D_{\mathrm{a}}} = p(a)$ *for all* $p \in P_k$*, where* P_k *is the spaces of polynomials of order up to* k *on* D_{a}*.*

2. $\|\eta_{\mathrm{a}}\|^2_{L^2_r(D_{\mathrm{a}})} \leq \frac{C}{\rho^2 r_{\mathrm{a}}}$*, where*

$$r_{\mathrm{a}} = \begin{cases} \rho & \text{in case 1.} \\ \min_{\mathrm{y} \in D_{\mathrm{a}}} r(\mathbf{y}) & \text{in case 2 and case 3.} \end{cases}$$

In line with Proposition 4.2.1, for a given triangulation $\mathscr{T}_h$ of D we define an associated domain D^h_{a} for each mesh vertex $\mathbf{a} \in \mathscr{T}_h$. We write $h = \max_{K \in \mathscr{T}_h} h_K$, where h_K is the diameter of K.

1. If $\mathbf{a}$ is on Γ_0 then D^h_{a} is chosen as in Case 1 in Figure 4-1 with $\rho = h\delta$.

2. If $\mathbf{a}$ is in the interior of D then D^h_{a} is chosen as in Case 2 in Figure 4-1 with $\rho = h\delta$.

3. If $\mathbf{a}$ is on Γ_1 then D^h_{a} is chosen as in Case 3 in Figure 4-1 with $\rho = h\delta$, i.e.,

$$D^h_{\mathrm{a}} = \left\{ \mathbf{y} \in \mathbb{R}^2_+ : |\mathbf{y} - \tilde{\mathbf{a}}| < h\delta \right\},$$

where $\tilde{\mathbf{a}} = (\tilde{a}_r, \tilde{a}_z)$ is obtained by

$$\begin{pmatrix} \tilde{a}_r \\ \tilde{a}_z \end{pmatrix} = \begin{pmatrix} a_r \\ a_z \end{pmatrix} + \begin{pmatrix} \cos\theta & -\sin\theta \\ \sin\theta & \cos\theta \end{pmatrix} \begin{pmatrix} 2h\delta \\ 0 \end{pmatrix},$$

for some fixed angle $\theta \geq 0$.

Next, we choose $0 < \delta < 1$ and an angle θ in the following way.

1. For $\mathbf{a}$ not on Γ_1 : There exists $0 < \delta_0 < 1$ such that $D^h_{\mathrm{a}} \subset D^{\mathrm{a}}_k$ for all $\mathbf{a}$, where D^{a}_k denotes the "vertex patch" domain formed by the union of all triangles in $\mathscr{T}_h$ connected to the mesh vertex $\mathbf{a}$, whenever $0 < \delta \leq \delta_0$. Choose $\delta \in (0, \delta_0]$.

2. For $\mathbf{a}$ on Γ_1 : For each $\mathbf{a}$, choose $\theta \geq 0$ so that $D^h_{\mathrm{a}} \subset \mathbb{R}^2_+ \backslash \bar{D}$.

Here, we summarize some notations that will be used in the remainder of the paper. We write $K = [\mathbf{a}_1, \mathbf{a}_2, \mathbf{a}_3]$ to indicate that $K \in \mathscr{T}_h$ is a triangle with vertices $\mathbf{a}_1$, $\mathbf{a}_2$, and $\mathbf{a}_3$. Additionally, $\mathfrak{e}_1 = [\mathbf{a}_2, \mathbf{a}_3]$, $\mathfrak{e}_2 = [\mathbf{a}_3, \mathbf{a}_1]$, and $\mathfrak{e}_3 = [\mathbf{a}_1, \mathbf{a}_2]$ denote the three edges of K with a fixed orientation (counter-clockwise), where $[\mathbf{a}_2, \mathbf{a}_3]$ denotes the edge from $\mathbf{a}_2$ to $\mathbf{a}_3$, etc.

Define $\kappa_i(\mathbf{y}_i) = r(\mathbf{y}_i)\eta_{\mathrm{a}_i}(\mathbf{y}_i)$ for $1 \leq i \leq 3$, where η_{a_i} is the function introduced in Proposition 4.2.1. We write $\kappa_{123} = \kappa_1\kappa_2\kappa_3$ and $\kappa_{12} = \kappa_1\kappa_2$, etc. Define $\tilde{\mathbf{x}}_{\mathrm{y}}$ by the same barycentric coordinates $\lambda_i(\mathbf{x})$, for $1 \leq i \leq 3$, as $\mathbf{x} \in K$ with respect to the triangle $[\mathbf{y}_1, \mathbf{y}_2, \mathbf{y}_3]$, i.e.,

$$\tilde{\mathbf{x}}_{\mathrm{y}}(\mathbf{x}, \mathbf{y}_1, \mathbf{y}_2, \mathbf{y}_3) = \sum_{i=1}^{3} \lambda_i(\mathbf{x})\mathbf{y}_i. \tag{4–10}$$

We now define the following mesh dependent smoothers which are similar to those by Schöberl [35]. Let $u, w \in L^2_r(\mathbb{R}^2_+)$ and $\mathbf{v} \in L^2_r(\mathbb{R}^2_+)^2$. Then

$$\begin{aligned}
S^g u(\mathbf{x}) &= \int_{D^h_{\mathrm{a}_1}} \int_{D^h_{\mathrm{a}_2}} \int_{D^h_{\mathrm{a}_3}} \kappa_{123} u(\tilde{\mathbf{x}}_{\mathrm{y}}) d\mathbf{y}_3 d\mathbf{y}_2 d\mathbf{y}_1, \\
S^c \mathbf{v}(\mathbf{x}) &= \int_{D^h_{\mathrm{a}_1}} \int_{D^h_{\mathrm{a}_2}} \int_{D^h_{\mathrm{a}_3}} \kappa_{123} [\sum_{i=1}^{3} \mathbf{y}_i \cdot \mathbf{v}(\tilde{\mathbf{x}}_{\mathrm{y}}) \mathbf{grad}_{rz} \lambda_i(\mathbf{x})] d\mathbf{y}_3 d\mathbf{y}_2 d\mathbf{y}_1, \\
S^o w(\mathbf{x}) &= \int_{D^h_{\mathrm{a}_1}} \int_{D^h_{\mathrm{a}_2}} \int_{D^h_{\mathrm{a}_3}} \kappa_{123} [(\sum_{m=1}^{3} (\partial_r \lambda_m(\mathbf{x})))\mathbf{y}_m) \times (\sum_{n=1}^{3} (\partial_z \lambda_n(\mathbf{x}))\mathbf{y}_n)] w(\tilde{\mathbf{x}}_{\mathrm{y}}) d\mathbf{y}_3 d\mathbf{y}_2 d\mathbf{y}_1,
\end{aligned} \tag{4–11}$$

where for two dimensional vectors $\mathbf{c} = (c_r, c_z)$ and $\mathbf{d} = (d_r, d_z)$, we write $\mathbf{c} \times \mathbf{d}$ to denote $c_r d_z - c_z d_r$.

In section 4.2.2, we will often need to compute the unisolvent node, edge, and element degrees of freedom for $S^g u$, $S^c \mathbf{v}$, and $S^o w$ respectively, so let us do this computation here.

Let $K \in \mathscr{T}_h$ such that $K = [\mathbf{a}_1, \mathbf{a}_3, \mathbf{a}_3]$. Then

$$\begin{aligned} S^g u(\mathbf{a}_1) &= \int_{D^h_{\mathrm{a}_1}} \int_{D^h_{\mathrm{a}_2}} \int_{D^h_{\mathrm{a}_3}} \kappa_{123} u(\mathbf{y}_1) d\mathbf{y}_3 d\mathbf{y}_2 d\mathbf{y}_1 \quad \text{since } \tilde{\mathbf{x}}_{\mathrm{y}} = \mathbf{y}_1 \text{ if } \mathbf{x} = \mathbf{a}_1, \\ &= \int_{D^h_{\mathrm{a}_1}} \kappa_1 u(\mathbf{y}_1) d\mathbf{y}_1. \end{aligned} \tag{4–12}$$

Similarly,

$$S^g u(\mathbf{a}_i) = \int_{D^h_{\mathrm{a}_i}} \kappa_i u(\mathbf{y}_i) d\mathbf{y}_i \text{ for all } 1 \le i \le 3.$$

Next, for $q(s) = (1-s)\mathbf{a}_2 + s\mathbf{a}_3$, $0 \le s \le 1$, and $\mathfrak{e}_1 = [\mathbf{a}_2, \mathbf{a}_3]$, we have that

$$\begin{aligned} &\int_{\mathfrak{e}_1} S^c \mathbf{v} \cdot \mathbf{t} ds \\ &= \int_0^1 S^c \mathbf{v}(q(s)) q'(s) ds, \\ &= \int_0^1 \int_{D^h_{\mathrm{a}_1}} \int_{D^h_{\mathrm{a}_2}} \int_{D^h_{\mathrm{a}_3}} \kappa_{123} [(\sum_{1 \le i \le 3} \mathbf{y}_i \cdot \mathbf{v}((1-s)\mathbf{y}_2 + s\mathbf{y}_3) \mathbf{grad}_{rz} \lambda_i) \cdot (\mathbf{a}_3 - \mathbf{a}_2)] d\mathbf{y}_3 d\mathbf{y}_2 d\mathbf{y}_1 ds, \\ &= \int_0^1 \int_{D^h_{\mathrm{a}_1}} \int_{D^h_{\mathrm{a}_2}} \int_{D^h_{\mathrm{a}_3}} \kappa_{123} (\mathbf{y}_3 - \mathbf{y}_2) \mathbf{v}((1-s)\mathbf{y}_2 + s\mathbf{y}_3) d\mathbf{y}_3 d\mathbf{y}_2 d\mathbf{y}_1 ds, \\ &= \int_{D^h_{\mathrm{a}_1}} \int_{D^h_{\mathrm{a}_2}} \int_{D^h_{\mathrm{a}_3}} \kappa_{123} \int_{[\mathrm{y}_2, \mathrm{y}_3]} \mathbf{v} \cdot \mathbf{t} ds d\mathbf{y}_3 d\mathbf{y}_2 d\mathbf{y}_1, \\ &= \int_{D^h_{\mathrm{a}_2}} \int_{D^h_{\mathrm{a}_3}} \kappa_{23} \int_{[\mathrm{y}_2, \mathrm{y}_3]} \mathbf{v} \cdot \mathbf{t} ds d\mathbf{y}_3 d\mathbf{y}_2. \end{aligned} \tag{4–13}$$

The third equality holds, since

$$\mathbf{grad}_{rz} \lambda_1 \cdot (\mathbf{a}_3 - \mathbf{a}_2) = 0,$$

$$\mathbf{grad}_{rz} \lambda_2 \cdot (\mathbf{a}_3 - \mathbf{a}_2) = -1,$$

$$\mathbf{grad}_{rz} \lambda_3 \cdot (\mathbf{a}_3 - \mathbf{a}_2) = 1.$$

Similarly,

$$\int_{\mathfrak{e}_2} S^c \mathbf{v} \cdot \mathbf{t} ds = \int_{D^h_{\mathrm{a}_1}} \int_{D^h_{\mathrm{a}_3}} \kappa_{13} \int_{[\mathrm{y}_3, \mathrm{y}_1]} \mathbf{v} \cdot \mathbf{t} ds d\mathbf{y}_3 d\mathbf{y}_1,$$

and

$$\int_{\mathfrak{e}_3} S^c \mathbf{v} \cdot \mathbf{t} ds = \int_{D^h_{\mathrm{a}_1}} \int_{D^h_{\mathrm{a}_2}} \kappa_{12} \int_{[\mathrm{y}_1, \mathrm{y}_2]} \mathbf{v} \cdot \mathbf{t} ds d\mathbf{y}_2 d\mathbf{y}_1.$$

Finally, it is straight forward to show that $\frac{1}{(\sum_{m=1}^{3}(\partial_r\lambda_m(\mathrm{x}))\mathrm{y}_m)\times(\sum_{n=1}^{3}(\partial_z\lambda_n(\mathrm{x}))\mathrm{y}_n)}$ is the Jacobian arising from change of variables from $\mathbf{x}$ to $\tilde{\mathbf{x}}_{\mathrm{y}}$. Therefore,

$$\frac{1}{|K|}\int_K S^o w d\mathbf{x} = \frac{1}{|K|}\int_{D^h_{\mathrm{a}_1}}\int_{D^h_{\mathrm{a}_2}}\int_{D^h_{\mathrm{a}_3}}\kappa_{123}\int_{[\mathrm{y}_1,\mathrm{y}_2,\mathrm{y}_3]} w(\mathbf{z})d\mathbf{z}d\mathbf{y}_3 d\mathbf{y}_2 d\mathbf{y}_1. \tag{4–14}$$

After applying these smoothers to functions in appropriate spaces, we can then apply the classical nodal interpolation operators which requires higher-order regularity. Thus, we may define the following Schöberl quasi-interpolators in weighted spaces.

From here on, let us assume that $u, w \in L^2_r(D)$ and $\mathbf{v} \in L^2_r(D)^2$. The extension of these functions to $L^2_r(\mathbb{R}^2_+)$ and $L^2_r(\mathbb{R}^2_+)^2$ will be denoted as $\tilde{u}$, $\tilde{w}$, and $\tilde{\mathbf{v}}$ respectively.

Define R^g_h, R^c_h, and R^o_h on $H^1_{r,\diamond}(D)$, $\mathbf{H}_{r,\diamond}(\mathrm{curl}, D)$, and $L^2_r(D)$ respectively by

$$R^g_h u = I^g_h S^g \tilde{u},$$

$$R^c_h \mathbf{v} = I^c_h S^c \tilde{\mathbf{v}},$$

$$R^o_h w = I^o_h S^o \tilde{w},$$

where $\tilde{}$ denotes the extension by zero, i.e., $\tilde{u} \in L^2_r(\mathbb{R}^2_+)$ such that $\tilde{u}|_D = u$ and zero elsewhere.

Note that these operators are not projectors as they do not preserve functions that are already in their projected spaces. In section 4.2.2, we will modify these quasi-interpolators into projectors. Before we end this section, we verify that these quasi-interpolators commute.

Lemma 4.2.1. *R^g_h, R^c_h, and R^o_h satisfy the following commuting diagram properties:*

1. $R^c_h(\mathbf{grad}_{rz} u) = \mathbf{grad}_{rz}(R^g_h u)$ *for all* $u \in H^1_{r,\diamond}(D)$.
2. $\mathrm{curl}_{rz}(R^c_h \mathbf{v}) = R^o_h(\mathrm{curl}_{rz}\mathbf{v})$ *for all* $\mathbf{v} \in \mathbf{H}_{r,\diamond}(\mathrm{curl}, D)$.

Proof. 1. Since both the left hand side and the right hand side are functions in $W_{h,\diamond}$, it suffices to show that the unisolvent edge functionals agree on $K = [\mathbf{a}_1, \mathbf{a}_2, \mathbf{a}_3]$, i.e.,

$$\int_{\mathfrak{e}_i}(\mathbf{grad}_{rz} R^g_h u)\cdot \mathbf{t} ds = \int_{\mathfrak{e}_i} R^c_h(\mathbf{grad}_{rz} u)\cdot \mathbf{t} ds,$$

for all $1 \leq i \leq 3$. It suffices to check for $\mathfrak{e}_1 = [\mathbf{a}_2, \mathbf{a}_3]$, as the result will hold for $\mathfrak{e}_2$ and $\mathfrak{e}_3$ in an identical way. This is true, since

$$\begin{aligned}
\int_{\mathfrak{e}_1} (\mathbf{grad}_{rz} R_h^g u) \cdot \mathbf{t} ds &= R_h^g u(\mathbf{a}_3) - R_h^g u(\mathbf{a}_2), \\
&= S^g \tilde{u}(\mathbf{a}_3) - S^g \tilde{u}(\mathbf{a}_2), \\
&= \int_{D_{\mathrm{a}_3}^h} \kappa_3 \tilde{u}(\mathbf{y}_3) d\mathbf{y}_3 - \int_{D_{\mathrm{a}_2}^h} \kappa_2 \tilde{u}(\mathbf{y}_2) d\mathbf{y}_2 \qquad \text{by (4–12)},
\end{aligned}$$

and since

$$\begin{aligned}
\int_{\mathfrak{e}_1} (R_h^c \mathbf{grad}_{rz} u) \cdot \mathbf{t} ds &= \int_{\mathfrak{e}_1} (S^c \mathbf{grad}_{rz} \tilde{u}) \cdot \mathbf{t} ds, \\
&= \int_{D_{\mathrm{a}_2}^h} \int_{D_{\mathrm{a}_3}^h} \kappa_{23} \int_{[\mathrm{y}_2, \mathrm{y}_3]} (\mathbf{grad}_{rz} \tilde{u}) \cdot \mathbf{t} ds d\mathbf{y}_3 d\mathbf{y}_2 \qquad \text{by (4–13)}, \\
&= \int_{D_{\mathrm{a}_2}^h} \int_{D_{\mathrm{a}_3}^h} \kappa_{23} [\tilde{u}(\mathbf{y}_3) - \tilde{u}(\mathbf{y}_2)] d\mathbf{y}_3 d\mathbf{y}_2, \\
&= \int_{D_{\mathrm{a}_3}^h} \kappa_3 \tilde{u}(\mathbf{y}_3) d\mathbf{y}_3 - \int_{D_{\mathrm{a}_2}^h} \kappa_2 \tilde{u}(\mathbf{y}_2) d\mathbf{y}_2,
\end{aligned}$$

for all smooth functions $u \in H^1_{r,\diamond}(D)$. The result follows from the density of smooth functions in $H^1_{r,\diamond}(D)$.

2. Now, since both quantities are in S_h, it is enough to check that

$$\frac{1}{|K|} \int_K \mathrm{curl}_{rz}(R_h^c \mathbf{v}) d\mathbf{x} = \frac{1}{|K|} \int_K R_h^o (\mathrm{curl}_{rz} \mathbf{v}) d\mathbf{x}.$$

By using integration by parts,

$$\begin{aligned}
\frac{1}{|K|} \int_K \mathrm{curl}_{rz}(R_h^c \mathbf{v}) d\mathbf{x} &= \frac{1}{|K|} \sum_{i=1}^{3} \int_{\mathfrak{e}_i} R_h^c \mathbf{v} \cdot \mathbf{t} ds, \\
&= \frac{1}{|K|} \sum_{i=1}^{3} \int_{\mathfrak{e}_i} S^c \tilde{\mathbf{v}} \cdot \mathbf{t} ds, \\
&= \frac{1}{|K|} \int_{D_{\mathrm{a}_1}^h} \int_{D_{\mathrm{a}_2}^h} \int_{D_{\mathrm{a}_3}^h} \kappa_{123} \int_{[\mathrm{y}_1, \mathrm{y}_2] + [\mathrm{y}_2, \mathrm{y}_3] + [\mathrm{y}_3, \mathrm{y}_1]} \tilde{\mathbf{v}} \cdot \mathbf{t} ds d\mathbf{y}_3 d\mathbf{y}_2 d\mathbf{y}_1 \qquad \text{by (4–13)}.
\end{aligned}$$

Additionally,

$$\begin{aligned}\frac{1}{|K|}\int_K R_h^o(\mathrm{curl}_{rz}\mathbf{v})d\mathbf{x} &= \frac{1}{|K|}\int_K S^o(\mathrm{curl}_{rz}\tilde{\mathbf{v}})d\mathbf{x},\\ &= \frac{1}{|K|}\int_{D^h_{\mathrm{a}_1}}\int_{D^h_{\mathrm{a}_2}}\int_{D^h_{\mathrm{a}_3}}\kappa_{123}\int_{[\mathrm{y}_1,\mathrm{y}_2,\mathrm{y}_3]}(\mathrm{curl}_{rz}\tilde{\mathbf{v}})(\mathbf{z})d\mathbf{z}d\mathbf{y}_3d\mathbf{y}_2d\mathbf{y}_1 \qquad \text{by (4–14)},\\ &= \frac{1}{|K|}\int_{D^h_{\mathrm{a}_1}}\int_{D^h_{\mathrm{a}_2}}\int_{D^h_{\mathrm{a}_3}}\kappa_{123}\int_{[\mathrm{y}_1,\mathrm{y}_2]+[\mathrm{y}_2,\mathrm{y}_3]+[\mathrm{y}_3,\mathrm{y}_1]}\tilde{\mathbf{v}}\cdot\mathbf{t}dsd\mathbf{y}_3d\mathbf{y}_2d\mathbf{y}_1,\end{aligned}$$

for all smooth functions $\mathbf{v}\in\mathbf{H}_{r,\diamond}(\mathrm{curl},D)$. The proof is then complete by the density of smooth functions in $\mathbf{H}_{r,\diamond}(\mathrm{curl},D)$.

□

4.2.2 Construction

In this section, we will show that the quasi-interpolators R_h^g, R_h^c, and R_h^o are uniformly bounded in the L_r^2-norm, and that these operators are invertible when restricted to their projected spaces. By using these results, we will then modify these operators into projectors and verify their error estimates.

The proofs of Lemma 4.2.2, 4.2.3, and 4.2.4 follow the lines of [35]. We must, however, pay close attention to the weight function r, since we are modifying these proofs to weighted spaces.

Lemma 4.2.2. *There exists a constant C independent of h and δ such that*

1. $\|R_h^g u\|^2_{L_r^2(D)} \le \frac{C}{\delta^3}\|u\|^2_{L_r^2(D)}$, *for all* $u\in L_r^2(D)$.
2. $\|R_h^g u_h - u_h\|_{L_r^2(D)} \le C\delta\|u_h\|_{L_r^2(D)}$, *for all* $u_h\in V_{h,\diamond}$.

Proof. Let $K=[\mathbf{a}_1,\mathbf{a}_2,\mathbf{a}_3]$ be a fixed triangle in $\mathscr{T}_h$, and let D_K denote the union of $D^h_{\mathrm{a}_1}$, $D^h_{\mathrm{a}_2}$, and $D^h_{\mathrm{a}_3}$. Then, due to the shape regularity property of $\mathscr{T}_h$ and the fact that $\tilde{u}$ and $\tilde{u}_h$ are extensions of u and u_h by zero respectively, to complete the proof it suffices to prove local estimates:

$$\|R_h^g u\|^2_{L_r^2(K)} \le \frac{C}{\delta^3}\|\tilde{u}\|^2_{L_r^2(D_K)},$$

$$\|R_h^g u_h - u_h\|_{L_r^2(K)} \le C\delta\|\tilde{u}_h\|_{L_r^2(D_K)}.$$

We have that

$$R_h^g u|_K = \sum_{i=1}^{3} S^g \tilde{u}(\mathbf{a}_i)\lambda_i \tag{4–15}$$

and that for each $1 \leq i \leq 3$,

$$\begin{aligned}
|S^g \tilde{u}(\mathbf{a}_i)| &= |\int_{D_{\mathrm{a}_i}^h} \kappa_i \tilde{u}(\mathbf{y}_i) d\mathbf{y}_i| && \text{by (4–12)},\\
&= |(\eta_{\mathrm{a}_i}, \tilde{u})_{r, D_{\mathrm{a}_i}^h}| && \text{by definition of } \kappa_i,\\
&\leq \|\eta_{\mathrm{a}_i}\|_{L_r^2(D_{\mathrm{a}_i}^h)} \|\tilde{u}\|_{L_r^2(D_{\mathrm{a}_i}^h)}, && (4–16)\\
&\leq \frac{C}{\sqrt{(h\delta)^2 r_{\mathrm{a}_i}}} \|\tilde{u}\|_{L_r^2(D_{\mathrm{a}_i}^h)} && \text{by Proposition 4.2.1 item 2},\\
&\leq \frac{C}{\sqrt{(h\delta)^3}} \|\tilde{u}\|_{L_r^2(D_{\mathrm{a}_i}^h)}.
\end{aligned}$$

The last inequality holds, since $r_{\mathrm{a}_i} \geq h\delta$ for each $1 \leq i \leq 3$, by definition of r_{a_i} and by the criterion of choosing δ. Therefore, it follows that

$$\begin{aligned}
\|R_h^g u\|_{L_r^2(K)}^2 &= \int_K |\sum_{i=1}^{3} S^g \tilde{u}(\mathbf{a}_i)\lambda_i(\mathbf{x})|^2 r(\mathbf{x}) d\mathbf{x} && \text{by (4–15)},\\
&\leq C \sum_{i=1}^{3} |S^g \tilde{u}(\mathbf{a}_i)|^2 \int_K |\lambda_i(\mathbf{x})|^2 r(\mathbf{x}) d\mathbf{x},\\
&\leq C \sum_{i=1}^{3} \frac{C}{(h\delta)^3} \|\tilde{u}\|_{L_r^2(D_{\mathrm{a}_i}^h)}^2 Ch^2 \max_{\mathrm{x}\in K} r(\mathbf{x}) && \text{by (4–16)},\\
&\leq \frac{C}{\delta^3} \|\tilde{u}\|_{L_r^2(D_K)}^2.
\end{aligned}$$

The last inequality holds, since $\max_{\mathrm{x}\in K} r(\mathbf{x}) \leq Ch$. From now on, we will write r_K to denote $\max_{\mathrm{x}\in K} r(\mathbf{x})$ for simplicity of the notation. Therefore, this completes the proof of item 1.

For item 2, we note that for all $1 \le i \le 3$,

$$
\begin{aligned}
((S^g\tilde{u}_h)(\mathbf{a}_i) - u_h(\mathbf{a}_i))|_K &= \int_{D^h_{\mathrm{a}_i}} \kappa_i(\tilde{u}_h(\mathbf{y}_i) - u_h(\mathbf{a}_i))d\mathbf{y}_i, \\
&\le \max_{\mathrm{y}_i \in D^h_{\mathrm{a}_i}} |\mathbf{grad}_{rz}\tilde{u}_h(\mathbf{y}_i)| \max_{\mathrm{y}_i \in D^h_{\mathrm{a}_i}} |\mathbf{a}_i - \mathbf{y}_i|, \qquad (4\text{–}17) \\
&\le Ch\delta \left\|\mathbf{grad}_{rz}\tilde{u}_h\right\|_{L^\infty(D^h_{\mathrm{a}_i})}.
\end{aligned}
$$

Hence,

$$
\begin{aligned}
\|R^g_h u_h - u_h\|^2_{L^2_r(K)} &= \int_K |\sum_{i=1}^{3}((S^g\tilde{u}_h)(\mathbf{a}_i) - u_h(\mathbf{a}_i))\lambda_i(\mathbf{x})|^2 r(\mathbf{x})d\mathbf{x}, \\
&\le C\sum_{i=1}^{3}|(S^g\tilde{u}_h)(\mathbf{a}_i) - u_h(\mathbf{a}_i)|^2 \int_K |\lambda_i(\mathbf{x})|^2 r(\mathbf{x})d\mathbf{x}, \\
&\le C\sum_{i=1}^{3}(h\delta)^2 \left\|\mathbf{grad}_{rz}\tilde{u}_h\right\|^2_{L^\infty(D^h_{\mathrm{a}_i})} h^2 r_K && \text{by (4–17)}, \\
&\le C(h\delta)^2 \left\|\mathbf{grad}_{rz}\tilde{u}_h\right\|^2_{L^2_r(D_K)}, \\
&\le C\delta^2 \left\|\tilde{u}_h\right\|^2_{L^2_r(D_K)} && \text{by the inverse inequality.}
\end{aligned}
$$

This completes the proof. □

Lemma 4.2.3. *There exists a constant C independent of h and δ such that*

1. $\|R^c_h\mathbf{v}\|^2_{L^2_r(D)} \le \frac{C}{\delta^3}\|\mathbf{v}\|^2_{L^2_r(D)}$ *for all* $\mathbf{v} \in L^2_r(D)^2$.
2. $\|R^c_h\mathbf{v}_h - \mathbf{v}_h\|_{L^2_r(D)} \le C\delta\|\mathbf{v}_h\|_{L^2_r(D)}$ *for all* $\mathbf{v}_h \in W_{h,\diamond}$.

Proof. Fix $K \in \mathscr{T}_h$ such that $K = [\mathbf{a}_1, \mathbf{a}_2, \mathbf{a}_3]$, and let C_K denote the convex hull of $D^h_{\mathrm{a}_1}$, $D^h_{\mathrm{a}_2}$, and $D^h_{\mathrm{a}_3}$. As in the proof of Lemma 4.2.2, it suffices to prove the local estimates:

$$
\|R^c_h\mathbf{v}\|^2_{L^2_r(K)} \le \frac{C}{\delta^3}\|\tilde{\mathbf{v}}\|^2_{L^2_r(C_K)}
$$

and

$$
\|R^c_h\mathbf{v}_h - \mathbf{v}_h\|_{L^2_r(K)} \le C\delta\|\tilde{\mathbf{v}}_h\|_{L^2_r(C_K)}.
$$

We have that

$$R_h^c\mathbf{v}|_K = \sum_{i=1}^{3}(\int_{\mathfrak{e}_i} S^c\tilde{\mathbf{v}}\cdot\mathbf{t}ds)\phi_{\mathfrak{e}_i},$$

and that $\|\phi_{\mathfrak{e}_i}\|^2_{L^2_r(K)} \le Cr_K$ for all $1 \le i \le 3$, since $\phi_{\mathfrak{e}_i} = \pm(\lambda_j\mathbf{grad}_{rz}\lambda_k - \lambda_k\mathbf{grad}_{rz}\lambda_j)$, where $\mathbf{a}_j$ and $\mathbf{a}_k$ are the two vertices of the edge $\mathfrak{e}_i$. Therefore,

$$\begin{aligned}
\|R_h^c\mathbf{v}\|^2_{L^2_r(K)} &= \int_K |\sum_{i=1}^{3}(\int_{\mathfrak{e}_i} S^c\tilde{\mathbf{v}}\cdot\mathbf{t}ds)\phi_{\mathfrak{e}_i}(\mathbf{x})|^2 r(\mathbf{x})d\mathbf{x},\\
&\le C\sum_{i=1}^{3}|\int_{\mathfrak{e}_i} S^c\tilde{\mathbf{v}}\cdot\mathbf{t}ds|^2\int_K|\phi_{\mathfrak{e}_i}(\mathbf{x})|^2 r(\mathbf{x})d\mathbf{x},\\
&\le Cr_K\sum_{i=1}^{3}|\int_{\mathfrak{e}_i} S^c\tilde{\mathbf{v}}\cdot\mathbf{t}ds|^2.
\end{aligned} \tag{4–18}$$

We will first bound the summand involving $\mathfrak{e}_1 = [\mathbf{a}_2, \mathbf{a}_3]$ since the others will follow by the same way.

$$\begin{aligned}
|\int_{\mathfrak{e}_1} S^c\tilde{\mathbf{v}}\cdot\mathbf{t}ds| &= |\int_{D^h_{\mathrm{a}_2}}\int_{D^h_{\mathrm{a}_3}}\kappa_{23}\int_0^1\tilde{\mathbf{v}}((1-s)\mathbf{y}_2+s\mathbf{y}_3)\cdot(\mathbf{y}_3-\mathbf{y}_2)dsd\mathbf{y}_3d\mathbf{y}_2| \quad \text{by (4–13)},\\
&\le Ch|\int_{D^h_{\mathrm{a}_2}}\int_{D^h_{\mathrm{a}_3}}\kappa_{23}\int_0^1\tilde{\mathbf{v}}((1-s)\mathbf{y}_2+s\mathbf{y}_3)dsd\mathbf{y}_3d\mathbf{y}_2|.
\end{aligned} \tag{4–19}$$

Next, we analyze the above integral with respect to s in two separate pieces, i.e., where $0 \le s \le \frac{1}{2}$ and $\frac{1}{2} < s \le 1$. First of all,

$$\begin{aligned}
&|\int_{D^h_{\mathrm{a}_3}}\kappa_3\int_0^{\frac{1}{2}}\int_{D^h_{\mathrm{a}_2}}\kappa_2\tilde{\mathbf{v}}((1-s)\mathbf{y}_2+s\mathbf{y}_3)d\mathbf{y}_2dsd\mathbf{y}_3|,\\
&= |\int_{D^h_{\mathrm{a}_3}}\kappa_3\int_0^{\frac{1}{2}}(\eta_{\mathrm{a}_2},\tilde{\mathbf{v}}((1-s)\mathbf{y}_2+s\mathbf{y}_3))_{r,D^h_{\mathrm{a}_2}}dsd\mathbf{y}_3|,\\
&\le |\int_{D^h_{\mathrm{a}_3}}\kappa_3\int_0^{\frac{1}{2}}\|\eta_{\mathrm{a}_2}\|_{L^2_r(D^h_{\mathrm{a}_2})}\|\tilde{\mathbf{v}}((1-s)\mathbf{y}_2+s\mathbf{y}_3))\|_{L^2_r(D^h_{\mathrm{a}_2})}dsd\mathbf{y}_3|,\\
&\le \frac{C}{\sqrt{(h\delta)^3}}|\int_{D^h_{\mathrm{a}_3}}\kappa_3\int_0^{\frac{1}{2}}(\int_{D^h_{\mathrm{a}_2}}|\tilde{\mathbf{v}}((1-s)\mathbf{y}_2+s\mathbf{y}_3))|^2 r(\mathbf{y}_2)d\mathbf{y}_2)^{\frac{1}{2}}dsd\mathbf{y}_3| \text{ by Proposition 4.2.1},\\
&\le \frac{C}{\sqrt{(h\delta)^3}}|\int_{D^h_{\mathrm{a}_3}}\kappa_3\int_0^{\frac{1}{2}}(\int_{D^h_{\mathrm{a}_2}}|\tilde{\mathbf{v}}((1-s)\mathbf{y}_2+s\mathbf{y}_3))|^2 r((1-s)\mathbf{y}_2+s\mathbf{y}_3))d\mathbf{y}_2)^{\frac{1}{2}}dsd\mathbf{y}_3|.
\end{aligned} \tag{4–20}$$

The last inequality holds, since when $0 \le s \le \frac{1}{2}$,

$$r(\mathbf{y}_2) \le 2(1-s)r(\mathbf{y}_2) \le 2((1-s)r(\mathbf{y}_2) + sr(\mathbf{y}_3)).$$

By change of variables from $\mathbf{y}_2$ to $\mathbf{z} = (1-s)\mathbf{y}_2 + s\mathbf{y}_3$, we have

$$\int_{D^h_{\mathrm{a}_2}} |\tilde{\mathbf{v}}((1-s)\mathbf{y}_2 + s\mathbf{y}_3))|^2 r((1-s)\mathbf{y}_2 + s\mathbf{y}_3))d\mathbf{y}_2 = \int_{\widetilde{D^h_{\mathrm{a}_2}}} |\tilde{\mathbf{v}}(\mathbf{z})|^2 r(\mathbf{z}) \frac{1}{(1-s)^2} d\mathbf{z},$$

where $\widetilde{D^h_{\mathrm{a}_2}} \subset C_K$. Therefore, by continuing from (4–20),

$$\begin{aligned}
&|\int_{D^h_{\mathrm{a}_3}} \kappa_3 \int_0^{\frac{1}{2}} \int_{D^h_{\mathrm{a}_2}} \kappa_2 \tilde{\mathbf{v}}((1-s)\mathbf{y}_2 + s\mathbf{y}_3) d\mathbf{y}_2 ds d\mathbf{y}_3| \\
&\le \frac{C}{\sqrt{(h\delta)^3}} |\int_{D^h_{\mathrm{a}_3}} \kappa_3 \int_0^{\frac{1}{2}} (\int_{C_K} |\tilde{\mathbf{v}}(\mathbf{z})|^2 r(\mathbf{z}) \frac{1}{(1-s)^2} d\mathbf{z})^{\frac{1}{2}} ds d\mathbf{y}_3|, \\
&\le \frac{C}{\sqrt{(h\delta)^3}} |\int_{D^h_{\mathrm{a}_3}} \kappa_3 (\int_{C_K} |\tilde{\mathbf{v}}(\mathbf{z})|^2 r(\mathbf{z}) d\mathbf{z})^{\frac{1}{2}} d\mathbf{y}_3| \qquad \text{since } \frac{1}{(1-s)^2} \le 4, \\
&= \frac{C}{\sqrt{(h\delta)^3}} |\int_{D^h_{\mathrm{a}_3}} \kappa_3 \|\tilde{\mathbf{v}}\|_{L^2_r(C_K)} d\mathbf{y}_3|, \\
&\le \frac{C}{\sqrt{(h\delta)^3}} \|\tilde{\mathbf{v}}\|_{L^2_r(C_K)} |\int_{D^h_{\mathrm{a}_3}} \kappa_3 d\mathbf{y}_3|, \\
&= \frac{C}{\sqrt{(h\delta)^3}} \|\tilde{\mathbf{v}}\|_{L^2_r(C_K)}.
\end{aligned}$$

Similarly, we get such a bound for $|\int_{D^h_{\mathrm{a}_3}} \kappa_3 \int_{\frac{1}{2}}^1 \int_{D^h_{\mathrm{a}_2}} \kappa_2 \tilde{\mathbf{v}}((1-s)\mathbf{y}_2 + s\mathbf{y}_3) d\mathbf{y}_2 ds d\mathbf{y}_3|$ as well, so we have that

$$|\int_{D^h_{\mathrm{a}_2}} \int_{D^h_{\mathrm{a}_3}} \kappa_{23} \int_0^1 \tilde{\mathbf{v}}((1-s)\mathbf{y}_2 + s\mathbf{y}_3) ds d\mathbf{y}_3 d\mathbf{y}_2| \le \frac{C}{\sqrt{(h\delta)^3}} \|\tilde{\mathbf{v}}\|_{L^2_r(C_K)}. \tag{4–21}$$

Therefore, by (4–19),

$$|\int_{\mathfrak{e}_1} S^c \tilde{\mathbf{v}} \cdot \mathbf{t} ds|^2 \le \frac{C}{h\delta^3} \|\tilde{\mathbf{v}}\|^2_{L^2_r(C_K)}.$$

Clearly, by similar arguments, such estimate holds for $|\int_{\mathfrak{e}_2} S^c\tilde{\mathbf{v}}\cdot\mathbf{t}ds|^2$ and $|\int_{\mathfrak{e}_3} S^c\mathbf{v}\cdot\mathbf{t}ds|^2$ as well. Therefore, by (4–18),

$$\begin{aligned}\|R_h^c\mathbf{v}\|^2_{L^2_r(K)} &\leq \frac{Cr_K}{h\delta^3}\|\tilde{\mathbf{v}}\|^2_{L^2_r(C_K)},\\ &\leq \frac{C}{\delta^3}\|\tilde{\mathbf{v}}\|^2_{L^2_r(C_K)}.\end{aligned}$$

To prove item 2, we again use (4–13). We find a bound for $|\int_{\mathfrak{e}_1}(S^c\tilde{\mathbf{v}}_h-\mathbf{v}_h)\cdot\mathbf{t}ds|$ as in the proof of item 1.

$$|\int_{\mathfrak{e}_1}(S^c\tilde{\mathbf{v}}_h-\mathbf{v}_h)\cdot\mathbf{t}ds| = \int_{D^h_{\mathrm{a}_2}}\int_{D^h_{\mathrm{a}_3}}\kappa_{23}(\int_{[\mathrm{y}_2,\mathrm{y}_3]}\tilde{\mathbf{v}}_h\cdot\mathbf{t}ds-\int_{[\mathrm{a}_2,\mathrm{a}_3]}\mathbf{v}_h\cdot\mathbf{t}ds)d\mathbf{y}_3d\mathbf{y}_2. \tag{4–22}$$

Denote L for the area enclosed by the line segments $[\mathbf{a}_2,\mathbf{a}_3]$, $[\mathbf{a}_3,\mathbf{y}_3]$, $[\mathbf{y}_3,\mathbf{y}_2]$ and $[\mathbf{y}_2,\mathbf{a}_2]$. Then, by integration by parts, we have that

$$\int_L \mathrm{curl}_{rz}\tilde{\mathbf{v}}_h d\mathbf{x} = \int_{[\mathrm{a}_2,\mathrm{a}_3]+[\mathrm{a}_3,\mathrm{y}_3]+[\mathrm{y}_3,\mathrm{y}_2]+[\mathrm{y}_2,\mathrm{a}_2]}\tilde{\mathbf{v}}_h\cdot\mathbf{t}ds.$$

Therefore, from (4–22), we have that

$$\begin{aligned}&|\int_{\mathfrak{e}_1}(S^c\tilde{\mathbf{v}}_h-\mathbf{v}_h)\cdot\mathbf{t}ds|\\ &\leq \int_{D^h_{\mathrm{a}_2}}\int_{D^h_{\mathrm{a}_3}}\kappa_{23}(|\int_L \mathrm{curl}_{rz}\tilde{\mathbf{v}}_h d\mathbf{x}|+|\int_{[\mathrm{a}_2,\mathrm{y}_2]}\tilde{\mathbf{v}}_h\cdot\mathbf{t}ds|+|\int_{[\mathrm{a}_3,\mathrm{y}_3]}\tilde{\mathbf{v}}_h\cdot\mathbf{t}ds|)d\mathbf{y}_3d\mathbf{y}_2,\\ &\leq \int_{D^h_{\mathrm{a}_2}}\int_{D^h_{\mathrm{a}_3}}\kappa_{23}(\|\mathrm{curl}_{rz}\tilde{\mathbf{v}}_h\|_{L^\infty(L)}Ch(h\delta)+\|\tilde{\mathbf{v}}_h\|_{L^\infty([\mathrm{a}_2,\mathrm{y}_2]\cup[\mathrm{a}_3,\mathrm{y}_3])}h\delta)d\mathbf{y}_3d\mathbf{y}_2,\\ &\leq \int_{D^h_{\mathrm{a}_2}}\int_{D^h_{\mathrm{a}_3}}\kappa_{23}Ch\delta(\|\tilde{\mathbf{v}}_h\|_{L^\infty(L)}+\|\tilde{\mathbf{v}}_h\|_{L^\infty([\mathrm{a}_2,\mathrm{y}_2]\cup[\mathrm{a}_3,\mathrm{y}_3])})d\mathbf{y}_3d\mathbf{y}_2 \text{ by the inverse inequality,}\\ &\leq Ch\delta\|\tilde{\mathbf{v}}_h\|_{L^\infty(C_K)}.\end{aligned} \tag{4–23}$$

The last inequality holds, since $L\subset C_K$ and $[\mathbf{a}_2,\mathbf{y}_2]\cup[\mathbf{a}_3,\mathbf{y}_3]\subset C_K$. Obviously, such result holds for $|\int_{\mathfrak{e}_2}(S^c\tilde{\mathbf{v}}_h-\mathbf{v}_h)\cdot\mathbf{t}ds|$ and $|\int_{\mathfrak{e}_3}(S^c\tilde{\mathbf{v}}_h-\mathbf{v}_h)\cdot\mathbf{t}ds|$ as well by similar arguments. Thus,

$$\sum_{i=1}^3|\int_{\mathfrak{e}_i}(S^c\tilde{\mathbf{v}}_h-\mathbf{v}_h)\cdot\mathbf{t}ds|^2\leq Ch^2\delta^2\|\tilde{\mathbf{v}}_h\|^2_{L^\infty(C_K)}.$$

Hence, by similar arguments as in (4–18), we reach,

$$\begin{aligned}\|R_h^c \mathbf{v}_h - \mathbf{v}_h\|^2_{L^2_r(K)} &\leq C r_K h^2 \delta^2 \|\tilde{\mathbf{v}}_h\|^2_{L^\infty(C_K)}, \\ &\leq C\delta^2 \|\tilde{\mathbf{v}}_h\|^2_{L^2_r(C_K)}.\end{aligned}$$

□

Lemma 4.2.4. *There exists a constant C independent of h and δ such that*

1. $\|R_h^o w\|^2_{L^2_r(D)} \leq \frac{C}{\delta} \|w\|^2_{L^2_r(D)}$ *for all* $w \in L^2_r(D)$.
2. $\|R_h^o w_h - w_h\|_{L^2_r(D)} \leq C\delta \|w_h\|_{L^2_r(D)}$ *for all* $w_h \in S_h$.

Proof. Fix $K = [\mathbf{a}_1, \mathbf{a}_2, \mathbf{a}_3] \in \mathscr{T}_h$, and let C_K denote the convex hull of $D^h_{\mathrm{a}_1}$, $D^h_{\mathrm{a}_2}$, and $D^h_{\mathrm{a}_3}$. As in the proofs of Lemmas 4.2.2 and 4.2.3, it is enough to show that

$$\|R_h^o w\|^2_{L^2_r(K)} \leq \frac{C}{\delta} \|\tilde{w}\|^2_{L^2_r(C_K)}$$

and

$$\|R_h^o w_h - w_h\|_{L^2_r(K)} \leq C\delta \|\tilde{w}_h\|_{L^2_r(C_K)}.$$

We will write $J = (\sum_{m=1}^3 (\partial_r \lambda_m)\mathbf{y}_m) \times (\sum_{n=1}^3 (\partial_z \lambda_n)\mathbf{y}_n)$ in the definition of S^o. Then,

$$\begin{aligned}|R_h^o w|_K| &\leq \frac{1}{|K|} \int_K |\int_{D^h_{\mathrm{a}_1}} \int_{D^h_{\mathrm{a}_2}} \int_{D^h_{\mathrm{a}_3}} \kappa_{123} w(\tilde{\mathbf{x}}_{\mathrm{y}}) J d\mathbf{y}_3 d\mathbf{y}_2 d\mathbf{y}_1| d\mathbf{x}, \\ &\leq \frac{1}{|K|} \sum_{i=1}^3 \int_{T_i} |\int_{D^h_{\mathrm{a}_1}} \int_{D^h_{\mathrm{a}_2}} \int_{D^h_{\mathrm{a}_3}} \kappa_{123} w(\tilde{\mathbf{x}}_{\mathrm{y}}) J d\mathbf{y}_3 d\mathbf{y}_2 d\mathbf{y}_1| d\mathbf{x},\end{aligned} \tag{4–24}$$

where $T_i = \left\{\mathbf{x} \in K : \lambda_i(\mathbf{x}) > \frac{1}{3}\right\}$, for $1 \le i \le 3$. We first bound the summand involving T_1. The other summands are also bounded in an identical way.

$$
\begin{aligned}
&\int_{T_1} \Big| \int_{D^h_{\mathrm{a}_1}} \int_{D^h_{\mathrm{a}_2}} \int_{D^h_{\mathrm{a}_3}} \kappa_{123} \tilde{w}(\tilde{\mathbf{x}}_{\mathrm{y}}) J d\mathbf{y}_3 d\mathbf{y}_2 d\mathbf{y}_1 \Big| d\mathbf{x} \\
&\le \int_{T_1} \int_{D^h_{\mathrm{a}_2}} \int_{D^h_{\mathrm{a}_3}} \kappa_{23} \big| (\eta_{\mathrm{a}_1}, \tilde{w}(\tilde{\mathbf{x}}_{\mathrm{y}}) J)_{r, D^h_{\mathrm{a}_1}} \big| d\mathbf{y}_3 d\mathbf{y}_2 d\mathbf{x}, \\
&\le \int_{T_1} \int_{D^h_{\mathrm{a}_2}} \int_{D^h_{\mathrm{a}_3}} \kappa_{23} \left\| \eta_{\mathrm{a}_1} \right\|_{L^2_r(D^h_{\mathrm{a}_1})} \left\| \tilde{w}(\tilde{\mathbf{x}}_{\mathrm{y}}) J \right\|_{L^2_r(D^h_{\mathrm{a}_1})} d\mathbf{y}_3 d\mathbf{y}_2 d\mathbf{x}, \\
&\le \int_{T_1} \int_{D^h_{\mathrm{a}_2}} \int_{D^h_{\mathrm{a}_3}} \kappa_{23} \frac{C}{\sqrt{(h\delta)^3}} \Big(\int_{D^h_{\mathrm{a}_1}} r(\mathbf{y}_1) |\tilde{w}(\tilde{\mathbf{x}}_{\mathrm{y}})|^2 |J|^2 d\mathbf{y}_1 \Big)^{\frac{1}{2}} d\mathbf{y}_3 d\mathbf{y}_2 d\mathbf{x} \qquad \text{by Proposition 4.2.1,} \\
&\le \frac{C}{\sqrt{(h\delta)^3}} \int_{D^h_{\mathrm{a}_2}} \int_{D^h_{\mathrm{a}_3}} \kappa_{23} |T_1|^{\frac{1}{2}} \Big(\int_{T_1} \int_{D^h_{\mathrm{a}_1}} r(\tilde{\mathbf{x}}_{\mathrm{y}}) |\tilde{w}(\tilde{\mathbf{x}}_{\mathrm{y}})|^2 |J|^2 d\mathbf{y}_1 d\mathbf{x} \Big)^{\frac{1}{2}} d\mathbf{y}_3 d\mathbf{y}_2.
\end{aligned}
\tag{4–25}
$$

$r(\mathbf{y}_1) \le C r(\tilde{\mathbf{x}}_{\mathrm{y}})$ in the last inequality, since $\mathbf{x} \in T_1$ and by definition of T_1:

$$
r(\mathbf{y}_1) = \frac{1}{\lambda_1(\mathbf{x})} \lambda_1(\mathbf{x}) r(\mathbf{y}_1) \le 3 r(\lambda_1(\mathbf{x})\mathbf{y}_1) \le 3\big(r(\lambda_1(\mathbf{x})\mathbf{y}_1) + r(\lambda_1(\mathbf{x})\mathbf{y}_2) + r(\lambda_1(\mathbf{x})\mathbf{y}_3)\big) = 3 r(\tilde{\mathbf{x}}_{\mathrm{y}}).
$$

Now, $|T_1|^{\frac{1}{2}} \le Ch$, and $J \le C$, since $J = \frac{|\tilde{K}|}{|K|}$, where $\tilde{K} = [\mathbf{y}_1, \mathbf{y}_2, \mathbf{y}_3]$. Therefore, by (4–25),

$$
\begin{aligned}
&\int_{T_1} \Big| \int_{D^h_{\mathrm{a}_1}} \int_{D^h_{\mathrm{a}_2}} \int_{D^h_{\mathrm{a}_3}} \kappa_{123} \tilde{w}(\tilde{\mathbf{x}}_{\mathrm{y}}) J d\mathbf{y}_3 d\mathbf{y}_2 d\mathbf{y}_1 \Big| d\mathbf{x} \\
&\le \frac{Ch}{\sqrt{(h\delta)^3}} \int_{D^h_{\mathrm{a}_2}} \int_{D^h_{\mathrm{a}_3}} \kappa_{23} \Big(\int_{T_1} \int_{D^h_{\mathrm{a}_1}} r(\tilde{\mathbf{x}}_{\mathrm{y}}) |\tilde{w}(\tilde{\mathbf{x}}_{\mathrm{y}})|^2 |J| d\mathbf{y}_1 d\mathbf{x} \Big)^{\frac{1}{2}} d\mathbf{y}_3 d\mathbf{y}_2, \\
&= \frac{Ch}{\sqrt{(h\delta)^3}} \int_{D^h_{\mathrm{a}_2}} \int_{D^h_{\mathrm{a}_3}} \kappa_{23} \Big(\int_{D^h_{\mathrm{a}_1}} \int_{T_1} r(\tilde{\mathbf{x}}_{\mathrm{y}}) |\tilde{w}(\tilde{\mathbf{x}}_{\mathrm{y}})|^2 |J| d\mathbf{x} d\mathbf{y}_1 \Big)^{\frac{1}{2}} d\mathbf{y}_3 d\mathbf{y}_2, \\
&= \frac{Ch}{\sqrt{(h\delta)^3}} \int_{D^h_{\mathrm{a}_2}} \int_{D^h_{\mathrm{a}_3}} \kappa_{23} \Big(\int_{D^h_{\mathrm{a}_1}} \int_{\tilde{T}_1} r(\mathbf{z}) |\tilde{w}(\mathbf{z})|^2 d\mathbf{z} d\mathbf{y}_1 \Big)^{\frac{1}{2}} d\mathbf{y}_3 d\mathbf{y}_2 \qquad \text{by change of variables,} \\
&\le \frac{Ch}{\sqrt{(h\delta)^3}} |D^h_{\mathrm{a}_1}|^{\frac{1}{2}} \left\| \tilde{w} \right\|_{L^2_r(\tilde{T}_1)}, \\
&\le \frac{Ch}{\sqrt{h\delta}} \left\| \tilde{w} \right\|_{L^2_r(C_K)}.
\end{aligned}
\tag{4–26}
$$

Therefore, by (4–24), we have that

$$
\begin{aligned}
|R_h^o w|_K|^2 &\leq \frac{1}{|K|^2}\frac{Ch^2}{h\delta}\,\|\tilde{w}\|^2_{L^2_r(C_K)} \\
&\leq \frac{C}{h^3\delta}\,\|\tilde{w}\|^2_{L^2_r(C_K)}\,.
\end{aligned}
$$

Hence,

$$
\begin{aligned}
\|R_h^o w\|^2_{L^2_r(K)} &\leq Ch^2 r_K |R_h^o w|^2_K|, \\
&\leq \frac{Ch^3}{h^3\delta}\,\|\tilde{w}\|^2_{L^2_r(C_K)}\,, \\
&\leq \frac{C}{\delta}\,\|\tilde{w}\|^2_{L^2_r(C_K)}\,.
\end{aligned}
$$

This proves item 1 of the Lemma.

Now we prove item 2. It is clear that

$$
\begin{aligned}
|R_h^o w_h - w_h|_K| &= |\frac{1}{|K|}\int_K S^o \tilde{w}_h d\mathbf{x} - \frac{1}{|K|}\int_K w_h d\mathbf{x}|, \\
&= |\frac{1}{|K|}\int_{D^h_{a_1}}\int_{D^h_{a_2}}\int_{D^h_{a_3}}(\int_{\tilde{K}}\tilde{w}_h(\mathbf{z})d\mathbf{z} - \int_K w_h(\mathbf{x})d\mathbf{x})d\mathbf{y}_3 d\mathbf{y}_2 d\mathbf{y}_1| \quad \text{by (4–14)}, \\
&\leq \frac{1}{|K|}\int_{D^h_{a_1}}\int_{D^h_{a_2}}\int_{D^h_{a_3}}\int_{(\tilde{K}\backslash K)\cup(K\backslash\tilde{K})}|\tilde{w}_h(\mathbf{x})|d\mathbf{x}d\mathbf{y}_3 d\mathbf{y}_2 d\mathbf{y}_1,
\end{aligned}
\tag{4–27}
$$

where $\tilde{K} = [\mathbf{y}_1, \mathbf{y}_2, \mathbf{y}_3]$. Notice that both $\tilde{K}\backslash K$ and $K\backslash\tilde{K}$ will always be inside the union of $conv(D^h_{a_1}, D^h_{a_2})$, and $conv(D^h_{a_2}, D^h_{a_3})$, and $conv(D^h_{a_3}, D^h_{a_1})$, where $conv(A, B)$ denotes the convex hull of A and B. Therefore, $area((\tilde{K}\backslash K) \cup (K\backslash\tilde{K})) \leq Ch(h\delta)$, and so continuing (4–27),

$$
\begin{aligned}
|R_h^o w_h - w_h|_K| &\leq \frac{1}{|K|}\int_{D^h_{a_1}}\int_{D^h_{a_2}}\int_{D^h_{a_3}} Ch(h\delta)\,\|\tilde{w}_h\|_{L^\infty(C_K)}\,d\mathbf{y}_3 d\mathbf{y}_2 d\mathbf{y}_1, \\
&\leq C\delta\,\|\tilde{w}_h\|_{L^\infty(C_K)}\,.
\end{aligned}
\tag{4–28}
$$

Hence,

$$\begin{aligned}
\|R_h^o w_h - w_h\|_{L_r^2(K)}^2 &\leq Ch^2 r_K |R_h^o w_h - w_h|_K|^2, \\
&\leq Ch^2 r_K \delta^2 \|\tilde{w}_h\|_{L^\infty(C_K)}^2 && \text{by (4–28)}, \\
&\leq C\delta^2 \|\tilde{w}_h\|_{L_r^2(C_K)}^2 .
\end{aligned}$$

□

Due to the second result of Lemmas 4.2.2, 4.2.3, and 4.2.4, there is a $0 < \delta_1 \leq \delta_0$ such that the operators $R_h^g|_{V_{h,\diamond}}$, $R_h^c|_{\mathbf{W}_{h,\diamond}}$, and $R_h^o|_{S_h}$ are invertible for all $0 < \delta \leq \delta_1$. We denote these inverse operators by $J_h^g : V_{h,\diamond} \to V_{h,\diamond}$, $J_h^c : \mathbf{W}_{h,\diamond} \to \mathbf{W}_{h,\diamond}$, and $J_h^o : S_h \to S_h$ respectively. For the rest of the paper, we fix $\delta \in (0, \delta_1]$. Then by construction, these inverse operators preserve the commuting diagram properties, and they are also uniformly bounded in the L_r^2-norm. Hence, we modify the quasi-interpolators as in [17] to construct projectors.

Define $\Pi_h^g : L_r^2(D) \to V_{h,\diamond}$, $\Pi_h^c : L_r^2(D)^2 \to \mathbf{W}_{h,\diamond}$, and $\Pi_h^o : L_r^2(D) \to S_h$ by

1. $\Pi_h^g = J_h^g R_h^g$.
2. $\Pi_h^c = J_h^c R_h^c$.
3. $\Pi_h^o = J_h^o R_h^o$.

Theorem 4.2.1. *Projectors Π_h^g, Π_h^c, and Π_h^o satisfy the following error estimates for all $0 \leq s \leq 1$.*

1. $\|u - \Pi_h^g u\|_r \leq Ch^s \|u\|_{H_r^s(D)}$ *for all* $u \in H_r^s(D)$.
2. $\|\mathbf{v} - \Pi_h^c \mathbf{v}\|_r \leq Ch^s \|\mathbf{v}\|_{H_r^s(D)^2}$ *for all* $\mathbf{v} \in H_r^s(D)^2$.
3. $\|w - \Pi_h^o w\|_r \leq Ch^s \|w\|_{H_r^s(D)}$ *for all* $w \in H_r^s(D)$.

If $s = 1$ the norms on the right hand side of all three inequalities above can be replaced by semi-norms.

Proof. We will only prove the error estimate for Π_h^c as the proof follows similarly for the other projectors as well. Let $\Pi_h : L_r^2(D)^2 \to \mathbf{W}_{h,\diamond}$ be the L_r^2-orthogonal projection. Since

$$\|\mathbf{v} - \Pi_h^c \mathbf{v}\|_r \leq (1 + C_\delta) \|\mathbf{v}\|_r \qquad \text{by Lemma 4.2.3 item 1,}$$

and

$$\begin{aligned} \|\mathbf{v} - \Pi_h^c \mathbf{v}\|_r &= \|(\mathbf{v} - \Pi_h \mathbf{v}) - \Pi_h^c(\mathbf{v} - \Pi_h \mathbf{v})\|_r , \\ &\leq (1 + C_\delta) \|(\mathbf{v} - \Pi_h \mathbf{v})\|_r , \\ &\leq (1 + C_\delta) Ch |\mathbf{v}|_{H_r^1(D)^2}, \end{aligned}$$

it follows that

$$\|\mathbf{v} - \Pi_h^c \mathbf{v}\|_r \leq Ch^s \|\mathbf{v}\|_{H_r^s(D)^2} ,$$

for all $0 \leq s \leq 1$, by interpolation theory [4]. □

The following corollary is immediate by the commuting diagram property.

Corollary 4.2.1. $\|\mathbf{v} - \Pi_h^c \mathbf{v}\|_\wedge \leq Ch^s(\|\mathbf{v}\|_{H_r^s(D)^2} + \|\mathrm{curl}_{rz}\mathbf{v}\|_{H_r^s(D)})$ *if* $\mathbf{v} \in H_r^s(D)^2$ *and* $\mathrm{curl}_{rz}\mathbf{v} \in H_r^s(D)$ *for all* $0 \leq s \leq 1$.

CHAPTER 5
ANALYSIS OF A DUAL MIXED PROBLEM IN WEIGHTED SPACES

In this chapter, we analyze a mixed problem in weighted spaces, that will provide main ingredients for the analysis of the meridian problem in Chapter 6 and 7. This problem is interesting in its own right, since it is related to the azimuthal problem as we shall see. We will prove that the problem is well posed and provide error estimates for the discrete solution. Much of the results in this chapter are contained in [20].

5.1 Problem Statement and Analysis

The problem can be stated as follows: Find $\mathbf{z}$ in $\mathbf{H}_{r,\diamond}(\mathrm{curl}, D)$ and p in $L^2_r(D)$ satisfying

$$\begin{aligned} (\mathbf{z}, \mathbf{w})_r - (p, \mathrm{curl}_{rz}\mathbf{w})_r &= 0, && \text{for all } \mathbf{w} \text{ in } \mathbf{H}_{r,\diamond}(\mathrm{curl}, D), \\ (s, \mathrm{curl}_{rz}\mathbf{z})_r &= (s, f)_r, && \text{for all } s \text{ in } L^2_r(D). \end{aligned} \tag{5–1}$$

Observe that this is a variational formulation of the boundary value problem

$$\begin{aligned} \mathbf{z} &= \mathbf{curl}_{rz}\, p && \text{on } D, \\ \mathrm{curl}_{rz}\mathbf{z} &= f && \text{on } D, \\ \mathbf{z}\cdot\mathbf{t} &= 0 && \text{on } \Gamma_1, \end{aligned}$$

which can also be written as the second-order boundary value problem

$$\mathrm{curl}_{rz}\, \mathbf{curl}_{rz}\, p = f \quad \text{on } D, \qquad \text{and} \qquad \mathbf{curl}_{rz}\, p \cdot \mathbf{t} = 0 \quad \text{on } \Gamma_1. \tag{5–2}$$

The differential operator appearing here is the same as the second order operator appearing in the azimuthal problem (1–9) defining the θ-component of the electric field in the time harmonic Maxwell equations under axial symmetry. Interestingly, this "azimuthal" operator plays an important role in the finite element analysis and the multigrid analysis of the "meridian" operator. Problem (5–1) is independently interesting because of the above mentioned connection to the azimuthal Maxwell system. Indeed, a

primal variational formulation of (5–2), but with different boundary conditions, is analyzed in [25]. In this section, we will analyze the dual variational formulation (5–1).

We begin with the following lemma, which will help in proving that the mixed problem (5–1) is well posed (cf. Lemma A.0.6 in Appendix A).

Lemma 5.1.1. *The map* $\mathrm{curl}_{rz} : \mathbf{H}_{r,\diamond}(\mathrm{curl}, D) \mapsto L^2_r(D)$ *is surjective.*

Proof. Let s be in $L^2_r(D)$. It is shown in [5, 25] that there exists a unique u in V^θ satisfying

$$(\mathbf{curl}_{rz} u, \mathbf{curl}_{rz} v)_r = (s, v)_r \quad \text{for all } v \in V^\theta, \tag{5–3}$$

where $V^\theta := \{v \in \widetilde{H}^1_r(D) : v = 0 \text{ on } \partial D\}$. This implies that $s = \mathrm{curl}_{rz}\mathbf{curl}_{rz} u$ in $L^2_r(D)$ by the density of $\mathcal{D}(D)$ in $L^2_r(D)$. Hence, setting $\mathbf{w} = \mathbf{curl}_{rz} u$, we find that

$$s = \mathrm{curl}_{rz}\mathbf{w}. \tag{5–4}$$

Note that $\mathbf{w}$ is in $L^2_r(D)^2$, since $\|\mathbf{curl}_{rz} u\|_r \leq C\|u\|_{\widetilde{H}^1_r(D)}$ by [25, Proposition 3.1]. In fact, these two norms are equivalent as u is in V^θ. Moreover, by (5–4) $\mathrm{curl}_{rz}\mathbf{w}$ is in $L^2_r(D)$, so $\mathbf{w}$ is in $\mathbf{H}_r(\mathrm{curl}, D)$. However, we want to express s as the curl of a function in $\mathbf{H}_{r,\diamond}(\mathrm{curl}, D)$.

To this end, we first define $\mathbf{W}^0$ by

$$\mathbf{W}^0 := \left\{\mathbf{w} \in \mathbf{H}_{r,\diamond}(\mathrm{curl}, D) : (\mathbf{w}, \mathbf{grad}_{rz} q)_r = 0 \text{ for all } q \in H^1_{r,\diamond}(D)\right\}$$

and let P^0 denote the orthogonal projection from $\mathbf{H}_r(\mathrm{curl}, D)$ to $\mathbf{W}^0$ in the $(\cdot,\cdot)_r$-inner product. Clearly, if we show that

$$s = \mathrm{curl}_{rz}(P^0\mathbf{w}), \tag{5–5}$$

the proof of the lemma will be complete.

Considering any ψ in $\mathcal{D}(D)$, it is easy to check that

$$\mathbf{curl}_{rz}\psi \text{ is in } \mathbf{W}^0. \tag{5–6}$$

Furthermore, since ψ is in $\mathcal{D}(D)$,

$$\begin{aligned}(\mathrm{curl}_{rz}(P^0\mathbf{w}), \psi)_r &= (P^0\mathbf{w}, \mathbf{curl}_{rz}\psi)_r && \text{by (2–8)},\\ &= (\mathbf{w}, \mathbf{curl}_{rz}\psi)_r && \text{by (5–6)},\\ &= (s, \psi)_r && \text{by (2–8) and (5–4)}.\end{aligned}$$

Since $\mathcal{D}(D)$ is dense in $L^2_r(D)$ (see e.g. [28]), we have proved (5–5). □

Theorem 5.1.1. *There exists a unique* $\mathbf{z}$ *in* $\mathbf{H}_{r,\diamond}(\mathrm{curl}, D)$ *and a unique* p *in* $L^2_r(D)$ *satisfying* (5–1)*. Moreover, there is a constant* $C_{\mathrm{stability}} > 0$ *independent of* f *such that*

$$\|\mathbf{z}\|_\Lambda + \|p\|_r \le C_{\mathrm{stability}}\|f\|_r.$$

Proof. By the Babuška-Brezzi theory of mixed methods [16], the theorem will follow once we verify the inf-sup condition

$$C_1\,\|s\|_r \le \sup_{\mathbf{v}\in\mathbf{H}_{r,\diamond}(\mathrm{curl},D)} \frac{(\mathrm{curl}_{rz}\mathbf{v}, s)_r}{\|\mathbf{v}\|_\Lambda} \qquad \text{for all } s \text{ in } L^2_r(D), \tag{5–7}$$

and coercivity on the kernel,

$$\|\mathbf{v}\|_\Lambda \le C_2\,\|\mathbf{v}\|_r \qquad \text{for all } \mathbf{v} \text{ in } \mathbf{G}, \tag{5–8}$$

where $\mathbf{G}$ is the kernel defined by

$$\mathbf{G} = \left\{\mathbf{w} \in \mathbf{H}_{r,\diamond}(\mathrm{curl}, D) : \quad (\mathrm{curl}_{rz}\mathbf{w}, s)_r = 0 \text{ for all } s \text{ in } L^2_r(D)\right\}.$$

Above, C_1 and C_2 are two constants independent of the functions involved.

The inf-sup condition (5–7) is equivalent to asserting that the adjoint of the operator

$$\mathrm{curl}_{rz} : \mathbf{H}_{r,\diamond}(\mathrm{curl}, D) \mapsto L^2_r(D)$$

is bounded from below, which is equivalent to the surjectivity of the above curl map (by standard arguments using the Closed Range Theorem, see e.g., [16, § II.1]). This surjectivity is precisely the assertion of Lemma 5.1.1. Hence, it only remains to

verify (5–8), which is obvious, since $\mathbf{v}$ is in $\mathbf{G}$ if and only if $\mathrm{curl}_{rz}\mathbf{v} = 0$, so that $\|\mathbf{v}\|_\Lambda = \|\mathbf{v}\|_r$ for all $\mathbf{v}$ in $\mathbf{G}$. $\square$

Next, we prove a regularity result. Recall that Ω is the revolution of D, and that we denote by $\breve{L}^2(\Omega)$ and $\breve{H}^k(\Omega)$ the subspaces of axisymmetric functions of $L^2(\Omega)$ and $H^k(\Omega)$, respectively, for $k \geq 1$. The restriction map $g(r,\theta,z) \mapsto g_D(r,z)$ given by

$$g_D(r,z) = g(r,0,z), \text{ for all } (r,z) \text{ in } D$$

is an isometry (up to a factor of $\sqrt{2\pi}$) from $\breve{L}^2(\Omega)$ onto $L^2_r(D)$ (See Theorem 2.3.1). The reverse operation will be denoted by superscripting functions with Ω, i.e., given $\eta(r,z)$ on D, the function η^Ω is defined by $\eta^\Omega(r,\theta,z) = \eta(r,z)$. Thus $(g_D)^\Omega = g$, for g in $\breve{L}^2(\Omega)$.

With the use of such notations, we will now prove the following estimates, which will be useful in our multigrid analysis.

Theorem 5.1.2. *The solution* $(\mathbf{z}, p)$ *of* (5–1) *satisfies*

$$\|\mathbf{z}\|_{H^s_r(D)^2} \leq C_{\text{regularity}} \|f\|_r ,$$
$$(\|p\|^2_{H^s_r(D)} + \|\mathbf{curl}_{rz} p\|^2_{H^s_r(D)^2})^{\frac{1}{2}} \leq C_{\text{regularity}} \|f\|_r ,$$

for any data f *in* $L^2_r(D)$*, where* $s = \frac{1}{2}$ *if* Ω *is a bounded Lipschitz domain, and* $s = 1$ *if* Ω *is convex. In fact, if* Ω *is convex* $\|p\|_{\widetilde{H}^2_r(D)} \leq C_{\text{regularity}} \|f\|_r$.

Proof. Let $(\mathbf{z}, p)$ solve (5–1). Define $\mathbf{p}_\theta = p^\Omega \mathbf{e}_\theta$. Then recalling the expression

$$\operatorname{div} \mathbf{q} = \frac{1}{r}\partial_r(rq_r) + \frac{1}{r}\partial_\theta q_\theta + \partial_z q_z \tag{5–9}$$

for divergence in cylindrical coordinates, we find that

$$\operatorname{div} \mathbf{p}_\theta = 0 \qquad \text{on } \Omega,$$
$$\mathbf{p}_\theta \cdot \mathbf{n} = 0 \qquad \text{on } \partial\Omega.$$

The last equality follows because the unit outward normal $\mathbf{n}$ on $\partial\Omega$ is orthogonal to $\mathbf{e}_\theta$. Furthermore, from the first equation of (5–1), we know that the equality $\mathbf{z} - \mathbf{curl}_{rz} p = 0$ holds in the distributional sense. Since $\mathbf{z}$ is in $L^2_r(D)^2$, the equality

$$\mathbf{z} = \mathbf{curl}_{rz} p \tag{5–10}$$

in fact holds in $L^2_r(D)^2$. By writing out the three-dimensional curl in cylindrical coordinates, we observe that

$$\mathbf{curl}\, \mathbf{p}_\theta = (\mathbf{curl}_{rz} p)^\Omega = \mathbf{z}^\Omega, \tag{5–11}$$

where for axisymmetric vector fields $\mathbf{v} = v_r \mathbf{e}_r + v_z \mathbf{e}_z$, the revolution is defined by $\mathbf{v}^\Omega = v_r^\Omega \mathbf{e}_r + v_z^\Omega \mathbf{e}_z$. Thus $\mathbf{curl}\, \mathbf{p}_\theta$ is in $L^2(\Omega)^3$. Combining these observations, we find that $\mathbf{p}_\theta$ is in $\mathbf{H}(\mathbf{curl}, \Omega) \cap \mathbf{H}_0(\mathrm{div}, \Omega)$, a space which is well-known to be continuously embedded in $H^{\frac{1}{2}}(\Omega)^3$ for bounded Lipschitz domains (Theorem 2.2.2). Thus, we have

$$\begin{aligned}
\|\mathbf{p}_\theta\|_{H^{\frac{1}{2}}(\Omega)^3} &\leq C\big(\|\mathbf{p}_\theta\|_{\mathrm{H(curl},\Omega)} + \|\mathbf{p}_\theta\|_{\mathrm{H(div},\Omega)}\big), \\
&\leq C\big(\|p\|_r + \|\mathbf{curl}_{rz} p\|_r\big), \\
&\leq C\big(\|p\|_r + \|\mathbf{z}\|_r\big), \\
&\leq C\|f\|_r,
\end{aligned} \tag{5–12}$$

where in the last step we have used Theorem 5.1.1.

The second equality of the variational problem (5–1) shows that $\mathrm{curl}_{rz}\mathbf{z} = f$ holds in $L^2_r(D)$. Translating this for $\mathbf{z}^\Omega$, we have

$$\begin{aligned}
\mathbf{curl}\, \mathbf{z}^\Omega &= f^\Omega \mathbf{e}_\theta && \text{on } \Omega, \\
\mathrm{div}\, \mathbf{z}^\Omega &= 0 && \text{on } \Omega, \\
\mathbf{z}^\Omega \times \mathbf{n} &= 0 && \text{on } \partial\Omega.
\end{aligned}$$

The last equality holds because $\gamma_t(\mathbf{z}) = 0$, and the second, $\mathrm{div}\, \mathbf{z}^\Omega = 0$, follows from (5–11). Now using the continuous embedding of $\mathbf{H}_0(\mathbf{curl}, \Omega) \cap \mathbf{H}(\mathrm{div}, \Omega)$ into

$H^{\frac{1}{2}}(\Omega)^3$ [22], we obtain

$$\|\mathbf{z}^{\Omega}\|_{H^{\frac{1}{2}}(\Omega)^3} = \|\,\mathbf{curl}\,\mathbf{p}_\theta\|_{H^{\frac{1}{2}}(\Omega)^3} \leq C\|f\|_r. \tag{5–13}$$

By using Theorem 2.3.1 item 3 which states the isomorphism between $\breve{H}^{\frac{1}{2}}(\Omega)^3$ and $H_r^{\frac{1}{2}}(D) \times H_r^{\frac{1}{2}}(D) \times H_r^{\frac{1}{2}}(D)$, the first inequality of the theorem follows immediately from the above estimate, since $\|\mathbf{z}\|_{H_r^{\frac{1}{2}}(D)^2} \leq C\|\mathbf{z}^{\Omega}\|_{H^{\frac{1}{2}}(\Omega)^3}$.

Again by using this isomorphism (Theorem 2.3.1 item 3), (5–12) and (5–13) we get

$$\begin{aligned} ||\mathbf{curl}_{rz}\,p||^2_{H_r^{\frac{1}{2}}(D)^2} + ||p||^2_{H_r^{\frac{1}{2}}(D)} &\leq C(||\,\mathbf{curl}\,\mathbf{p}_\theta||^2_{H^{\frac{1}{2}}(\Omega)^3} + ||\mathbf{p}_\theta||^2_{H^{\frac{1}{2}}(\Omega)^3}), \\ &\leq C||f||_r^2, \end{aligned}$$

which proves the second estimate of the theorem. If Ω is convex then we reach the result by using the continuous embedding result of $\mathbf{H}_0(\mathbf{curl}, \Omega) \cap \mathbf{H}(\mathrm{div}, \Omega)$ and $\mathbf{H}(\mathbf{curl}, \Omega) \cap \mathbf{H}_0(\mathrm{div}, \Omega)$ into $H^1(\Omega)^3$ (Theorem 2.2.1), and the isomorphism between $\breve{H}^1(\Omega)^3$ and $\widetilde{H}_r^1(D) \times \widetilde{H}_r^1(D) \times H_r^1(D)$ (Theorem 2.3.1 item 3). □

Let us now consider the mixed finite element approximation of (5–1). The discrete problem is to find $\mathbf{z}_h$ in $\mathbf{W}_{h,\diamond}$ and p_h in S_h satisfying

$$\begin{aligned} (\mathbf{z}_h, \mathbf{w}_h)_r - (p_h, \mathrm{curl}_{rz}\mathbf{w}_h)_r &= 0, && \text{for all } \mathbf{w}_h \text{ in } \mathbf{W}_{h,\diamond}, \\ (s_h, \mathrm{curl}_{rz}\mathbf{z}_h)_r &= (s_h, f)_r, && \text{for all } s_h \text{ in } S_h. \end{aligned} \tag{5–14}$$

At this point, we can proceed to analyze the discrete mixed method by verifying the conditions of the Babuška-Brezzi theory, which would yield *a priori* error estimates. However, for our multigrid analysis, we will need error estimates in a slightly more specialized form, so we will provide a direct error analysis. We will also prove a higher order estimate obtained via duality. These results are collected in the next theorem.

Theorem 5.1.3. *Suppose* $\mathbf{z}$ *in* $\mathbf{H}_{r,\diamond}(\mathrm{curl}, D)$ *and* p *in* $L_r^2(D)$ *solve* (5–1).

1. There is a unique $\mathbf{z}_h$ *in* $\mathbf{W}_{h,\diamond}$ *and a unique* p_h *in* S_h *satisfying* (5–14).

2. The following error estimate holds:

$$\|\mathbf{z} - \mathbf{z}_h\|_r = \left\|\mathbf{z} - \Pi_h^W \mathbf{z}\right\|_r .$$

3. If f is in S_h, then

$$\left\|\Pi_h^S p - p_h\right\|_r \leq Ch^{2s}\|f\|_r,$$

where $s = \frac{1}{2}$ if Ω is a bounded Lipschitz domain, and $s = 1$ if Ω is convex.

Proof. Proof of 1: Suppose $f = 0$ in (5–14). Then by setting $\mathbf{w}_h = \mathbf{z}_h$, we get $\mathbf{z}_h = 0$. Then

$$(p_h, \mathrm{curl}_{rz}\mathbf{w}_h)_r = 0 \text{ for all } \mathbf{w}_h \text{ in } \mathbf{W}_{h,\diamond},$$

which implies that $p_h = 0$ by the exactness of (4–3), and this completes the proof.

Proof of 2: Since, by (5–14),

$$(\mathbf{z}_h, \mathbf{grad}_{rz}\eta_h)_r = 0 = (\mathbf{z}, \mathbf{grad}_{rz}\eta_h)_r \text{ for all } \eta_h \in V_{h,\diamond}$$

and

$$(\mathrm{curl}_{rz}\mathbf{z}_h, s_h)_r = (f, s_h)_r = (\mathrm{curl}_{rz}\mathbf{z}, s_h)_r \text{ for all } s_h \in S_h,$$

by the unique solvability of (4–6), $\mathbf{z}_h = \Pi_h^W \mathbf{z}$. Therefore, item 2 holds.

Proof of 3: We proceed by a duality argument, suitably modified. Let ε_z in $\mathbf{H}_{r,\diamond}(\mathrm{curl}, D)$ and ε_p in $L_r^2(D)$ solve (5–1) with f set to $\Pi_h^S p - p_h$. Let their discrete counterparts be $\boldsymbol{\varepsilon}_{z,h}$ in $\mathbf{W}_{h,\diamond}$ and $\varepsilon_{p,h}$ in S_h, which solve (5–14) with f set to $\Pi_h^S p - p_h$. Then by (5–14) and (5–1),

$$\begin{aligned}
\left\|\Pi_h^S p - p_h\right\|_r^2 &= (\Pi_h^S p - p_h, \mathrm{curl}_{rz}\boldsymbol{\varepsilon}_{z,h})_r, \\
&= (p - p_h, \mathrm{curl}_{rz}\boldsymbol{\varepsilon}_{z,h})_r, \\
&= (\mathbf{z} - \mathbf{z}_h, \boldsymbol{\varepsilon}_{z,h})_r, \\
&= (\mathbf{z} - \mathbf{z}_h, \boldsymbol{\varepsilon}_{z,h} - \boldsymbol{\varepsilon}_z)_r + (\mathbf{z} - \mathbf{z}_h, \boldsymbol{\varepsilon}_z)_r. \qquad (5\text{–}15)
\end{aligned}$$

Now, since f is given to be in S_h,

$$\mathrm{curl}_{rz}\mathbf{z} = \mathrm{curl}_{rz}\mathbf{z}_h = f.$$

This together with the definition of $\{\varepsilon_z, \varepsilon_p\}$ imply that the last term in (5–15) vanishes:

$$(\varepsilon_z, \mathbf{z} - \mathbf{z}_h)_r = (\varepsilon_p, \operatorname{curl}_{rz}(\mathbf{z} - \mathbf{z}_h)) = 0.$$

Using this in (5–15) and continuing,

$$\begin{aligned}
\left\|\Pi_h^S p - p_h\right\|_r^2 &= (\mathbf{z} - \mathbf{z}_h, \varepsilon_{z,h} - \varepsilon_z)_r, \\
&\leq \|\mathbf{z} - \mathbf{z}_h\|_r \|\varepsilon_{z,h} - \varepsilon_z\|_r, \\
&= \left\|\mathbf{z} - \Pi_h^W \mathbf{z}\right\|_r \left\|\varepsilon_z - \Pi_h^W \varepsilon_z\right\|_r && \text{by item 2,} \\
&\leq Ch^{2s} \|\mathbf{z}\|_{H_r^s(D)^2} \|\varepsilon_z\|_{H_r^s(D)^2}, && \text{by Corollary 4.1.1, ,}
\end{aligned}$$

for all $0 \leq s \leq 1$. We choose $s = \frac{1}{2}$ for bounded Lipschitz Ω, and $s = 1$ for convex Ω in order to apply the regularity result of Theorem 5.1.2,

$$\|\varepsilon_z\|_{H_r^s(D)^2} \leq C\|\Pi_h^S p - p_h\|_r.$$

Thus,

$$\left\|\Pi_h^S p - p_h\right\|_r^2 \leq Ch^{2s} \|\mathbf{z}\|_{H_r^s(D)^2} \|\Pi_h^S p - p_h\|_r.$$

Canceling the common factor and applying Theorem 5.1.2 again, we obtain the required estimate. □

Remark 5.1.1. If Ω is convex then item 3 of Theorem 5.1.3 can be thought of as a superconvergence result, as it shows that we obtain quadratic convergence for $\Pi_h^S p - p_h$ even when using piecewise constant approximation spaces. In this respect, this result is similar to certain known superconvergence error estimates derived via duality arguments for the Raviart-Thomas mixed method [19, 23, 34], albeit without a degenerate weight function.

Remark 5.1.2. There is an analogue of the mixed problem (5–1) in the case of the fully three-dimensional **curl curl** operator, sometimes called the dual mixed formulation (see e.g. [8] where it used for eigenvalue analysis). However, this method is not practically

popular in the 3D case as its implementation requires a basis for exactly divergence-free finite element spaces, which is not easy to construct. This difficulty is absent in the axisymmetric case.

5.2 Numerical Results

In this section, we will report the observed convergence rate for the approximate solution of the dual mixed problem. This will serve as a test of the sharpness of our theoretical error estimates.

For computer implementation of the mixed method, we need to assemble the matrix representations of the operators $A_h : \mathbf{W}_{h,\diamond} \mapsto \mathbf{W}'_{h,\diamond}$ and $B_h : \mathbf{W}_{h,\diamond} \mapsto S'_h$ defined by

$$A_h\mathbf{u}_h(\mathbf{w}_h) = (\mathbf{u}_h, \mathbf{w}_h)_r \text{ for all } \mathbf{u}_h, \mathbf{w}_h \in \mathbf{W}_{h,\diamond},$$

$$B_h\mathbf{u}_h(s_h) = -(\mathrm{curl}_{rz}\mathbf{u}_h, s_h)_r \text{ for all } \mathbf{u}_h \in \mathbf{W}_{h,\diamond}, s_h \in S_h.$$

Let $\mathbf{A}$ and $\mathbf{B}$ denote the matrix representations of A_h and B_h, respectively, in terms of the standard local bases for $\mathbf{W}_{h,\diamond}$ and S_h (consisting of the Whitney functions $\Phi_{\mathfrak{e}}$, and the indicator functions of triangles). Then (5–14) can be rewritten as the linear system

$$\mathbf{A}z + \mathbf{B}^t p = 0,$$

$$-\mathbf{B}z = f,$$

where z and p denote the vectors of coefficients in the basis expansions of $\mathbf{z}_h$ and p_h, respectively. The vector f is computed from the right hand side of (5–14) as usual. In practice, we compute p and z by solving

$$\mathbf{C}p = f,$$

$$\mathbf{A}z = g,$$

where $\mathbf{C} = \mathbf{B}\mathbf{A}^{-1}\mathbf{B}^t$ and $g = -\mathbf{B}^t p$. Both these systems can be solved via the conjugate gradient method as $\mathbf{C}$ and $\mathbf{A}$ are symmetric and positive definite. Note that when solving

Table 5-1. Mixed problem convergence rates

level	$\|\mathbf{z}-\mathbf{z}_h\|_r$	order	$\|p-p_h\|_r$	order	$\|\Pi_h^S p - p_h\|_r$	order
1	0.305150		0.123463		0.044430	
2	0.152784	0.998	0.059647	1.05	0.011144	1.995
3	0.076486	0.998	0.029553	1.013	0.002791	1.997
4	0.038263	0.999	0.014743	1.003	0.000698	1.999
5	0.019135	1	0.007367	1.001	0.000175	2
6	0.009568	1	0.003683	1	0.000044	2
7	0.004784	1	0.001842	1	0.000011	1.999
8	0.002392	1	0.000921	1	0.000003	2

the first equation, for each application of $\mathbf{C}$, we use another inner conjugate gradient iteration to obtain the result of multiplication by $\mathbf{A}^{-1}$.

In Table 5-1, we report the $L_r^2(D)$-norm of the observed errors in the mixed method approximations of $\mathbf{z}$, p, and $\Pi_h^S p$. In this case, $f = -3$, $p = r^2$ and $\mathbf{z} = (0, 3r)$. The domain D was the chosen to be the unit square. Note that in this case, Ω is convex. The coarsest mesh is obtained by dividing the unit square into two uniform triangles by connecting the points (0,0) and (1,1). This is mesh level 0. Higher levels are obtained by successive refinements. Each refinement is performed by connecting the midpoints of each edge, so the meshsize reduces by $1/2$, and the finest mesh (level 8) is roughly of size $1/256$. The order of convergence is computed as $\log_2(e_{j-1}/e_j)$, where e_j is the computed $L_r^2(D)$-norm of the error at mesh level j.

From the table, we observe that the approximations for $\mathbf{z}$ and p converge at first order. This convergence for $\mathbf{z}$ is in accordance with Theorem 5.1.3 item 2. The convergence for p is also in accordance with the theorem, because by triangle inequality

$$\|p - p_h\|_r \leq \|p - \Pi_h^S p\|_r + \|\Pi_h^S p - p_h\|_r$$

and although Theorem 5.1.3 item 3 asserts that the last term is $O(h^2)$, the first term on the right hand side, being $O(h)$, dominates. That the last term indeed superconverges at double the order is verified in the last row of the table.

CHAPTER 6
FINITE ELEMENT ANALYSIS FOR THE MERIDIAN PROBLEM

In this chapter, we use the edge finite element method to find an approximate solution to the meridian problem (1–8). We will show that the the edge finite element method provides a good approximation to this problem under certain conditions.

6.1 The Edge Finite Element Method

The weak formulation of (1–8) in the simple case of unit material properties reads:

Find $\mathbf{u} = (E_r, E_z) \in \mathbf{H}_{r,\diamond}(\text{curl}, D)$ such that

$$(\text{curl}_{rz}\mathbf{u}, \text{curl}_{rz}\mathbf{v})_r - \kappa^2(\mathbf{u}, \mathbf{v})_r = (\mathbf{F}, \mathbf{v})_r, \tag{6–1}$$

for all $\mathbf{v} \in \mathbf{H}_{r,\diamond}(\text{curl}, D)$, where here and in the remainder of this dissertation we denote $\mathbf{F}$ for (F_r, F_z). Note that there is a countable set of real values for κ for which (6–1) does not have a unique solution [29]. For the remainder of this dissertation, we assume that κ is not one of such values so that (6–1) is uniquely solvable.

The finite element method reduces an infinite dimensional problem into a finite dimensional one (See Chapter 3 section 3.1). The first step is to construct a finite dimensional subspace of the infinite dimensional space $\mathbf{H}_{r,\diamond}(\text{curl}, D)$. We will use the lowest order Nédélec space $\mathbf{W}_{h,\diamond} \subset \mathbf{H}_{r,\diamond}(\text{curl}, D)$ for the finite element subspace. Recall that

$$\mathbf{W}_{h,\diamond} = \{\mathbf{v}_h \in \mathbf{H}_{r,\diamond}(\text{curl}, D) : \mathbf{v}_h|_K = (b - az, c + ar) \text{ for some } a, b, c \in \mathbb{R} \text{ for all } K \in \mathscr{T}_h\}.$$

Since functions in $\mathbf{W}_{h,\diamond}$ have the form $(b - az, c + ar)$ for some $a, b, c \in \mathbb{R}$ when restricted to each triangle in the triangulation of the domain, and there are finitely many triangles in the mesh, $\mathbf{W}_{h,\diamond}$ is clearly finite dimensional.

Next we solve the problem (6–1) on $\mathbf{W}_{h,\diamond}$ instead of $\mathbf{H}_{r,\diamond}(\text{curl}, D)$:

Find $\mathbf{u}_h \in \mathbf{W}_{h,\diamond}$ such that

$$(\text{curl}_{rz}\mathbf{u}_h, \text{curl}_{rz}\mathbf{v}_h)_r - \kappa^2(\mathbf{u}_h, \mathbf{v}_h)_r = (\mathbf{F}, \mathbf{v}_h)_r, \tag{6–2}$$

for all $\mathbf{v}_h \in \mathbf{W}_{h,\diamond}$.

Now we are ready to change this finite dimension problem (6–2) into a matrix system by using basis functions. Let $\{\phi_i\}_{i=1}^N$ denote the basis of $\mathbf{W}_{h,\diamond}$. Then the solution $\mathbf{u}_h = \sum_{i=1}^N c_i\phi_i$ for some $c_i \in \mathbb{R}, 1 \leq i \leq N$. Additionally, since (6–2) holds for all $\mathbf{v}_h \in \mathbf{W}_{h,\diamond}$, it holds for all $\left\{\phi_j\right\}_{j=1}^N$ in particular. Therefore,

$$(\mathrm{curl}_{rz}\sum_{i=1}^N c_i\phi_i, \mathrm{curl}_{rz}\phi_j)_r - \kappa^2(\sum_{i=1}^N c_i\phi_i, \phi_j)_r = (\mathbf{F}, \phi_j)_r \qquad \text{for all } 1 \leq j \leq N,$$

$$\sum_{i=1}^N((\mathrm{curl}_{rz}\phi_i, \mathrm{curl}_{rz}\phi_j)_r - \kappa^2(\phi_i, \phi_j)_r)c_i = (\mathbf{F}, \phi_j)_r \qquad \text{for all} 1 \leq j \leq N.$$

Hence, $\{c_i\}_{i=1}^N$ can be obtained by solving the matrix system

$$\mathbf{A}\vec{\mathbf{c}} = \vec{\mathbf{b}},$$

where $\mathbf{A}$ is the $N \times N$ matrix whose ji-th entry is $A_{ji} = (\mathrm{curl}_{rz}\phi_i, \mathrm{curl}_{rz}\phi_j)_r - \kappa^2(\phi_i, \phi_j)_r$ and $\vec{\mathbf{b}}$ is the vector of length N whose j-th entry is $(\mathbf{F}, \phi_j)_r$. Once we find this vector $\vec{\mathbf{c}}$, we can use the formula $\mathbf{u}_h = \sum_{i=1}^N c_i\phi_i$ to obtain the approximate solution $\mathbf{u}_h$.

Remark 6.1.1. Since there are three unknowns for each triangle and all functions in $\mathbf{W}_{h,\diamond} \subset \mathbf{H}_{r,\diamond}(\mathrm{curl}, D)$ must have continuous tangential components along each edge, it follows that the dimension N of $\mathbf{W}_{h,\diamond}$ is the number of edges in the corresponding mesh that is not on Γ_1. This is why we call such method the "edge" finite element method. For each edge not on Γ_1 we construct a basis function in the following way. Let ϕ_i be associated with the i-th edge not on Γ_1 denoted by e_i. Then $\phi_i|_K = C(\lambda_m\mathbf{grad}_{rz}\lambda_n - \lambda_n\mathbf{grad}_{rz}\lambda_m)$ for each triangle K, where λ_m and λ_n denotes the barycentric coordinates of the two vertices of e_i with respect to the triangle K. We choose C so that the tangential component of ϕ_i will be one on the i-th edge. Thus, ϕ_i has support on two triangles if e_i is not on Γ_0, and it is defined piecewise, but the tangential components on e_i will agree. This is the well-known Whitney basis function.

We now state the result that illustrates how accurately the discrete solution $\mathbf{u}_h$ of (6–2) approximates the exact solution $\mathbf{u}$ of (6–1).

Theorem 6.1.1 (Quasi-Optimality)**.** *Suppose Ω, the revolution of D, is a bounded Lipschitz domain. If (6–1) has a unique solution $\mathbf{u} \in \mathbf{H}_{r,\diamond}(\mathrm{curl}, D)$ then there is a constant h_0 and C such that, for all $0 < h < h_0$, (6–2) also has a unique solution $\mathbf{u}_h$, and*

$$\|\mathbf{u} - \mathbf{u}_h\|_\Lambda \leq C \inf_{\mathbf{w}_h \in \mathbf{W}_{h,\diamond}} \|\mathbf{u} - \mathbf{w}_h\|_\Lambda .$$

These constants are independent of $\mathbf{u}$ and $\mathbf{u}_h$.

This result will be proved in the next section. By using this theorem and Corollary 4.2.1, we have the following result.

Corollary 6.1.1. *Under the same conditions of Theorem 6.1.1, we have*

$$\|\mathbf{u} - \mathbf{u}_h\|_\Lambda \leq Ch^s(\|\mathbf{u}\|_{H_r^s(D)^2} + \|\mathrm{curl}_{rz}\mathbf{u}\|_{H_r^s(D)}),$$

for all $0 \leq s \leq 1$.

We will later see that $\|\mathbf{u}\|_{H_r^{\frac{1}{2}}(D)^2} + \|\mathrm{curl}_{rz}\mathbf{u}\|_{H_r^{\frac{1}{2}}(D)} \leq C\,\|\mathbf{F}\|_r$ when Ω is a bounded Lipschitz domain. This result shows that we can make the approximation $\mathbf{u}_h$ as close as we want to the exact solution $\mathbf{u}$ by refining the mesh and making the meshsize small.

6.2 Proof of the Quasi-Optimality Result

Before we prove Theorem 6.1.1, we prove two important Lemmas that will not only be used for the finite element approximation but also for the multigrid analysis in Chapter 7. Recall that Ω is the three dimensional rotational domain of D.

Lemma 6.2.1. *Let $\mathbf{w}_h \in \mathbf{W}_{h,\diamond}$ be a discrete divergence free function, i.e.,*

$$(\mathbf{w}_h, \mathbf{grad}_{rz}\phi_h)_r = 0 \qquad \text{for all } \phi_h \in V_{h,\diamond},$$

and suppose $\mathbf{S}\mathbf{w}_h \in \mathbf{H}_{r,\diamond}(\mathrm{curl}, D)$ *and* $p \in L^2_r(D)$ *is the solution of the following dual mixed problem.*

$$\begin{aligned} (\mathbf{S}\mathbf{w}_h, \mathbf{x})_r - (p, \mathrm{curl}_{rz}\mathbf{x})_r &= 0, && \textit{for all } \mathbf{x} \textit{ in } \mathbf{H}_{r,\diamond}(\mathrm{curl}, D), \\ (s, \mathrm{curl}_{rz}\mathbf{S}\mathbf{w}_h)_r &= (s, \mathrm{curl}_{rz}\mathbf{w}_h)_r, && \textit{for all } s \textit{ in } L^2_r(D). \end{aligned} \tag{6–3}$$

Then

$$\|\mathbf{S}\mathbf{w}_h - \mathbf{w}_h\|_r \leq Ch^s \|\mathrm{curl}_{rz}\mathbf{w}_h\|_r ,$$

where $s = \frac{1}{2}$ *if* Ω *is a bounded Lipschitz domain, and* $s = 1$ *if* Ω *is convex.*

Proof. Since $\mathbf{w}_h$ is discrete divergence free, by the discrete Helmholtz decomposition in weighted spaces, $\mathbf{w}_h = \mathrm{curl}'_{rz} p_h$, for some $p_h \in S_h$. Thus,

$$(\mathbf{w}_h, \mathbf{x}_h)_r - (p_h, \mathrm{curl}_{rz}\mathbf{x}_h)_r = 0 \text{ for all } \mathbf{x}_h \in \mathbf{W}_{h,\diamond}.$$

Therefore,

$$\begin{aligned} \|\mathbf{S}\mathbf{w}_h - \mathbf{w}_h\|_r &= \left\|\mathbf{S}\mathbf{w}_h - \Pi_h^W \mathbf{S}\mathbf{w}_h\right\|_r && \text{by Theorem 5.1.3 item 2,} \\ &\leq Ch^s \|\mathbf{S}\mathbf{w}_h\|_{H^s_r(D)^2} && \text{by Corollary 4.1.1,} \\ &\leq Ch^s \|\mathrm{curl}_{rz}\mathbf{w}_h\|_r && \text{by Theorem 5.1.2.} \end{aligned}$$

In using Theorem 5.1.2 in the last inequality, we have that $s = \frac{1}{2}$ when Ω is a bounded Lipschitz domain, and $s = 1$ when Ω is convex. This completes the proof. □

Let us denote by $A : \mathbf{H}_{r,\diamond}(\mathrm{curl}, D) \times \mathbf{H}_{r,\diamond}(\mathrm{curl}, D)$ the bilinear form:

$$A(\mathbf{u}, \mathbf{v}) = (\mathrm{curl}_{rz}\mathbf{u}, \mathrm{curl}_{rz}\mathbf{v})_r - \kappa^2(\mathbf{u}, \mathbf{v})_r.$$

Then we have the following regularity result for the meridian problem (6–1). Recall that given $v(r, z)$ on D that is invariant under rotation, the function v^Ω on Ω is defined by $v^\Omega(r, \theta, z) = v(r, z)$. For axisymmetric vector fields $\mathbf{v}(r, z) = (v_r(r, z), v_z(r, z))$ on D, we define $\mathbf{v}^\Omega$ on Ω by $\mathbf{v}^\Omega = (v_r^\Omega, 0, v_z^\Omega)$.

Lemma 6.2.2. *Given* $\mathbf{F} \in L^2_r(D)^2$ *such that*

$$(\mathbf{F}, \mathbf{grad}_{rz}\phi)_r = 0 \text{ for all } \phi \in H^1_{r,\diamond}(D), \tag{6–4}$$

suppose $\mathbf{u} \in \mathbf{H}_{r,\diamond}(\mathrm{curl}, D)$ *is the solution of*

$$A(\mathbf{u}, \mathbf{v}) = (\mathbf{F}, \mathbf{v})_r \text{ for all } \mathbf{v} \in \mathbf{H}_{r,\diamond}(\mathrm{curl}, D). \tag{6–5}$$

Then

$$\|\mathbf{u}\|_{H^s_r(D)^2} + \|\mathrm{curl}_{rz}\mathbf{u}\|_{H^s_r(D)} \leq C \|\mathbf{F}\|_r ,$$

where $s = \frac{1}{2}$ *if* Ω *is a bounded Lipschitz domain, and* $s = 1$ *if* Ω *is convex. In fact, if* Ω *is convex, then* $\mathrm{curl}_{rz}\mathbf{u} \in \widetilde{H}^1_r(D)$.

Proof. It was shown in [21] that condition (6–4) implies that

$$(\mathbf{F}^\Omega, \mathbf{grad}\,\zeta)_r = 0 \text{ for all } \zeta \in H^1_0(\Omega).$$

Therefore, by taking derivative in the sense of distributions,

$$(\mathrm{div}\,\mathbf{F}^\Omega, \zeta) = -(\mathbf{F}^\Omega, \mathbf{grad}\,\zeta) = 0 \text{ for all } \zeta \in \mathcal{D}(\Omega),$$

and so $\mathrm{div}\,\mathbf{F}^\Omega = 0$ in $L^2(\Omega)$.

Since

$$\mathbf{curl}_{rz}\mathrm{curl}_{rz}\mathbf{u} - \kappa^2\mathbf{u} = \mathbf{F},$$

direct calculation shows that

$$\mathbf{curl}\,\mathbf{curl}\,\mathbf{u}^\Omega - \kappa^2\mathbf{u}^\Omega = \mathbf{F}^\Omega.$$

Note that $\mathbf{u}^\Omega \in \breve{\mathbf{H}}_0(\mathrm{curl}, D)$ and $\mathbf{F}^\Omega \in \breve{L}^2(\Omega)^2$. Therefore, by [22],

$$||\mathbf{u}^\Omega||_{H^{\frac{1}{2}}(\Omega)^3} + ||\,\mathbf{curl}\,\mathbf{u}^\Omega||_{H^{\frac{1}{2}}(\Omega)^3} \leq ||\mathbf{F}^\Omega||. \tag{6–6}$$

Then, since the θ-component of $\mathbf{curl}\,\mathbf{u}^{\Omega}$ is $\mathrm{curl}_{rz}\mathbf{u}$, it follows from the isomorphism between $\breve{\mathbf{H}}^{\frac{1}{2}}(\Omega)$ and $H_r^{\frac{1}{2}}(D) \times H_r^{\frac{1}{2}}(D) \times H_r^{\frac{1}{2}}(D)$ (Theorem 2.3.1 item 3) and the isomorphism between $\breve{L}^2(\Omega)$ and $L_r^2(D)$ (Theorem 2.3.1 item 1) that

$$\|\mathbf{u}\|_{H_r^{\frac{1}{2}}(D)^2} + \|\mathrm{curl}_{rz}\mathbf{u}\|_{H_r^{\frac{1}{2}}(D)} \leq C\,\|\mathbf{F}\|_r\,.$$

If Ω is convex then we use the well-known result [30]

$$||\mathbf{u}^{\Omega}||_{H^1(\Omega)^3} + ||\,\mathbf{curl}\,\mathbf{u}^{\Omega}||_{H^1(\Omega)^3} \leq ||\mathbf{F}^{\Omega}||$$

instead of (6–6). This completes the proof. □

Note that in Chapter 7, we assume that the rotation of D, namely Ω, is convex. Therefore, in Chapter 7 we will use Lemmas 6.2.1 and 6.2.2 under the convexity assumption.

We are now ready to prove the main result of this chapter.

Proof of Theorem 6.1.1. If the result holds, then the well-posedness of problem (6–2) follows, so we only need to prove the error estimate given that the meshsize is sufficiently small. Let $\mathbf{e} = \mathbf{u} - \mathbf{u}_h$, and let $\mathbf{w}_h \in \mathbf{W}_{h,\diamond}$ be arbitrary. Then $A(\mathbf{e}, \mathbf{w}_h) = 0$. Thus,

$$\begin{aligned} \|\mathbf{e}\|_{\Lambda}^2 &= \Lambda(\mathbf{e}, \mathbf{u} - \mathbf{w}_h) + \Lambda(\mathbf{e}, \mathbf{w}_h - \mathbf{u}_h), \\ &\leq \|\mathbf{e}\|_{\Lambda}\,\|\mathbf{u} - \mathbf{w}_h\|_{\Lambda} + A(\mathbf{e}, \mathbf{w}_h - \mathbf{u}_h) + (1+\kappa^2)(\mathbf{e}, \mathbf{w}_h - \mathbf{u}_h)_r, \\ &= \|\mathbf{e}\|_{\Lambda}\,\|\mathbf{u} - \mathbf{w}_h\|_{\Lambda} + (1+\kappa^2)(\mathbf{e}, \mathbf{w}_h - \mathbf{u}_h)_r. \end{aligned} \tag{6–7}$$

We approximate $(\mathbf{e}, \mathbf{w}_h - \mathbf{u}_h)_r$.

Let $\mathbf{e} = \mathbf{grad}_{rz}\eta + \alpha$ be the continuous Helmholtz decomposition of $\mathbf{e}$ where $\eta \in \mathbf{H}^1_{r,\diamond}(D)$ and $\alpha \in \mathbf{H}_{r,\diamond}(\mathrm{curl}, D)$. Let $\mathbf{w}_h - \mathbf{u}_h = \mathbf{grad}_{rz}\xi_h + \mathrm{curl}'_{rz}s_h$ be the discrete

Helmholtz decomposition of $\mathbf{w}_h - \mathbf{u}_h$, and let $\mathbf{S}(\mathrm{curl}'_{rz} s_h)$ be as in (6–3). Then

$$
\begin{aligned}
(\mathbf{grad}_{rz}\eta, \mathbf{w}_h - \mathbf{u}_h)_r &= (\mathbf{grad}_{rz}\eta, \mathrm{curl}'_{rz} s_h)_r, \\
&= (\mathbf{grad}_{rz}\eta, \mathrm{curl}'_{rz} s_h - \mathbf{S}(\mathrm{curl}'_{rz} s_h))_r, \\
&\leq \|\mathbf{e}\|_r \, \|\mathrm{curl}'_{rz} s_h - \mathbf{S}(\mathrm{curl}'_{rz} s_h)\|_r \,, \\
&\leq C h^{\frac{1}{2}} \|\mathbf{e}\|_r \, \|\mathrm{curl}_{rz} \mathrm{curl}'_{rz} s_h\|_r && \text{by Lemma 6.2.1,} \\
&= C h^{\frac{1}{2}} \|\mathbf{e}\|_r \, \|\mathrm{curl}_{rz}(\mathbf{w}_h - \mathbf{u}_h)\|_r \,.
\end{aligned}
$$

The first equality holds, since

$$
(\mathbf{grad}_{rz}\eta, \mathbf{grad}_{rz}\xi_h)_r = (\mathbf{e}, \mathbf{grad}_{rz}\xi_h)_r = -\frac{1}{\kappa^2} A(\mathbf{e}, \mathbf{grad}_{rz}\xi_h) = 0.
$$

Therefore,

$$
(\mathbf{grad}_{rz}\eta, \mathbf{w}_h - \mathbf{u}_h)_r \leq C h^{\frac{1}{2}} \|\mathbf{e}\|_r \, \|\mathrm{curl}_{rz}(\mathbf{w}_h - \mathbf{u}_h)\|_r \,. \tag{6–8}
$$

Next, let $\mathbf{z} \in \mathbf{H}_{r,\diamond}(\mathrm{curl}, D)$ be the solution of

$$
A(\mathbf{z}, \mathbf{x}) = (\alpha, \mathbf{x})_r \text{ for all } \mathbf{x} \in \mathbf{H}_{r,\diamond}(\mathrm{curl}, D).
$$

Then,

$$
\begin{aligned}
\|\alpha\|_r^2 &= (\alpha, \mathbf{e})_r, \\
&= A(\mathbf{z}, \mathbf{e}), \\
&= A(\mathbf{z} - \Pi_h^c \mathbf{z}, \mathbf{e}), \\
&\leq C \, \|\mathbf{z} - \Pi_h^c \mathbf{z}\|_\Lambda \, \|\mathbf{e}\|_\Lambda \,, \\
&\leq C h^{\frac{1}{2}} (\|\mathbf{z}\|_{H_r^{\frac{1}{2}}(D)^2} + \|\mathrm{curl}_{rz}\mathbf{z}\|_{H_r^{\frac{1}{2}}(D)}) \, \|\mathbf{e}\|_\Lambda && \text{by Corollary 4.2.1,} \\
&\leq C h^{\frac{1}{2}} \|\alpha\|_r \, \|\mathbf{e}\|_\Lambda && \text{by Lemma 6.2.2.}
\end{aligned}
$$

Therefore,

$$
\|\alpha\|_r \leq C h^{\frac{1}{2}} \|\mathbf{e}\|_\Lambda \,. \tag{6–9}
$$

Thus, it follows from (6–7) that

$$
\begin{aligned}
\|\mathbf{e}\|_\Lambda^2 &\le \|\mathbf{e}\|_\Lambda \|\mathbf{u}-\mathbf{w}_h\|_\Lambda + (1+\kappa^2)(\mathbf{e}, \mathbf{w}_h - \mathbf{u}_h)_r, \\
&= \|\mathbf{e}\|_\Lambda \|\mathbf{u}-\mathbf{w}_h\|_\Lambda + (1+\kappa^2)((\mathbf{grad}_{rz}\eta, \mathbf{w}_h - \mathbf{u}_h)_r + (\alpha, \mathbf{w}_h - \mathbf{u}_h)_r), \\
&\le \|\mathbf{e}\|_\Lambda \|\mathbf{u}-\mathbf{w}_h\|_\Lambda + Ch^{\frac{1}{2}} \|\mathbf{e}\|_\Lambda \|\mathbf{w}_h - \mathbf{u}_h\|_\Lambda \qquad \text{by (6–8) and (6–9)}, \\
&\le \|\mathbf{e}\|_\Lambda \|\mathbf{u}-\mathbf{w}_h\|_\Lambda + Ch^{\frac{1}{2}} \|\mathbf{e}\|_\Lambda \|\mathbf{w}_h - \mathbf{u}\|_\Lambda + Ch^{\frac{1}{2}} \|\mathbf{e}\|_\Lambda \|\mathbf{u} - \mathbf{u}_h\|_\Lambda, \\
&\le (1 + Ch^{\frac{1}{2}}) \|\mathbf{e}\|_\Lambda \|\mathbf{u}-\mathbf{w}_h\|_\Lambda + Ch^{\frac{1}{2}} \|\mathbf{e}\|_\Lambda^2 .
\end{aligned}
$$

Therefore,

$$||\mathbf{u}-\mathbf{u}_h||_\Lambda \le \frac{1+Ch^{\frac{1}{2}}}{1-Ch^{\frac{1}{2}}} ||\mathbf{u}-\mathbf{w}_h||_\Lambda$$

if $1 - Ch^{\frac{1}{2}} > 0$. Hence, there exists some $h_0 > 0$ such that, for all $0 < h < h_0$,

$$\|\mathbf{u}-\mathbf{u}_h\|_\Lambda \le C \|\mathbf{u}-\mathbf{w}_h\|_\Lambda \qquad \text{for all } \mathbf{w}_h \in \mathbf{W}_{h,\diamond}.$$

In conclusion, for all $0 < h < h_0$,

$$\|\mathbf{u}-\mathbf{u}_h\|_\Lambda \le C \inf_{\mathbf{w}_h \in \mathbf{W}_{h,\diamond}} \|\mathbf{u}-\mathbf{w}_h\|_\Lambda .$$

□

6.3 Numerical Results

In this section, we report numerical results that provide empirical support to the convergence of edge finite element apporximation when applied to the indefinite bilinear form $A(\cdot,\cdot)$. The domain D is the unit square and mesh level 1 consist of two uniform right triangles with the common edge connecting $(0,0)$ and $(1,1)$. The next level mesh is obtained by connecting the midpoints of each edge. Note that, in this case, the rotational domain is convex.

Table 6-1 reports the $L_r^2(D)$-norm of the error between the exact solution $\mathbf{u}$ and discrete soltuion $\mathbf{u}_h$ of (6–1) and (6–2) respectively with $f = (-2\pi r \sin(\pi z), (-49r^2 +$

Table 6-1. FEM convergence rates

level	$\|\mathbf{u} - \mathbf{u}_h\|_r$	order
2	0.17539	
3	0.0987347	0.83
4	0.0456298	1.11
5	0.0213924	1.10
6	0.0104596	1.03
7	0.0051979	1.01
8	0.0025949	1.00
9	0.0012969	1.00

$45)\cos(\pi z))$ and wavenumber $\kappa = 7$. The order of convergence is computed as $\log_2(e_{j-1}/e_j)$, where e_j is the computed $L^2_r(D)$-norm of the error at mesh level j.

From the table, we observe that the approximations for $\mathbf{u}$ converge at first order. This convergence is in accordance with Theorem 6.1.1 when Ω is convex.

CHAPTER 7
MULTIGRID ANALYSIS FOR THE MERIDIAN PROBLEM

We have seen in Chapter 6 that the error between the finite element approximation of (6–2) and the exact solution of (6–1) approaches zero as the meshsize approaches zero (Corollary 6.1.1) under certain assumptions. This means that we have to solve a large matrix system in order to get a good approximation to the meridian problem, since the size of the matrix system obtained by the edge finite element method corresponds to the number of edges in the mesh. Multigrid is an efficient iterative method that is used to solve a matrix system obtained by the finite element method (See Chapter 3 section 3.2). In this chapter, we will show that the multigrid "backslash" cycle converges at a uniform rate independent of the meshsize when applied to the meridian problem under the assumption that the rotation of the domain D, namely Ω, is convex. Notice that the meridian problem (6–1) is an indefinite problem. Techniques from [12, 26] provide a way to analyze the error reduction operator of the indefinite problem by using the error reduction operator of the related positive definite problem. In particular, it is well known [11] that multigrid, as an iterative method, is connected through a linear error reduction operator $\mathcal{E}$, i.e.,

$$\mathbf{x} - \mathbf{x}_{n+1} = \mathcal{E}(\mathbf{x} - \mathbf{x}_n),$$

where $\mathbf{x}$ is the exact solution and $\mathbf{x}_n$ denotes the n-th iteration result. In other words,

$$||\mathbf{x} - \mathbf{x}_n||_\Lambda \leq ||\mathcal{E}||_\Lambda^n ||\mathbf{x} - \mathbf{x}_0||_\Lambda,$$

where $\mathbf{x}_0$ is the initial value of the iteration. Therefore, if we show that

$$||\mathcal{E}||_\Lambda < \delta,$$

where $0 < \delta < 1$ is a constant independent of the meshsize, then the uniform convergence result of the multigrid will follow.

Now, let $\widetilde{\mathcal{E}}$ denote the error reduction operator of the multigrid algorithm when applied to the related positive definite problem $\Lambda(\mathbf{u}, \mathbf{v}) = (\mathbf{F}, \mathbf{v})_r$. In other words, the related positive definite problem is obtained by replacing $-\kappa^2$ in the meridian problem (6–1) by one. The first step is to show that

$$||\widetilde{\mathcal{E}}||_\Lambda < \widetilde{\delta},$$

where $0 < \widetilde{\delta} < 1$ is independent of the meshsize. Then we will show that $\left\|\mathcal{E} - \widetilde{\mathcal{E}}\right\|_\Lambda < Ch_1$, where h_1 is the coarsest meshsize in the sequence of meshes used in the multigrid algorithm, to conclude that

$$\begin{aligned} \|\mathcal{E}\|_\Lambda &\leq \left\|\mathcal{E} - \widetilde{\mathcal{E}}\right\|_\Lambda + \left\|\widetilde{\mathcal{E}}\right\|_\Lambda, \\ &< Ch_1 + \widetilde{\delta}. \end{aligned}$$

Hence, $\|\mathcal{E}\|_\Lambda < \delta$, where $\delta = Ch_1 + \widetilde{\delta}$, and we conclude that the multigrid algorithm converges at a uniform rate ($0 < \delta < 1$) when applied to the meridian problem given that the coarsest meshsize is sufficiently small.

Throughout this chapter, we will assume additionally that Ω is convex.

7.1 Multigrid Analysis for the Related Positive Definite Problem

In this section we provide a multigrid analysis for the following positive definite problem related to the meridian problem:

Find $\mathbf{u}_h \in \mathbf{W}_{h,\diamond}$ such that

$$(\mathrm{curl}_{rz}\mathbf{u}_h, \mathrm{curl}_{rz}\mathbf{v}_h)_r + (\mathbf{u}_h, \mathbf{v}_h)_r = (\mathbf{F}, \mathbf{v}_h)_r,$$

for all $\mathbf{v}_h \in \mathbf{W}_{h,\diamond}$. The results in this section are contained in [20].

7.1.1 The Multigrid Algorithm

Here, we present the multigrid V-cycle algorithm and state a uniform convergence result for the algorithm. We now assume the typical geometrical multigrid setting, where the discrete solution space is based on the finest mesh in a sequence of nested

refinements of a coarse mesh. Let $\mathscr{T}_1$ be the coarsest mesh subdividing D. Typically $\mathscr{T}_1$ is small enough so that the cost of solving our finite element problem on it is negligible. For $k = 2, 3, \ldots, J$, the mesh $\mathscr{T}_k$ is obtained from $\mathscr{T}_{k-1}$ by connecting the midpoints of all edges. We want to efficiently solve a finite element problem on the mesh $\mathscr{T}_J$ by multigrid.

The multilevel finite element spaces are Nédélec spaces on each of the meshes, i.e., let

$$\mathbf{W}_k = \{\mathbf{v} \in \mathbf{H}_{r,\diamond}(\mathrm{curl}, D) : \mathbf{v}|_K \in \mathbf{N}_1 \text{ for all } K \in \mathscr{T}_k\}.$$

Define $\Lambda_k : \mathbf{W}_k \to \mathbf{W}_k$ by

$$(\Lambda_k \mathbf{u}_k, \mathbf{v}_k)_r = \Lambda(\mathbf{u}_k, \mathbf{v}_k) \qquad \text{for all } \mathbf{u}_k, \mathbf{v}_k \in \mathbf{W}_k.$$

The multigrid algorithm we present is for solving a linear system on the finest level, of the type $\Lambda_J \mathbf{u} = \mathbf{f}$.

To describe the algorithm, we first need to define certain smoothing operators $\widetilde{R}_k : \mathbf{W}_k \mapsto \mathbf{W}_k$. These could be additive or multiplicative subspace correction operators based on any of the subspace decompositions of [1] and [27]. To describe them, first let $D_k^{\mathfrak{v}}$ denote the "vertex patch" domain formed by the union of all triangles in $\mathscr{T}_k$ connected to the mesh vertex $\mathfrak{v}$. Define $\mathbf{W}_k^{\mathfrak{v}} = \{\mathbf{v} \in \mathbf{W}_k : \mathrm{supp}(\mathbf{v}) \subseteq D_k^{\mathfrak{v}}\}$. For every mesh edge $\mathfrak{e}$, let $\Phi_{\mathfrak{e}}$ denote the Whitney edge basis function, and let $\mathbf{W}_k^{\mathfrak{e}}$ denote $\mathrm{span}(\Phi_{\mathfrak{e}})$. The decomposition of [1], adapted to our setting, is

$$\mathbf{W}_k = \sum_{\mathfrak{v} \in \mathscr{V}_k} \mathbf{W}_k^{\mathfrak{v}} + \sum_{\mathfrak{e} \in \mathscr{E}_k^*} \mathbf{W}_k^{\mathfrak{e}}, \tag{7–1}$$

where $\mathscr{V}_k$ is the set of nodes in the mesh $\mathscr{T}_k$ that are not on $\bar{\Gamma}_1$, and $\mathscr{E}_k^*$ is the set of edges of the mesh $\mathscr{T}_k$ that are not on Γ_1 but have both nodes on Γ_1. The last set $\mathscr{E}_k^*$ may appear "pathological," but it is needed in mixed boundary condition cases like ours, as its edges are not covered by any of the vertex patches in the first sum of (7–1).

To be clear, let us exhibit the decomposition for a $\mathbf{u}_k$ in $\mathbf{W}_k$. Let $\mathscr{E}_k$ denote the set of edges in the mesh that are not on Γ_1. Then the basis expansion of $\mathbf{u}_k$ is

$$\mathbf{u}_k = \sum_{\mathfrak{e}\in\mathscr{E}_k} c_{\mathfrak{e}}\Phi_{\mathfrak{e}}.$$

Now, for each $\mathfrak{v} \in \mathscr{V}_k$, define $\mathscr{E}^1_{k,\mathfrak{v}}$ and $\mathscr{E}^2_{k,\mathfrak{v}}$ as

$$\mathscr{E}^1_{k,\mathfrak{v}} = \left\{\mathfrak{e} \in \mathscr{E}_k : \text{ one endpoint of } \mathfrak{e} \text{ is } \mathfrak{v} \text{ and the other is on } \bar{\Gamma}_1\right\},$$
$$\mathscr{E}^2_{k,\mathfrak{v}} = \left\{\mathfrak{e} \in \mathscr{E}_k : \text{ one endpoint of } \mathfrak{e} \text{ is } \mathfrak{v} \text{ and the other is not on } \bar{\Gamma}_1\right\}.$$

When summing over the vertex patches, the edges of $\mathscr{E}^2_{k,\mathfrak{v}}$ are counted twice. Hence, setting

$$\mathbf{u}^{\mathfrak{v}}_k := \sum_{\mathfrak{e}\in\mathscr{E}^1_{k,\mathfrak{v}}} c_{\mathfrak{e}}\Phi_{\mathfrak{e}} + \sum_{\mathfrak{e}\in\mathscr{E}^2_{k,\mathfrak{v}}} \frac{1}{2} c_{\mathfrak{e}}\Phi_{\mathfrak{e}},$$

we have

$$\mathbf{u}_k = \sum_{\mathfrak{v}\in\mathscr{V}_k} \mathbf{u}^{\mathfrak{v}}_k + \sum_{\mathfrak{e}\in\mathscr{E}^*_k} c_{\mathfrak{e}}\Phi_{\mathfrak{e}}.$$

This shows that $\mathbf{W}_k$ can indeed be decomposed as in (7–1).

The other subspace decomposition, due to [27], reads as follows in our application:

$$\mathbf{W}_k = \sum_{\mathfrak{e}\in\mathscr{E}_k} \mathbf{W}^{\mathfrak{e}}_k + \sum_{\mathfrak{v}\in\mathscr{V}_k} \mathbf{grad}_{rz} V^{\mathfrak{v}}_k, \tag{7–2}$$

where $V^{\mathfrak{v}}_k$ is the (one-dimensional) space of continuous scalar functions supported on $D^{\mathfrak{v}}_k$ which are linear on each triangle of $D^{\mathfrak{v}}_k$ and vanish on $\partial D^{\mathfrak{v}}_k$.

We can use either (7–1) or (7–2) to construct additive or multiplicative smoothers. The details are standard, so we present only the algorithm for the block Gauss-Seidel type multiplicative smoothing iteration

$$\mathbf{u}_{i+1} = \widetilde{GS}_k(\mathbf{u}_i, \mathbf{f})$$

where the procedure $\widetilde{GS}_k(\cdot,\cdot)$ is given below.

Let $\mathbf{W}_{k,i}$, $i = 1, 2, \ldots, N_k$ be an enumeration of the subspaces in either of the decompositions (7–1) or (7–2). Define $\Lambda_{k,i} : \mathbf{W}_{k,i} \mapsto \mathbf{W}_{k,i}$ by

$$(\Lambda_{k,i}\mathbf{v}_i, \mathbf{w}_i)_r = \Lambda(\mathbf{v}_i, \mathbf{w}_i), \qquad \text{for all } \mathbf{v}_i, \mathbf{w}_i \text{ in } \mathbf{W}_{k,i}.$$

Let the $L^2_r(D)^2$-orthogonal projection onto $\mathbf{W}_{k,i}$ be denoted by $Q_{k,i}$.

Algorithm 7.1.1 (Multiplicative smoothing). Given $\mathbf{u}_i$ in $\mathbf{W}_k$, calculate $\mathbf{u}_{i+1} = \widetilde{GS}_k(\mathbf{u}_i, \mathbf{f})$ in $\mathbf{W}_k$ as follows:

1. Set $\mathbf{u}_i^{(0)} = \mathbf{u}_i$.
2. For $j = 1, 2, \ldots, N_k$, compute
$$\mathbf{u}_i^{(j)} = \mathbf{u}_i^{(j-1)} + \Lambda_{k,j}^{-1} Q_{k,j}(\mathbf{f} - \Lambda_k \mathbf{u}_i^{(j-1)}).$$
3. Set the result $\mathbf{u}_{i+1}$ to be $\mathbf{u}_i^{(N_k)}$.

Standard arguments show that this iteration can be rewritten as

$$\mathbf{u}_{i+1} = \mathbf{u}_i + \widetilde{R}_k(\mathbf{f} - \Lambda_k \mathbf{u}_i),$$

with

$$\widetilde{R}_k = (I - (I - \widetilde{P}_{k,N_k})(I - \widetilde{P}_{k,N_k-1}) \cdots (I - \widetilde{P}_{k,1}))\Lambda_k^{-1},$$

where $\widetilde{P}_{k,j}$ is the orthogonal projection into $\mathbf{W}_{k,j}$ in the $\Lambda(\cdot,\cdot)$-inner product.

With such a smoother $\widetilde{R}_k$, or an additive Jacobi type smoother based on the same decompositions (whose details we omit), we can now describe the multigrid algorithm. Let the $L^2_r(D)^2$-orthogonal projection onto $\mathbf{W}_k$ be denoted by Q_k.

Algorithm 7.1.2 (V-cycle). Given $\mathbf{u}$ and $\mathbf{f}$ in $\mathbf{W}_k$, define the output $MG_k(\mathbf{u}, \mathbf{f})$ in $\mathbf{W}_k$ by the following recursive procedure:

1. Set $MG_1(\mathbf{u}, \mathbf{f}) = \Lambda_1^{-1}\mathbf{f}$.
2. For $k > 1$, define $MG_k(\mathbf{u}, \mathbf{f})$ recursively:
   (a) $\mathbf{v}^{(1)} = \mathbf{u} + \widetilde{R}_k(\mathbf{f} - \Lambda_k \mathbf{u})$.
   (b) $\mathbf{v}^{(2)} = \mathbf{v}^{(1)} + MG_{k-1}(\mathbf{0}, Q_{k-1}(\mathbf{f} - \Lambda_k \mathbf{v}^{(1)}))$.

(c) $\mathbf{v}^{(3)} = \mathbf{v}^{(2)} + \widetilde{R}_k^t(\mathbf{f} - \Lambda_k \mathbf{v}^{(2)})$.

(d) Set $MG_k(\mathbf{u}, \mathbf{f}) = \mathbf{v}^{(3)}$.

It is well known [11] that the V-cycle iterates $\mathbf{x}_{i+1} = MG_k(\mathbf{x}_i, \mathbf{f})$, approximating the exact solution $\mathbf{x} = \Lambda_k^{-1}\mathbf{f}$, are connected through a linear error reduction operator $\widetilde{\mathcal{E}}_k$, i.e.,

$$\mathbf{x} - \mathbf{x}_{i+1} = \widetilde{\mathcal{E}}_k(\mathbf{x} - \mathbf{x}_i).$$

The following is our main result on the convergence of the V-cycle algorithm. Its proof is given in the next section.

Theorem 7.1.1. *There exists a positive number $\widetilde{\delta} < 1$ such that*

$$0 \;\le\; \Lambda(\widetilde{\mathcal{E}}_k \mathbf{u}, \mathbf{u}) \;\le\; \widetilde{\delta}\, \Lambda(\mathbf{u}, \mathbf{u}), \qquad \textit{for all } \mathbf{u} \textit{ in } \mathbf{W}_k \textit{ and all } k \ge 1.$$

The number $\widetilde{\delta}$ is independent of the meshsize and refinement level.

7.1.2 Multigrid Analysis

In this subsection, we prove Theorem 7.1.1 by verifying two conditions in a standard abstract framework for multigrid analysis [1, 10, 11, 14]. We state the conditions and its implication as the next lemma and omit its well known proof. The analysis of this section is heavily based on the techniques introduced in [1]. Let $\widetilde{P}_k$ denote the orthogonal projection into $\mathbf{W}_k$ in the $\Lambda(\cdot,\cdot)$-inner product.

Lemma 7.1.1. *The assertion of Theorem 7.1.1 follows from the two conditions below:*

1. Existence of a stable decomposition: *There exists a constant $C_1 > 0$ independent of the meshsizes and k, such that for all $\mathbf{v}$ in $(I - \widetilde{P}_{k-1})\mathbf{W}_k$, there is a decomposition*

$$\mathbf{v} = \sum_{j=1}^{N_k} \mathbf{v}_j, \qquad \textit{with } \mathbf{v}_j \textit{ in } \mathbf{W}_{k,j},$$

satisfying

$$\sum_{j=1}^{N_k} \Lambda(\mathbf{v}_j, \mathbf{v}_j) \le C_1 \Lambda(\mathbf{v}, \mathbf{v}).$$

2. Limited interaction: *There exists a constant $C_2 > 0$, independent of k, such that*

$$\sum_{j=1}^{N_k}\sum_{l=1}^{N_k}|\Lambda(\mathbf{v}_j,\mathbf{w}_l)| \le C_2\left(\sum_{j=1}^{N_k}\Lambda(\mathbf{v}_j,\mathbf{v}_j)\right)^{\frac{1}{2}}\left(\sum_{l=1}^{N_k}\Lambda(\mathbf{w}_l,\mathbf{w}_l)\right)^{\frac{1}{2}}$$

for all $\mathbf{v}_j$ in $\mathbf{W}_{k,j}$, $\mathbf{w}_l$ in $\mathbf{W}_{k,l}$, and $k \ge 1$.

The remainder of this section is devoted to the verification of the two conditions of Lemma 7.1.1. Note that the first condition only involves functions on two levels, k and $k-1$. The second involves an inequality of functions in just one level k. For this reason, we can simplify our notation and use subscripts H and h for $k-1$ and k, respectively. The mesh $\mathscr{T}_h$ is a refinement of $\mathscr{T}_H$, and $H = 2h$. Previously defined notations with these new subscripts have the obvious definitions, e.g., Π_H^S denotes the weighted $L_r^2(D)$-orthogonal projection into S_H, the space of piecewise constant functions with respect to the mesh $\mathscr{T}_H$, etc. Before verifying the conditions, we need a number of preliminary results.

Lemma 7.1.2. *For all p_h in S_h,*

$$\left\|p_h - \Pi_H^S p_h\right\|_r \le CH\left\|\mathrm{curl}'_{rz}p_h\right\|_r. \tag{7–3}$$

Proof. Given p_h in S_h, define $\mathbf{z}$ in $\mathbf{H}_{r,\diamond}(\mathrm{curl}, D)$ and p in $L_r^2(D)$ as the solution of (5–1) with $f = \mathrm{curl}_{rz}\mathrm{curl}'_{rz}p_h$, i.e.,

$$\begin{aligned}(\mathbf{z},\mathbf{w})_r - (p,\mathrm{curl}_{rz}\mathbf{w})_r &= 0 && \text{for all } \mathbf{w} \text{ in } \mathbf{H}_{r,\diamond}(\mathrm{curl}, D),\\ (s,\mathrm{curl}_{rz}\mathbf{z})_r &= (s,\mathrm{curl}_{rz}\mathrm{curl}'_{rz}p_h)_r && \text{for all } s \text{ in } L_r^2(D).\end{aligned}$$

Then, with $\mathbf{z}_h = \mathrm{curl}'_{rz}p_h$, the pair $\{\mathbf{z}_h,\ p_h\}$ obviously satisfies

$$\begin{aligned}(\mathbf{z}_h,\mathbf{w}_h)_r - (p_h,\mathrm{curl}_{rz}\mathbf{w}_h)_r &= 0 && \text{for all } \mathbf{w}_h \text{ in } \mathbf{W}_{h,\diamond},\\ (s_h,\mathrm{curl}_{rz}\mathbf{z}_h)_r &= (s_h,\mathrm{curl}_{rz}\mathrm{curl}'_{rz}p_h)_r && \text{for all } s_h \text{ in } S_h.\end{aligned}$$

Moreover,

$$\mathrm{curl}_{rz}\mathbf{z} = \mathrm{curl}_{rz}\mathbf{z}_h \qquad \text{in } L_r^2(D). \tag{7–4}$$

By the triangle inequality,

$$\left\|p_h - \Pi_H^S p_h\right\|_r \leq \|p_h - p\|_r + \left\|p - \Pi_H^S p\right\|_r + \left\|\Pi_H^S p - \Pi_H^S p_h\right\|_r . \tag{7–5}$$

We now estimate each of the terms on the right hand side above.

Beginning with the middle term, and using a standard weighted norm approximation estimate (see e.g. [3, 13]), we have

$$\left\|p - \Pi_H^S p\right\|_r^2 \leq CH^2 \left|p\right|_{H_r^1(D)}^2 \leq CH^2\big(\|p\|_{H_r^1(D)}^2 + \|r^{-1}p\|_r^2\big).$$

The right hand side is bounded because p is in $\widetilde{H}_r^2(D)$, by Theorem 5.1.2. Moreover, as in [25, Proposition 3.1], it can be bounded further by $CH^2(\|r^{-1}\partial_r(rp)\|_r^2 + \|\partial_z p\|_r^2)$, which is the same as $CH^2\|\mathbf{curl}_{rz}p\|_r^2$. Thus,

$$\left\|p - \Pi_H^S p\right\|_r \leq CH\|\mathbf{curl}_{rz}p\|_r. \tag{7–6}$$

Furthermore, since

$$\begin{aligned}
\|\mathbf{curl}_{rz}p\|_r^2 &= (\mathbf{curl}_{rz}p, \mathbf{z})_r && \text{cf. (5–10)},\\
&= (p, \mathrm{curl}_{rz}\mathbf{z})_r && \text{by (2–8)},\\
&= (p, \mathrm{curl}_{rz}\mathbf{z}_h)_r && \text{by (7–4)},\\
&= (\mathbf{curl}_{rz}p, \mathbf{z}_h)_r && \text{by (2–8)},\\
&= (\mathbf{curl}_{rz}p, \mathrm{curl}'_{rz}p_h)_r,
\end{aligned}$$

by the Cauchy-Schwarz inequality, we obtain $\|\mathbf{curl}_{rz}p\|_r \leq \|\mathrm{curl}'_{rz}p_h\|_r$. Thus (7–6) yields

$$\left\|p - \Pi_H^S p\right\|_r \leq CH \left\|\mathrm{curl}'_{rz}p_h\right\|_r . \tag{7–7}$$

Next, consider the first term on the right hand side of (7–5). Using triangle inequality,

$$\|p - p_h\|_r \leq \left\|p - \Pi_h^S p\right\|_r + \left\|\Pi_h^S p - p_h\right\|_r .$$

The term $\left\|p - \Pi_h^S p\right\|_r$ can be bounded by the same type of argument that led to (7–7). Theorem 5.1.3 item 3 provides a bound for the other term. Then the inverse estimate [3, Lemma 4] yields

$$\begin{aligned} \|p - p_h\|_r &\leq Ch \|\mathrm{curl}'_{rz} p_h\|_r + Ch^2 \|\mathrm{curl}_{rz}\mathrm{curl}'_{rz} p_h\|_r , \\ &\leq Ch \|\mathrm{curl}'_{rz} p_h\|_r . \end{aligned} \tag{7–8}$$

The only remaining term on the right hand side of (7–5) is bounded by using (7–8) and the fact that orthogonal projectors have unit norm:

$$\left\|\Pi_H^S p - \Pi_H^S p_h\right\|_r \leq \|p - p_h\|_r \leq Ch \|\mathrm{curl}'_{rz} p_h\|_r . \tag{7–9}$$

Collecting the estimates of (7–7), (7–8) and (7–9) in (7–5), we have

$$\left\|p_h - \Pi_H^S p_h\right\|_r \leq C(H + h) \|\mathrm{curl}'_{rz} p_h\|_r .$$

Since $h \leq CH$, this completes the proof. □

The next lemma is crucial in proving the uniform convergence of the multigrid V-cycle and is modeled after the lemmas in [1]. We shall make significant use of the weighted discrete Helmholtz decomposition discussed in Section 4.1. Recall that as per our previous remarks on the notation, $\widetilde{P}_H$ denotes the Λ-orthogonal projection into the coarser of the two spaces.

Lemma 7.1.3. *Let $\mathbf{w}_h$ be in $\mathbf{W}_{h,\diamond}$. If the weighted discrete Helmholtz decomposition of $\mathbf{w}_h - \widetilde{P}_H \mathbf{w}_h$ is*

$$\mathbf{w}_h - \widetilde{P}_H \mathbf{w}_h = \mathbf{grad}_{rz}\phi_h + \mathrm{curl}'_{rz} a_h,$$

with ϕ_h in $V_{h,\diamond}$ and a_h in S_h, then

$$\begin{aligned} \|\phi_h\|_r &\leq CH \left\|(I - \widetilde{P}_H)\mathbf{w}_h\right\|_r , \\ \|\mathrm{curl}'_{rz} a_h\|_r &\leq CH \left\|(I - \widetilde{P}_H)\mathbf{w}_h\right\|_\Lambda . \end{aligned}$$

Proof. We first prove the second inequality. Define $\mathbf{z}_h$ in $\mathbf{W}_{h,\diamond}$, given the above a_h, by

$$\Lambda(\mathbf{z}_h, \mathbf{q}_h) = (\mathrm{curl}'_{rz} a_h, \mathbf{q}_h)_r \qquad \text{for all } \mathbf{q}_h \text{ in } \mathbf{W}_{h,\diamond}. \tag{7–10}$$

Observe that $\mathbf{z}_h$ is orthogonal to $\mathbf{grad}_{rz} V_{h,\diamond}$. By setting $\mathbf{q}_h = \mathrm{curl}'_{rz} a_h$ above,

$$\begin{aligned}
\|\mathrm{curl}'_{rz} a_h\|_r^2 &= \Lambda(\mathbf{z}_h, \mathrm{curl}'_{rz} a_h), \\
&= \Lambda(\mathbf{z}_h, (I - \widetilde{P}_H)\mathbf{w}_h - \mathbf{grad}_{rz}\phi_h), && (7–11)\\
&= \Lambda(\mathbf{z}_h, (I - \widetilde{P}_H)\mathbf{w}_h), \\
&= \Lambda(\mathbf{z}_h - \mathbf{z}_H, (I - \widetilde{P}_H)\mathbf{w}_h), && (7–12)\\
&\le \|\mathbf{z}_h - \mathbf{z}_H\|_\Lambda \left\|(I - \widetilde{P}_H)\mathbf{w}_h\right\|_\Lambda, && (7–13)
\end{aligned}$$

for any $\mathbf{z}_H$ in $\mathbf{W}_{H,\diamond}$. Next, we choose a suitable $\mathbf{z}_H$ and estimate $\|\mathbf{z}_h - \mathbf{z}_H\|_\Lambda$.

To this end, first define $\mathbf{z}$ in $\mathbf{H}_{r,\diamond}(\mathrm{curl}, D)$, given the above $\mathbf{z}_h$, by (5–1) with $f = \mathrm{curl}_{rz}\mathbf{z}_h$, i.e.,

$$\begin{aligned}
(\mathbf{z}, \mathbf{w})_r - (p, \mathrm{curl}_{rz}\mathbf{w})_r &= 0 && \text{for all } \mathbf{w} \text{ in } \mathbf{H}_{r,\diamond}(\mathrm{curl}, D),\\
(s, \mathrm{curl}_{rz}\mathbf{z})_r &= (s, \mathrm{curl}_{rz}\mathbf{z}_h)_r && \text{for all } s \text{ in } L^2_r(D).
\end{aligned}$$

Then define $\mathbf{z}_H$ in $\mathbf{W}_{H,\diamond}$ by the analogue of (5–14) on the coarser of the meshes, i.e.,

$$\begin{aligned}
(\mathbf{z}_H, \mathbf{w}_H)_r - (p_H, \mathrm{curl}_{rz}\mathbf{w}_H)_r &= 0 && \text{for all } \mathbf{w}_H \text{ in } \mathbf{W}_{H,\diamond},\\
(s_H, \mathrm{curl}_{rz}\mathbf{z}_H)_r &= (s_H, \mathrm{curl}_{rz}\mathbf{z}_h)_r && \text{for all } s_H \text{ in } S_H.
\end{aligned}$$

Since $\mathbf{z}_h$ is orthogonal to $\mathbf{grad}_{rz} V_{h,\diamond}$, it is clear that $\mathbf{z}_h$ is in the range of curl'_{rz} by the weighted discrete Helmholtz decomposition of $\mathbf{W}_{h,\diamond}$. Thus, there is a unique p_h in S_h such that $\mathrm{curl}'_{rz} p_h = \mathbf{z}_h$. In other words,

$$(\mathbf{z}_h, \mathbf{w}_h)_r - (p_h, \mathrm{curl}_{rz}\mathbf{w}_h)_r = 0 \qquad \text{for all } \mathbf{w}_h \text{ in } \mathbf{W}_{h,\diamond},$$

which is the first equation of the formulation (5–14). The second equation of (5–14) is also satisfied by $\mathbf{z}_h$ trivially since $f = \mathrm{curl}_{rz}\mathbf{z}_h$. Therefore, by Theorem 5.1.3 item 2,

$$\|\mathbf{z} - \mathbf{z}_h\|_r = \left\|\mathbf{z} - \Pi_h^W \mathbf{z}\right\|_r ,$$
$$\|\mathbf{z} - \mathbf{z}_H\|_r = \left\|\mathbf{z} - \Pi_H^W \mathbf{z}\right\|_r ,$$

which implies

$$\begin{aligned} \|\mathbf{z}_h - \mathbf{z}_H\|_r &\le \left\|\mathbf{z} - \Pi_h^W \mathbf{z}\right\|_r + \left\|\mathbf{z} - \Pi_H^W \mathbf{z}\right\|_r && \text{by the triangle inequality,} \\ &\le CH|\mathbf{z}|_{H_r^1(D)^2} && \text{by Corollary 4.1.1,} \\ &\le CH\,\|\mathrm{curl}_{rz}\mathbf{z}_h\|_r && \text{by Theorem 5.1.2.} \end{aligned} \tag{7–14}$$

We also need to estimate $\|\mathrm{curl}_{rz}(\mathbf{z}_h - \mathbf{z}_H)\|_r$. By the definition of $\mathbf{z}_H$ and Lemma 7.1.2,

$$\begin{aligned} \|\mathrm{curl}_{rz}(\mathbf{z}_h - \mathbf{z}_H)\|_r &= \left\|\mathrm{curl}_{rz}\mathbf{z}_h - \Pi_H^S \mathrm{curl}_{rz}\mathbf{z}_h\right\|_r , \\ &\le CH\,\|\mathrm{curl}'_{rz}\mathrm{curl}_{rz}\mathbf{z}_h\|_r . \end{aligned}$$

Combining this with (7–14), we get

$$\|\mathbf{z}_h - \mathbf{z}_H\|_\Lambda^2 \le CH^2\big(\,\|\mathrm{curl}_{rz}\mathbf{z}_h\|_r^2 + \|\mathrm{curl}'_{rz}\mathrm{curl}_{rz}\mathbf{z}_h\|_r^2\,\big) \tag{7–15}$$

This estimate is not yet in a form we can use in (7–13). To simplify its right hand side, define $\Lambda_h : \mathbf{W}_{h,\diamond} \to \mathbf{W}_{h,\diamond}$ by

$$(\Lambda_h \mathbf{v}_h, \mathbf{w}_h)_r = \Lambda(\mathbf{v}_h, \mathbf{w}_h) \qquad \text{for all } \mathbf{w}_h \text{ in } \mathbf{W}_{h,\diamond},$$

we observe that $\Lambda_h \mathbf{z}_h = \mathrm{curl}'_{rz} a_h$ by (7–10), and

$$\begin{aligned}
\|\Lambda_h \mathbf{z}_h\|_r^2 &= (\Lambda_h \mathbf{z}_h, \Lambda_h \mathbf{z}_h)_r = \Lambda(\mathbf{z}_h, \Lambda_h \mathbf{z}_h), \\
&= (\mathbf{z}_h, \Lambda_h \mathbf{z}_h)_r + (\mathrm{curl}_{rz} \mathbf{z}_h, \mathrm{curl}_{rz}(\Lambda_h \mathbf{z}_h))_r, \\
&= \Lambda(\mathbf{z}_h, \mathbf{z}_h) + \Lambda(\mathrm{curl}'_{rz} \mathrm{curl}_{rz} \mathbf{z}_h, \mathbf{z}_h), \\
&= \|\mathbf{z}_h\|_r^2 + 2\,\|\mathrm{curl}_{rz} \mathbf{z}_h\|_r^2 + \|\mathrm{curl}'_{rz} \mathrm{curl}_{rz} \mathbf{z}_h\|_r^2 .
\end{aligned}$$

Hence, returning to (7–15) and overestimating its right hand side,

$$\|\mathbf{z}_h - \mathbf{z}_H\|_\Lambda^2 \le CH^2\,\|\Lambda_h \mathbf{z}_h\|_r^2 = CH^2\,\|\mathrm{curl}'_{rz} a_h\|_r^2 .$$

Using this estimate in (7–13), we have

$$\|\mathrm{curl}'_{rz} a_h\|_r^2 \le\ CH\,\|\mathrm{curl}'_{rz} a_h\|_r\ \|(I - \widetilde{P}_H)\mathbf{w}_h\|_\Lambda,$$

from which the second inequality of the lemma follows.

It now only remains to prove the first estimate of the lemma. Let ψ in $H^1_{r,\diamond}(D)$ be the unique solution (see [25]) of

$$(\mathbf{grad}_{rz}\psi, \mathbf{grad}_{rz}\eta)_r = (\phi_h, \eta)_r \qquad \text{for all } \eta \text{ in } H^1_{r,\diamond}(D). \tag{7–16}$$

Then [25, Theorem 2.1] gives the regularity estimate

$$|\psi|_{H^2_r(D)} \le C\,\|\phi_h\|_r . \tag{7–17}$$

Observe that for any ψ_H in $V_{H,\diamond}$,

$$\begin{aligned}
(\mathbf{grad}_{rz}\phi_h, \mathbf{grad}_{rz}\psi_H)_r &= \Lambda(\mathbf{grad}_{rz}\phi_h, \mathbf{grad}_{rz}\psi_H), \\
&= \Lambda(\mathbf{w}_h - \widetilde{P}_H \mathbf{w}_h, \mathbf{grad}_{rz}\psi_H) = 0.
\end{aligned} \tag{7–18}$$

We will use this with $\psi_H = \widehat{\Pi}_H^V \psi$, where $\widehat{\Pi}_H^V$ is the previously mentioned projection of [21]. Proceeding by a standard duality argument [33],

$$\begin{aligned}
\|\phi_h\|_r^2 = (\phi_h, \phi_h)_r &= (\mathbf{grad}_{rz}\psi, \mathbf{grad}_{rz}\phi_h)_r && \text{by (7–16)},\\
&= (\mathbf{grad}_{rz}\psi - \mathbf{grad}_{rz}\widehat{\Pi}_H^V\psi, \mathbf{grad}_{rz}\phi_h)_r && \text{by (7–18)},\\
&\le CH|\psi|_{H_r^2(D)} \|\mathbf{grad}_{rz}\phi_h\|_r && \text{by [21, Lemma 5.3]},\\
&\le CH \|\phi_h\|_r \|\mathbf{grad}_{rz}\phi_h\|_r && \text{by (7–17)}.
\end{aligned}$$

Canceling the common factor, and using the stability estimate (4–4),

$$\begin{aligned}
\|\phi_h\|_r &\le CH \|\mathbf{grad}_{rz}\phi_h\|_r ,\\
&\le CH \left\|\mathbf{w}_h - \widetilde{P}_H \mathbf{w}_h\right\|_r ,
\end{aligned}$$

which finishes the proof of the lemma. □

We can now prove the convergence of multigrid as an iterative method.

Proof of Theorem 7.1.1. By Lemma 7.1.1, we only need to verify the two conditions there. For verifying the second condition on the limited interaction of smoothing subspaces, we can use standard techniques [1, 14]. Hence we omit it.

Let us now verify the first condition on the existence of a stable decomposition for the case of the smoothing subspaces of [1], namely (7–1). Given any $\mathbf{w}_k$ in $(I - \widetilde{P}_{k-1})\mathbf{W}_k$, let

$$\mathbf{w}_k = \mathbf{grad}_{rz}\phi_k + \mathbf{r}_k$$

be its weighted discrete Helmholtz decomposition, with ϕ_k in $V_k = \{v \in H^1_{r,\diamond}(D) : v|_K \in P_1$ for all $K \in \mathscr{T}_k\}$ and $\mathbf{r}_k$ in $\mathbf{W}_k$. By Lemma 7.1.3,

$$\|\phi_k\|_r \le Ch_{k-1} \|\mathbf{w}_k\|_r , \tag{7–19}$$

$$\|\mathbf{r}_k\|_r \le Ch_{k-1} \|\mathbf{w}_k\|_\wedge . \tag{7–20}$$

Let $V_k^{\mathfrak{v}} = \{v \in V_k : \mathrm{supp}(v) \subseteq D_k^{\mathfrak{v}}\}$. Then, by using the decomposition

$$V_k = \sum_{\mathfrak{v}\in\mathscr{V}_k} V_k^{\mathfrak{v}}, \tag{7–21}$$

we split

$$\phi_k = \sum_{\mathfrak{v}\in\mathscr{V}_k} \phi_k^{\mathfrak{v}}, \qquad \text{with } \phi_k^{\mathfrak{v}} \text{ in } V_k^{\mathfrak{v}},$$

while we split $\mathbf{r}_k$ by the decomposition of (7–1) as

$$\mathbf{r}_k = \sum_{\mathfrak{v}\in\mathscr{V}_k} \mathbf{r}_k^{\mathfrak{v}} + \sum_{\mathfrak{e}\in\mathscr{E}_k^*} \mathbf{r}_k^{\mathfrak{e}}, \qquad \text{with } \mathbf{r}_k^{\mathfrak{v}} \text{ in } \mathbf{W}_k^{\mathfrak{v}},\ \mathbf{r}_k^{\mathfrak{e}} \text{ in } \mathbf{W}_k^{\mathfrak{e}}.$$

Setting $\mathbf{w}_k^{\mathfrak{v}} = \mathbf{grad}_{rz}\phi_k^{\mathfrak{v}} + \mathbf{r}_k^{\mathfrak{v}}$, we want to show that

$$\sum_{\mathfrak{v}\in\mathscr{V}_k} \Lambda(\mathbf{w}_k^{\mathfrak{v}}, \mathbf{w}_k^{\mathfrak{v}}) + \sum_{\mathfrak{e}\in\mathscr{E}_k^*} \Lambda(\mathbf{r}_k^{\mathfrak{e}}, \mathbf{r}_k^{\mathfrak{e}}) \le C\Lambda(\mathbf{w}_k, \mathbf{w}_k). \tag{7–22}$$

Expanding the terms and using the orthogonality of the discrete Helmholtz decomposition and the weighted inverse estimate [3, Lemma 4], we obtain

$$\begin{aligned}
\sum_{\mathfrak{v}\in\mathscr{V}_k} \|\mathbf{w}_k^{\mathfrak{v}}\|_\Lambda^2 + \sum_{\mathfrak{e}\in\mathscr{E}_k^*} \|\mathbf{r}_k^{\mathfrak{e}}\|_\Lambda^2 &= \sum_{\mathfrak{v}\in\mathscr{V}_k} \|\mathbf{grad}_{rz}\phi_k^{\mathfrak{v}} + \mathbf{r}_k^{\mathfrak{v}}\|_\Lambda^2 + \sum_{\mathfrak{e}\in\mathscr{E}_k^*} \|\mathbf{r}_k^{\mathfrak{e}}\|_\Lambda^2, \\
&= \sum_{\mathfrak{v}\in\mathscr{V}_k} \left(\|\mathbf{grad}_{rz}\phi_k^{\mathfrak{v}}\|_r^2 + \|\mathbf{r}_k^{\mathfrak{v}}\|_r^2 + \|\mathrm{curl}_{rz}\mathbf{r}_k^{\mathfrak{v}}\|_r^2 \right) + \sum_{\mathfrak{e}\in\mathscr{E}_k^*} \|\mathbf{r}_k^{\mathfrak{e}}\|_\Lambda^2, \\
&\le C \sum_{\mathfrak{v}\in\mathscr{V}_k} \left(h_k^{-2} \|\phi_k^{\mathfrak{v}}\|_r^2 + (1 + h_k^{-2}) \|\mathbf{r}_k^{\mathfrak{v}}\|_r^2 \right) + C \sum_{\mathfrak{e}\in\mathscr{E}_k^*} h_k^{-2} \|\mathbf{r}_k^{\mathfrak{e}}\|_r^2, \\
&\le C h_k^{-2} \left(\|\phi_k\|_r^2 + \|\mathbf{r}_k\|_r^2 \right).
\end{aligned}$$

By (7–19) and (7–20),

$$\sum_{\mathfrak{v}\in\mathscr{V}_k} \|\mathbf{w}_k^{\mathfrak{v}}\|_\Lambda^2 + \sum_{\mathfrak{e}\in\mathscr{E}_k^*} \|\mathbf{r}_k^{\mathfrak{e}}\|_\Lambda^2 \le C h_k^{-2} h_{k-1}^2 \|\mathbf{w}_k\|_\Lambda^2,$$

which proves (7–22). Thus the condition on the existence of the stable decomposition is verified for the smoothing subspaces of (7–1).

A similar and simpler argument verifies the existence of a stable decomposition for the subspaces of (7–2) as well. We omit the details. □

7.1.3 Numerical Results

In this subsection, we will report the iteration counts for the multigrid V-cycle applied to $\Lambda_h \mathbf{x} = f$ for a few choices of the domain and f. Note that the V-cycle operator can also be used as a preconditioner for Λ_h and numerical experiments using it so have already been reported in [21] in the context of solving a div-curl system.

We will verify the uniform convergence of the multigrid V-cycle algorithm for $\Lambda_h \mathbf{x} = f$. We apply the V-cycle algorithm to the three different domains shown in Figure 7-1. Domain I is convex and its revolution is also convex, while Domain II is convex, but its revolution is nonconvex, and Domain III and its revolution are both nonconvex. The initial mesh (level 1) for domain I and II consists of two congruent right triangles, and for domain III, it consists of four congruent right triangles. In all cases, we obtain the next level mesh by connecting the edge midpoints of all triangles.

Table 7-1 reports the convergence rate when $f = 0$. We apply the Gauss-Seidel smoother with the subspace decomposition (7–2). For succesive finite element spaces $\mathbf{W}_{H,\diamond} \subset \mathbf{W}_{h,\diamond}$, the prolongation matrix that we used for implementation is the matrix whose (i,j)-th entry is $\int_{e_i} \phi_j \cdot \mathbf{t}_i ds$, where e_i denotes the i-th edge of mesh $\mathscr{T}_h$ that is not on Γ_1, $\mathbf{t}_i$ denotes the unit tangent vector of this edge, and ϕ_j is the j-th basis function of $\mathbf{W}_{H,\diamond}$. The restriction matrix is the transpose of the prolongation matrix. For each fine level mesh, the initial value $\mathbf{x}_0$ was chosen randomly in C++. The stopping criterion is $\|\mathbf{x}_n\|_\Lambda / \|\mathbf{x}_0\|_\Lambda < 10^{-7}$, where $\mathbf{x}_n$ is the result of the n-th iteration (which measures the reduction in the error since the exact solution is zero). The convergence rate is computed by taking the average of $\|\mathbf{x}_n\|_\Lambda / \|\mathbf{x}_{n-1}\|_\Lambda$.

As we see from the table, the convergence rate is nearly constant and seems bounded independently of the meshsize. Additionally, although we assumed that the revolution of the two-dimensional domain is convex throughout the paper in order to

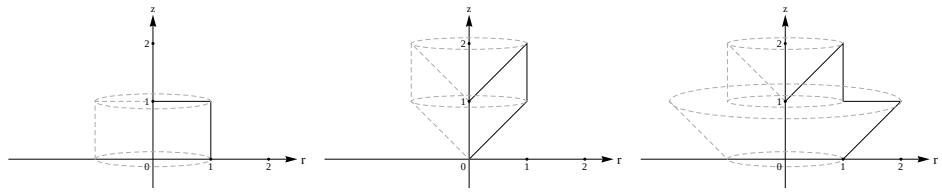

A Domain I B Domain II C Domain III

Figure 7-1. Domains

Table 7-1. V-cycle convergence rates

	Convergence rate		
Level	Domain I	Domain II	Domain III
2	0.27	0.29	0.32
3	0.37	0.35	0.41
4	0.43	0.41	0.40
5	0.42	0.40	0.40
6	0.41	0.41	0.41
7	0.41	0.41	0.41
8	0.41	0.41	0.41
9	0.41	0.41	0.41

prove the uniform convergence result, it appears that even when the revolution of the domain is nonconvex, the convergence rate is independent of the meshsize.

7.2 Multigrid Analysis for the Indefinite Problem

In this section, we will study the multigrid backslash cycle. We will also state our main theorem that implies the uniform convergence of the multigrid backslash cycle independent of the meshsize when applied to the discrete meridian problem (6–2) provided that the coarsest mesh is sufficiently fine.

It was shown in Chapter 6 that if the indefinite problem (6–1) is uniquely solvable, then the discrete problem (6–2) is also well-posed, and that the discrete solution of (6–2) approximates the exact solution of (6–1) given that the meshsize is sufficiently small. Therefore, throughout this section, we assume that (6–1) has a unique solution and that all meshes considered here have small enough meshsize so that this result (Theorem 6.1.1) holds.

7.2.1 The Multigrid Algorithm

As in section 7.1, we assume that we have a sequence of nested triangulations of D, which we will denote by $\mathscr{T}_k$ for the kth mesh where $k = 1, \cdots, J$. $\mathscr{T}_1$ is the coarsest mesh while $\mathscr{T}_J$ is the finest mesh. Let h_k be the representative meshsize of $\mathscr{T}_k$. We will later see that for theoretical and practical purposes, the initial meshsize h_1 must be sufficiently small. Let $\mathbf{W}_k$ be the finite element subspace $\mathbf{W}_{h,\diamond}$ with respect to $\mathscr{T}_k$ (See section 7.1.1). Define $P_k : \mathbf{H}_{r,\diamond}(\text{curl}, D) \to \mathbf{W}_k$ to be the orthogonal projection with respect to $A(\cdot,\cdot)$, where

$$A(\mathbf{u}, \mathbf{v}) = (\text{curl}_{rz}\mathbf{u}, \text{curl}_{rz}\mathbf{v})_r - \kappa^2(\mathbf{u}, \mathbf{v})_r$$

as in Chapter 6. Recall that $Q_k : \mathbf{H}_{r,\diamond}(\text{curl}, D) \to \mathbf{W}_k$ is the orthogonal projection with respect to the L^2_r-inner product, i.e.,

$$A(P_k\mathbf{u}, \mathbf{v}_k) = A(\mathbf{u}, \mathbf{v}_k) \text{ for all } \mathbf{v}_k \in \mathbf{W}_k,$$

$$(Q_k\mathbf{u}, \mathbf{v}_k)_r = (\mathbf{u}, \mathbf{v}_k)_r \text{ for all } \mathbf{v}_k \in \mathbf{W}_k.$$

Note that P_k is well-defined since we are assuming the unique solvability of (6–1). We also define $A_k : \mathbf{H}_{r,\diamond}(\text{curl}, D) \to \mathbf{W}_k$ by

$$(A_k\mathbf{u}, \mathbf{v}_k)_r = A(\mathbf{u}, \mathbf{v}_k) \text{ for all } \mathbf{v} \in \mathbf{W}_k.$$

Since the meshes are nested,

$$\mathbf{W}_1 \subset \cdots \subset \mathbf{W}_J,$$

and $\mathbf{W}_J$ is the finite element subspace in which we will solve the given problem, but we go through each $\mathbf{W}_k$ as the following algorithm illustrates.

Algorithm 7.2.1 (backslash cycle). Given $\mathbf{u}$ and $\mathbf{f}$ in $\mathbf{W}_k$, define the output $MG_k(\mathbf{u}, \mathbf{f})$ in $\mathbf{W}_k$ by the following recursive procedure:

1. Set $MG_1(\mathbf{u}, \mathbf{f}) = A_1^{-1}\mathbf{f}$.

2. For $k > 1$, define $MG_k(\mathbf{u}, \mathbf{f})$ recursively:

(a) $\mathbf{v}^{(1)} = \mathbf{u} + R_k(\mathbf{f} - A_k\mathbf{u})$.

(b) $\mathbf{v}^{(2)} = \mathbf{v}^{(1)} + MG_{k-1}(\mathbf{0}, Q_{k-1}(\mathbf{f} - A_k\mathbf{v}^{(1)}))$.

(c) Set $MG_k(\mathbf{u}, \mathbf{f}) = \mathbf{v}^{(2)}$.

Here $R_k : \mathbf{W}_k \to \mathbf{W}_k$ is a linear smoothing operator. Note that in this multigrid algorithm (often called the "backslash cycle") we smooth only once as we proceed to coarser grids. Our smoothing operators will always be based on a generalized block Jacobi or block Gauss-Seidel iteration as in section 7.1. For these additive and multiplicative subspace correction smoothers, we need a subspace decomposition of $\mathbf{W}_k$. As in section 7.1.1, we will use the decomposition (7–1) or (7–2) to construct additive or multiplicative smoothers. Let $\mathbf{W}_k = \sum_{i=1}^{N_k} \mathbf{W}_{k,i}$ be either decomposition (7–1) or (7–2), and define $A_{k,i} : \mathbf{W}_k \to \mathbf{W}_{k,i}$ as

$$(A_{k,i}\mathbf{u}, \mathbf{v}_i)_r = A(\mathbf{u}, \mathbf{v}_i),$$

and define $P_{k,i} : \mathbf{W}_k \to \mathbf{W}_{k,i}$ as

$$A(P_{k,i}\mathbf{u}, \mathbf{v}_i) = A(\mathbf{u}, \mathbf{v}_i),$$

for all $\mathbf{v}_i \in \mathbf{W}_{k,i}$. It can be shown, by the same way as in [26, Proposition 3.1] with Lemma 7.2.1, that $A_{k,i}$ is invertible and that $P_{k,i}$ is well defined given that the meshsize is sufficiently small.

Now we can state the following algorithm that defines the block Gauss-Seidel smoother for the indefinite problem, which is the same as Algorithm 7.1.1 with Λ replaced by A, i.e.,

Algorithm 7.2.2 (Indefinite Gauss-Seidel). Given $\mathbf{u}_i$ in $\mathbf{W}_k$, calculate $\mathbf{u}_{i+1} = GS_k(\mathbf{u}_i, \mathbf{f})$ in $\mathbf{W}_k$ as follows:

1. Set $\mathbf{u}_i^{(0)} = \mathbf{u}_i$.

2. For $j = 1, 2, \ldots, N_k$, compute

$$\mathbf{u}_i^{(j)} = \mathbf{u}_i^{(j-1)} + A_{k,j}^{-1} Q_{k,j}(\mathbf{f} - A_k \mathbf{u}_i^{(j-1)}).$$

3. Set the result $\mathbf{u}_{i+1}$ to be $\mathbf{u}_i^{(N_k)}$.

This iteration can be rewritten as

$$\mathbf{u}_{i+1} = \mathbf{u}_i + R_k(\mathbf{f} - A_k \mathbf{u}_i),$$

with

$$R_k = (I - (I - P_{k,N_k})(I - P_{k,N_k-1}) \cdots (I - P_{k,1}))A_k^{-1}, \tag{7–23}$$

and this is the smoothing operator that we will use in the multigrid backslash cycle.

The backslash cycle iterates $\mathbf{x}_{i+1} = MG_k(\mathbf{x}_i, \mathbf{f})$, approximating the exact solution $\mathbf{x} = A_k^{-1}\mathbf{f}$, are connected through a linear error reduction operator $\mathcal{E}_k$ [11], i.e.,

$$\mathbf{x} - \mathbf{x}_{n+1} = \mathcal{E}_k(\mathbf{x} - \mathbf{x}_n).$$

The following is our main result on the convergence of the backslash cycle algorithm. Its proof is given in the next section.

Theorem 7.2.1. *There exists $h_0 > 0$ such that if $0 < h_1 < h_0$ then $\|\mathcal{E}_k\|_\wedge < \delta$ for some positive number $\delta < 1$ for all $k \geq 1$. The number δ is independent of the meshsize and the refinement level.*

Before we end this subsection, let us prove a lemma that will be used in proving the previous theorem.

Lemma 7.2.1. *If $\mathbf{u} \in \mathbf{W}_k$ is a discrete divergence free functions in $\mathbf{W}_k^{\mathfrak{v}}$ for any $\mathfrak{v} \in \mathscr{V}_k$ in decomposition (7–1) or if it is in $\mathbf{W}_k^{\mathfrak{e}}$ for any $\mathfrak{e} \in \mathscr{E}_k$ in decomposition (7–2), then*

$$\|\mathbf{u}\|_r \leq Ch_k \|\mathrm{curl}_{rz}\mathbf{u}\|_r .$$

Proof. We first show that the result holds for all edge element basis functions in $\mathbf{W}_k$. Then the result will hold for all $\mathbf{u} \in \mathbf{W}_k^{\mathfrak{e}}$ for any $\mathfrak{e} \in \mathscr{E}_k$. For edge basis functions that

correspond to an edge on a triangle that have empty intersection with Γ_0, we can extend such result on unweighted norms trivially, so we only have to prove the lemma for edge basis functions for triangles that do intersect Γ_0.

We consider two different type of triangles that intersect the axis of symmetry. Triangles that intersect Γ_0 at exactly one vertex are catagorized as type one triangle. Triangles that intersect Γ_0 at two vertices are catagorized as type two. Now let us consider two reference triangles. $\widehat{K}_1$ denotes the triangle with vertices $(1,-1)$, $(0,0)$, and $(1,1)$, and $\widehat{K}_2$ denotes the triangle with vertices $(1,0)$, $(0,1)$, and $(0,-1)$. First of all, let K be a type one triangle, and let F be an affine homeomorphism that maps $\widehat{K}_1$ onto K such that F maps $(0,0)$ to the one vertex of K on the axis. Map $\mathbf{u}(r,z)$ covariantly to define the function $\widehat{\mathbf{u}}(\widehat{r},\widehat{z}) = J(F)^t\mathbf{u}(r,z)$ on $\widehat{K}_1$, where $J(F)$ is the Frechet derivative of F. Observe that $r = r_1\lambda_1 + r_2\lambda_2$ on K, where r_i and λ_i denotes the r-coordinate and the barycentric coordinate respectively of the i-th vertex of K not on the axis. Also r_1/h and r_2/h are bounded above and below by fixed constants(independent of the meshsize, but depending on element angles and the angle Γ_1 makes with Γ_0). It is staight forward to show that

$$\begin{aligned} \|\mathbf{u}\|_{r,K}^2 &\leq Ch\,\|\widehat{\mathbf{u}}\|_{r,\widehat{K}_1}^2 , \\ \|\mathrm{curl}_{rz}\widehat{\mathbf{u}}\|_{r,\widehat{K}_1}^2 &\leq Ch\,\|\mathrm{curl}_{rz}\mathbf{u}\|_{r,K}^2 . \end{aligned} \tag{7–24}$$

Since each edge basis function $\widehat{\phi}_i$ for $1 \leq i \leq 3$ on $\widehat{K}_1$ satisfies

$$\left\|\widehat{\phi}_i\right\|_{r,\widehat{K}_1} \leq \left\|\mathrm{curl}_{rz}\widehat{\phi}_i\right\|_{r,\widehat{K}_1} ,$$

by using (7–24) we have that

$$\|\phi\|_{r,K} \leq Ch\,\|\mathrm{curl}_{rz}\phi\|_{r,K} , \tag{7–25}$$

for all edge basis functions ϕ on any type one triangle K.

Similarly, for all type two triangles a similar proof goes through, except that we now use a mapping from the other reference element $\widehat{K}_2$. Let K be a type two triangle now,

and let v_3 denote its vertex not on the axis. Suppose λ_3 and h_3 denote the barycentric coordinate and the r-coordinate of v_3 respectively. Then $r = h_3\lambda_3$, and inequalities like (7–24) continue to hold. Since each edge basis function $\widehat{\phi}_i$ for $1 \leq i \leq 3$ on $\widehat{K}_2$ satisfies

$$\left\|\widehat{\phi}_i\right\|_{r,\widehat{K}_2} \leq \left\|\mathrm{curl}_{rz}\widehat{\phi}_i\right\|_{r,\widehat{K}_2},$$

we conclude that

$$\|\phi\|_{r,K} \leq Ch\,\|\mathrm{curl}_{rz}\phi\|_{r,K}, \tag{7–26}$$

for all edge basis functions ϕ on any type two triangle K. Hence, by (7–25) and (7–26), it follows that for all edge basis functions ϕ corresponding to an edge of a triangle that has nonempty intersection with Γ_0, we have

$$\|\phi\|_r \leq Ch\,\|\mathrm{curl}_{rz}\phi\|_r,$$

which completes the proof for decomposition (7–2).

Next, we prove the lemma for discrete divergence free functions in $\mathbf{W}_k^{\mathfrak{v}}$ for decomposition (7–1). Fix a vertex patch $D_k^{\mathfrak{v}}$, and let v_0 denote the vertex on which all triangles in this vertex patch meet. Let $\mathbf{w} \in \mathbf{W}_k^{\mathfrak{v}}$ be discrete divergence free, and let ψ_0 be the nodal basis function corresponding to v_0. Then define $\mathbf{z}_\mu = \mu\mathbf{grad}_{rz}\psi_0 + \mathbf{w}$, for some $\mu \in \mathbb{R}$.

For each triangle connected to v_0, we use local coordinates as in the proof of [26, Lemma 3.1], to prove that the result holds for $\mathbf{w}$. There are finitely many triangles in this vertex patch by the shape regularity property of $\mathscr{T}_k$. Denote the l-th triangle by T_l, where $1 \leq l \leq N$. Then, consider the local coordiates $(r^{(l)}, z^{(l)})$ on T_l such that the $r^{(l)}$-axis contains the edge of T_l that does not intersect v_0. We will call this edge e_l. Also, let the $z^{(l)}$-axis be the perpendicular axis to such $r^{(l)}$-axis that meets v_0. Then, we use the notation $\mathbf{z}_\mu^{(l)}$, for $1 \leq l \leq N$, to denote $\mathbf{z}_\mu|_{T_l}$ in local coordinates $(r^{(l)}, z^{(l)})$ on T_l.

Since $\mathbf{z}_\mu$ is in $\mathbf{W}_k^{\mathfrak{v}}$, it has support only in the interior of the vertex patch, so the tangential component of $\mathbf{z}_\mu$ on e_l is zero, so we have that

$$\mathbf{z}_\mu^{(l)} = (-b^{(l)} z^{(l)}, c^{(l)} + b^{(l)} r^{(l)}), \tag{7–27}$$

for some $c^{(l)}, b^{(l)} \in \mathbb{R}$. We also have that

$$\mathrm{curl}_{rz} \mathbf{z}_\mu^{(l)} = -2b^{(l)}, \tag{7–28}$$

for all $1 \leq l \leq N$.

Now, let us consider the first triangle T_1 in the vertex patch $\mathbf{W}_k^{\mathfrak{v}}$. Let v_1 denote one of the vertices of T_1 that is not v_0. Without loss of generality, suppose that the edge connecting v_0 and v_1 is an edge of both T_1 and T_2, and let $\mathbf{t}^{(i)}$ be the unit tangent vector of the edge that connects v_0 and v_1 in local coordinates $(r^{(i)}, z^{(i)})$ for $i = 1, 2$. Then, direct calculation shows that

$$\mathbf{z}_\mu^{(1)} \cdot \mathbf{t}^{(1)} = \frac{-c^{(1)} v_{0,z}^{(1)} - \frac{1}{2}\mathrm{curl}_{rz} \mathbf{z}_\mu^{(1)} \mathbf{v}_0^{(1)} \wedge \mathbf{v}_1^{(1)}}{|\mathbf{v}_1^{(1)} - \mathbf{v}_0^{(1)}|}, \tag{7–29}$$

where $\mathbf{v}_i^{(1)} = (v_{i,r}^{(1)}, v_{i,z}^{(1)})$ for $i = 1, 2$, and $\mathbf{v}_0^{(1)} \wedge \mathbf{v}_1^{(1)} = v_{0,z}^{(1)}(v_{1,z}^{(1)} - v_{1,r}^{(1)})$. Then, we choose $\mu \in \mathbb{R}$ so that $c^{(1)} = 0$. Therefore, with such fixed $\mu \in \mathbb{R}$, we have that

$$\mathbf{z}_\mu^{(1)} = (-b^{(1)} z^{(1)}, b^{(1)} r^{(1)}),$$

so by using (7–28), we have

$$|\mathbf{z}_\mu^{(1)}| \leq Ch |\mathrm{curl}_{rz} \mathbf{z}_\mu^{(1)}|.$$

Additionally, since $c^{(1)} = 0$, by (7–29), we have that

$$\mathbf{z}_\mu^{(1)} \cdot \mathbf{t}^{(1)} = \frac{-\frac{1}{2}\mathrm{curl}_{rz} \mathbf{z}_\mu^{(1)} \mathbf{v}_0^{(1)} \wedge \mathbf{v}_1^{(1)}}{|\mathbf{v}_1^{(1)} - \mathbf{v}_0^{(1)}|}. \tag{7–30}$$

Next, as in (7–29) but this time using local cooridantes $(r^{(2)}, z^{(2)})$, we derive that

$$\mathbf{z}_\mu^{(2)} \cdot \mathbf{t}^{(2)} = \frac{-c^{(2)} v_{0,z}^{(2)} - \frac{1}{2}\mathrm{curl}_{rz} \mathbf{z}_\mu^{(2)} \mathbf{v}_0^{(2)} \wedge \mathbf{v}_1^{(2)}}{|\mathbf{v}_1^{(2)} - \mathbf{v}_0^{(2)}|}. \tag{7–31}$$

Although we are in local coordinate systems, the tangential components still agree, so by (7–30) and (7–31), we have

$$c^{(2)} = \frac{\frac{1}{2}\mathrm{curl}_{rz}\mathbf{z}_\mu^{(1)}\mathbf{v}_0^{(1)} \wedge \mathbf{v}_1^{(1)} - \frac{1}{2}\mathrm{curl}_{rz}\mathbf{z}_\mu^{(2)}\mathbf{v}_0^{(2)} \wedge \mathbf{v}_1^{(2)}}{v_{0,z}^{(2)}}.$$

Thus,

$$|c^{(2)}| \leq Ch(|\mathrm{curl}_{rz}\mathbf{z}_\mu^{(1)}| + |\mathrm{curl}_{rz}\mathbf{z}_\mu^{(2)}|),$$

and it follows from (7–27) and (7–28) that

$$|\mathbf{z}_\mu^{(2)}| \leq Ch(|\mathrm{curl}_{rz}\mathbf{z}_\mu^{(1)}| + |\mathrm{curl}_{rz}\mathbf{z}_\mu^{(2)}|).$$

In general, by induction, we have that

$$|\mathbf{z}_\mu^{(l)}| \leq Ch(|\mathrm{curl}_{rz}\mathbf{z}_\mu^{(1)}| + |\mathrm{curl}_{rz}\mathbf{z}_\mu^{(2)}| + \cdots + |\mathrm{curl}_{rz}\mathbf{z}_\mu^{(l)}|), \tag{7–32}$$

for all $1 \leq l \leq N$.

Since

$$|\mathbf{z}_\mu(r,z)|_{T_l}| \leq C|\mathbf{z}_\mu^{(l)}(r^{(l)}, z^{(l)})|$$

and

$$|\mathrm{curl}_{rz}\mathbf{z}_\mu^{(l)}(r^{(l)}, z^{(l)})| \leq C|\mathrm{curl}_{rz}\mathbf{z}_\mu(r,z)|_{T_l}|,$$

where C depends on the shape regularity constant, it follows from (7–32) that

$$|\mathbf{z}_\mu|_{T_l}| \leq Ch(|\mathrm{curl}_{rz}\mathbf{z}_\mu|_{T_1}| + |\mathrm{curl}_{rz}\mathbf{z}_\mu|_{T_2}| + \cdots + |\mathrm{curl}_{rz}\mathbf{z}_\mu|_{T_l}|),$$

for all $1 \leq l \leq N$. Therefore, we conclude that

$$\|\mathbf{z}_\mu\|_r \leq Ch\,\|\mathrm{curl}_{rz}\mathbf{z}_\mu\|_r\,.$$

Since $\mathbf{z}_\mu = \mu\mathbf{grad}_{rz}\psi_0 + \mathbf{w}$ is an orthogonal decomposition, this implies that

$$\|\mathbf{w}\|_r \leq Ch\,\|\mathrm{curl}_{rz}\mathbf{w}\|_r\,.$$

As $\mathbf{w} \in \mathbf{W}_k^{\mathfrak{p}}$ were an arbitrary discrete divergence free function, this completes the proof. $\square$

7.2.2 Multigrid Analysis

In this subsection, we will prove our main result, the uniform convergence of the multigrid backslash cycle. Our analysis will be based on perturbation from the uniform multigrid convergence estimates for a related symmetric positive definite problem as done in [12] and [26].

In section 7.1, we analyzed the multigrid convergence when applied to the bilinear form Λ. Although we analyzed the multigrid V-cycle there, such results can be extended to the multigrid backslash cycle as well [15, Lemma 2.2]. Here and in the remaining of this chapter, let $\widetilde{\mathcal{E}}_k$ denote the error reduction operator of Algorithm 7.2.1 with A_k replaced by Λ_k and R_k replaced by $\widetilde{R}_k$ described in section 7.1.1. We use the same decomposition (7–1) or (7–2).

Then the following result follows from Theorem 7.1.1. See Chapter 3 section 3.2 for details.

Theorem 7.2.2. *There exists a positive number $\widetilde{\delta} < 1$ such that*

$$\left\|\widetilde{\mathcal{E}}_k\right\|_{\Lambda} < \widetilde{\delta},$$

for all $k \geq 1$. The number $\widetilde{\delta}$ is independent of the meshsize and refinement level.

Now, let us study the error reduction operator $\mathcal{E}_k$ and $\widetilde{\mathcal{E}}_k$ further. Note that, for error reduction operators, the subscript k indicates that $J = k$. Define $T_k : \mathbf{W}_J \to \mathbf{W}_k$ as $T_1 = P_1$ and $T_k = R_k A_k P_k$ for $k > 1$. Then by using consistency and linearity of $MG_k(\cdot,\cdot)$, it is straightforward to show that

$$\mathcal{E}_k = (I - T_1)(I - T_2)\cdots(I - T_k), \tag{7–33}$$

where I is the identity operator. Similarly, if $\widetilde{T}_1 = \widetilde{P}_1$ and $\widetilde{T}_k = \widetilde{R}_k \Lambda_k \widetilde{P}_k$ for $k > 1$, then we get

$$\widetilde{\mathcal{E}}_k = (I - \widetilde{T}_1)(I - \widetilde{T}_2) \cdots (I - \widetilde{T}_k). \tag{7–34}$$

We will analyze the multigrid algorithm by using another operator $Z_k = T_k - \widetilde{T}_k$. Suppose we have

$$\begin{aligned} &\|Z_1\|_\Lambda \leq Ch_1, \\ &\|Z_k\|_\Lambda \leq Ch_k \text{ for } k = 2, \cdots J. \end{aligned} \tag{7–35}$$

Then, by an argument of [12], it follows that $\left\|\widetilde{\mathcal{E}}_k - \mathcal{E}_k\right\|_\Lambda$ is small. In particular, since $I - T_k = I - \widetilde{T}_k - Z_k$ and $\left\|I - \widetilde{T}_k\right\|_\Lambda \leq 1$,

$$\|I - T_k\|_\Lambda \leq 1 + Ch_k,$$

and so by (7–33),

$$\|\mathcal{E}_k\|_\Lambda \leq \prod_{i=1}^{k} (1 + Ch_i),$$

which can be bounded by a convergent infinite product. Thus, $\|\mathcal{E}_k\|_\Lambda \leq C$. Additionally, since

$$\mathcal{E}_k - \widetilde{\mathcal{E}}_k = (\mathcal{E}_{k-1} - \widetilde{\mathcal{E}}_{k-1})(I - \widetilde{T}_k) - \mathcal{E}_{k-1} Z_k,$$

by (7–33) and (7–34), it follows that

$$\left\|\mathcal{E}_k - \widetilde{\mathcal{E}}_k\right\|_\Lambda \leq Ch_1. \tag{7–36}$$

By combining Theorem 7.2.2 and (7–36), it is easy to show that $\|\mathcal{E}_k\|_\Lambda$ is bounded by some positive constant less than 1 given that h_1 is small enough. So we will show that conditions (7–35) do in fact hold.

Lemma 7.2.2. *For all* $\mathbf{x}_J \in \mathbf{W}_J$ *and* $\mathbf{v}_1 \in \mathbf{W}_1$,

$$(\mathbf{x}_J - P_1 \mathbf{x}_J, \mathbf{v}_1)_r \leq Ch_1 \|\mathbf{x}_J - P_1 \mathbf{x}_J\|_\Lambda \|\mathbf{v}_1\|_\Lambda .$$

Proof. For given $\mathbf{x}_J \in \mathbf{W}_J$ and $\mathbf{v}_1 \in \mathbf{W}_1$, let $\mathbf{x}_J - P_1\mathbf{x}_J = \mathbf{grad}_{rz}\phi_J + \mathrm{curl}^J_{rz} r_J$ be the discrete Helmholz decomposition in $\mathbf{W}_J$, and let $\mathbf{v}_1 = \mathbf{grad}_{rz}\psi_1 + \mathrm{curl}^1_{rz} s_1$, be the discrete Helmholz decomposition in $\mathbf{W}_1$.

By definition of P_1,

$$A(\mathbf{x}_J - P_1\mathbf{x}_J, \mathbf{v}_1) = 0$$

so

$$(\mathbf{x}_J - P_1\mathbf{x}_J, \mathbf{grad}_{rz}\psi_1) = 0.$$

Therefore,

$$(\mathbf{x}_J - P_1\mathbf{x}_J, \mathbf{v}_1)_r = (\mathbf{x}_J - P_1\mathbf{x}_J, \mathrm{curl}^1_{rz} s_1)_r. \tag{7–37}$$

Let $\mathbf{S}\mathbf{w}_1 \in \mathbf{H}_{r,\diamond}(\mathrm{curl}, D)$ be the solution of (6–3), where $\mathbf{w}_1 = \mathrm{curl}^1_{rz} s_1$. Then,

$$\begin{aligned}
(\mathbf{grad}_{rz}\phi_J, \mathrm{curl}^1_{rz} s_1)_r &= (\mathbf{grad}_{rz}\phi_J, \mathbf{w}_1 - S\mathbf{w}_1)_r, \\
&\le \|\mathbf{x}_J - P_1\mathbf{x}_J\|_r \, Ch_1 \, \|\mathrm{curl}_{rz}\mathbf{w}_1\|_r \quad \text{by Lemma 6.2.1}, \\
&\le Ch_1 \, \|\mathbf{x}_J - P_1\mathbf{x}_J\|_r \, \|\mathbf{v}_1\|_\Lambda .
\end{aligned} \tag{7–38}$$

Next, let $\mathbf{z} \in \mathbf{H}_{r,\diamond}(\mathrm{curl}, D)$ be the solution of

$$A(\mathbf{z}, \mathbf{x}) = (\mathbf{w}_J, \mathbf{x}) \qquad \text{for all } \mathbf{x} \in \mathbf{H}_{r,\diamond}(\mathrm{curl}, D),$$

where $\mathbf{w}_J = \mathrm{curl}^J_{rz} r_J$. Since

$$\begin{aligned}
\left\|\mathrm{curl}^J_{rz} r_J\right\|_r^2 &= (\mathrm{curl}^J_{rz} r_J, \mathbf{x}_J - P_1\mathbf{x}_J)_r, \\
&= A(\mathbf{z}, \mathbf{x}_J - P_1\mathbf{x}_J), \\
&= A(\mathbf{z} - \Pi^W_{h_1}\mathbf{z}, \mathbf{x}_J - P_1\mathbf{x}_J), \\
&\le C \left\|\mathbf{z} - \Pi^W_{h_1}\mathbf{z}\right\|_\Lambda \|\mathbf{x}_J - P_1\mathbf{x}_J\|_\Lambda , \\
&\le Ch_1(|\mathbf{z}|_{H^1_r(D)^2} + |\mathrm{curl}_{rz}\mathbf{z}|_{H^1_r(D)}) \, \|\mathbf{x}_J - P_1\mathbf{x}_J\|_\Lambda \qquad \text{by Corollary 4.1.1}, \\
&\le Ch_1 \, \|\mathbf{w}_J\|_r \, \|\mathbf{x}_J - P_1\mathbf{x}_J\|_\Lambda \qquad \text{by Lemma 6.2.2}.
\end{aligned}$$

It follows that

$$
\begin{aligned}
(\mathrm{curl}^J_{rz} r_J, \mathrm{curl}^1_{rz} s_1)_r &\leq \left\|\mathrm{curl}^J_{rz} r_J\right\|_r \|\mathbf{v}_1\|_r \,, \\
&\leq Ch_1 \|\mathbf{x}_J - P_1\mathbf{x}_J\|_\Lambda \|\mathbf{v}_1\|_r \,.
\end{aligned} \tag{7–39}
$$

Hence, by (7–37),

$$
\begin{aligned}
(\mathbf{x}_J - P_1\mathbf{x}_J, \mathbf{v}_1)_r &= (\mathbf{grad}_{rz}\phi_J, \mathrm{curl}^1_{rz} s_1)_r + (\mathrm{curl}^J_{rz} r_J, \mathrm{curl}^1_{rz} s_1)_r, \\
&\leq Ch_1 \|\mathbf{x}_J - P_1\mathbf{x}_J\|_\Lambda \|\mathbf{v}_1\|_\Lambda && \text{by (7–38) and (7–39),}
\end{aligned}
$$

which is the desired result. □

Now we use this lemma to prove the first condition of (7–35).

Lemma 7.2.3. *There exists a constant $H_1 > 0$ such that, for all $0 < h_1 < H_1$,*

$$
\|Z_1\|_\Lambda \leq Ch_1.
$$

Proof. The proof follows as in [26, Lemma 4.3]. Let $\mathbf{u}_J, \mathbf{v}_J \in \mathbf{W}_J$. Then

$$
\begin{aligned}
\Lambda(Z_1\mathbf{u}_J, \mathbf{v}_J) &= \Lambda(P_1\mathbf{u}_J - \mathbf{u}_J, \widetilde{P}_1\mathbf{v}_J), \\
&= A(P_1\mathbf{u}_J - \mathbf{u}_J, \widetilde{P}_1\mathbf{v}_J) + (1+\kappa^2)(P_1\mathbf{u}_J - \mathbf{u}_J, \widetilde{P}_1\mathbf{v}_J)_r, \\
&= (1+\kappa^2)(P_1\mathbf{u}_J - \mathbf{u}_J, \widetilde{P}_1\mathbf{v}_J)_r, \\
&\leq Ch_1 \|P_1\mathbf{u}_J - \mathbf{u}_J\|_\Lambda \left\|\widetilde{P}_1\mathbf{v}_J\right\|_\Lambda && \text{by Lemma 7.2.2,} \\
&\leq Ch_1 \|\mathbf{u}_J\|_\Lambda \|\mathbf{v}_J\|_\Lambda \,.
\end{aligned}
$$

In the last step, we are again using Lemma 7.2.2. That is,

$$
\begin{aligned}
\|P_1\mathbf{u}_J - \mathbf{u}_J\|^2_\Lambda &= \Lambda(P_1\mathbf{u}_J - \mathbf{u}_J, P_1\mathbf{u}_J) - \Lambda(P_1\mathbf{u}_J - \mathbf{u}_J, \mathbf{u}_J), \\
&= (1+\kappa^2)(P_1\mathbf{u}_J - \mathbf{u}_J, P_1\mathbf{u}_J)_r - \Lambda(P_1\mathbf{u}_J - \mathbf{u}_J, \mathbf{u}_J), \\
&\leq Ch_1 \|P_1\mathbf{u}_J - \mathbf{u}_J\|_\Lambda \|P_1\mathbf{u}_J\|_\Lambda + \|P_1\mathbf{u}_J - \mathbf{u}_J\|_\Lambda \|\mathbf{u}_J\|_\Lambda && \text{by Lemma 7.2.2,} \\
&\leq Ch_1 \|P_1\mathbf{u}_J - \mathbf{u}_J\|^2_\Lambda + (Ch_1 + 1) \|P_1\mathbf{u}_J - \mathbf{u}_J\|_\Lambda \|\mathbf{u}_J\|_\Lambda \,.
\end{aligned}
$$

Therefore, by canceling the common factor, we see that there exists a constant $H_1 > 0$ such that

$$\|P_1\mathbf{u}_J - \mathbf{u}_J\|_\Lambda \leq C\,\|\mathbf{u}_J\|_\Lambda\,,$$

for all $0 < h_1 < H_1$. This completes the proof. □

The next two lemmas verify the second condition of (7–35). These proofs proceed exactly as the proofs of [26, Lemma 4.4, 4.5] by using Lemma 7.2.1. We include the outline of the proof here for the sake of completeness.

Lemma 7.2.4. *There exists a constant C such that*

$$(\mathbf{u}_k - P_{k,i}\mathbf{u}_k, \mathbf{v}_{k,i}) \leq Ch_k\,\|\mathbf{u}_k - P_{k,i}\mathbf{u}_k\|_r\,\|\mathrm{curl}_{rz}\mathbf{v}_{k,i}\|_r$$

for all $\mathbf{u}_k \in \mathbf{W}_k$ and $\mathbf{v}_{k,i} \in \mathbf{W}_{k,i}$, where $\mathbf{W}_k = \sum_{i=1}^{N_k}\mathbf{W}_{k,i}$, $k = 2, \cdots J$, is decomposition (7–1) or (7–2).

Proof. For decomposition (7–1), $\mathbf{v}_{k,i} \in \mathbf{W}_k^{\mathfrak{v}}$ for some $\mathfrak{v} \in \mathscr{V}_k$ or $\mathbf{v}_{k,i} \in \mathbf{W}_k^{\mathfrak{e}}$ for some $\mathfrak{e} \in \mathscr{E}_k^*$. If $\mathbf{v}_{k,i} \in \mathbf{W}_k^{\mathfrak{v}}$ then let $\mathbf{v}_{k,i} = \mathbf{grad}_{rz}w_{k,i} + \mathbf{x}_{k,i}$ be the discrete Helmholz decompostion of $\mathbf{v}_{k,i}$. Then, since $(\mathbf{u}_k - P_{k,i}\mathbf{u}_k, \mathbf{grad}_{rz}w_{k,i})_r = \frac{1}{\kappa^2}A(\mathbf{u}_k - P_{k,i}\mathbf{u}_k, \mathbf{grad}_{rz}w_{k,i}) = 0$,

$$\begin{aligned}(\mathbf{u}_k - P_{k,i}\mathbf{u}_k, \mathbf{v}_{k,i})_r &= (\mathbf{u}_k - P_{k,i}\mathbf{u}_k, \mathbf{x}_{k,i})_r,\\ &\leq Ch_k\,\|\mathbf{u}_k - P_{k,i}\mathbf{u}_k\|_r\,\|\mathrm{curl}_{rz}\mathbf{x}_{k,i}\|_r \qquad \text{by Lemma 7.2.1,}\\ &= Ch_k\,\|\mathbf{u}_k - P_{k,i}\mathbf{u}_k\|_r\,\|\mathrm{curl}_{rz}\mathbf{v}_{k,i}\|_r\,.\end{aligned}$$

If $\mathbf{v}_{k,i} \in \mathbf{W}_k^{\mathfrak{e}}$ then the result follows directly from Cauchy-Shwartz inequality and Lemma 7.2.1. For decomposition (7–2) $\mathbf{v}_{k,i} \in \mathbf{grad}_{rz}V_k^{\mathfrak{v}}$ for some $\mathfrak{v} \in \mathscr{V}_k$ or $\mathbf{v}_{k,i} \in \mathbf{W}_k^{\mathfrak{e}}$ for some $\mathfrak{e} \in \mathscr{E}_k$. In the former case, there is nothing to prove as both sides of the inequality we wish to prove are both zero. In the latter case, the result follows again by Cauchy-Shwartz inequality and Lemma 7.2.1. □

Lemma 7.2.5. *There exists a constant $H_2 > 0$ such that, for all $0 < h_1 < H_2$,*

$$\|Z_k\|_\Lambda \leq Ch_k \text{ for } k = 2, \cdots J.$$

Proof. Define

$$E_i = (I - P_{k,i})(I - P_{k,i-1}) \cdots (I - P_{k,1}),$$
$$\widetilde{E}_i = (I - \widetilde{P}_{k,i})(I - \widetilde{P}_{k,i-1}) \cdots (I - \widetilde{P}_{k,1}),$$

and let $E_0 = \widetilde{E}_0 = I$. Then, by (7–23),

$$Z_k = T_k - \widetilde{T}_k = \widetilde{E}_{N_k} - E_{N_k}.$$

As in the proof of [26, Lemma 4.5] it can be shown that

$$\left\|(\widetilde{E}_{N_k} - E_{N_k})\mathbf{u}\right\|_\Lambda^2 \leq Ch_k^2 \sum_{i=1}^{N_k} \|E_{i-1}\mathbf{u}\|_\Lambda^2 \leq Ch_k^2 \|\mathbf{u}\|_\Lambda^2 .$$

Note that, by using Lemma 7.2.4, there exists a constant $H_2 > 0$ such that the above second inequality holds, for all $0 < h_1 < H_2$. See the proof of [26, Theorem 4.5] for details. Therefore, for all $k > 1$,

$$\|Z_k\|_\Lambda \leq Ch_k.$$

□

By putting all of these pieces together, we can prove our main result.

Proof of Theorem 7.2.1. By Lemma 7.2.3 and Lemma 7.2.5, (7–36) holds for sufficiently small h_1, so for all $k \geq 1$,

$$\begin{aligned} \|\mathcal{E}_k\|_\Lambda &\leq \left\|\mathcal{E}_k - \widetilde{\mathcal{E}}_k\right\|_\Lambda + \left\|\widetilde{\mathcal{E}}_k\right\|_\Lambda , \\ &\leq Ch_1 + \widetilde{\delta} && \text{by (7–36) and Theorem 7.2.2.} \end{aligned}$$

Hence, there exists $h_0 > 0$ such that $h_0 < H_1$, $h_0 < H_2$, and for all $0 < h_1 < h_0$, we have that

$$\|\mathcal{E}_k\|_\Lambda < \delta,$$

where $\delta = Ch_1 + \widetilde{\delta} < 1$, and this completes the proof. □

7.2.3 Numerical Results

In this section, we report numerical results that provide empirical support to the uniform convergence of the multigrid backslash cycle when applied to the indefinite bilinear form $A(\cdot,\cdot)$ provided that the coarsest mesh is sufficiently fine. Additionally, for different wavenumbers, we compare the coarsest meshsize that guarantees multigrid convergence. In all experiments, our domain is the unit square and mesh level 1 consist of two uniform right triangles with the common edge connecting $(0,0)$ and $(1,1)$. The next level mesh is obtained by connecting the midpoints of each edge.

We compute the convergence rate for the multigrid backslash cycle when $f = 0$. We apply the Indefinite Gauss-Seidel smoother with the subspace decomposition (7–2). In order to choose the initial value independent of the mesh level, we first choose $\mathbf{x}_0$ in the finite element space of mesh level 1 to be the function that corresponds to the vector with one on each entry with respect to the standard basis functions. Then we use this $\mathbf{x}_0$ as the initial value for all level meshes, which is possible, since the finite element space of mesh level 1 is contained in the finite element space of all higher level meshes. The stopping criterion is $\|\mathbf{x}_n\|_\Lambda / \|\mathbf{x}_0\|_\Lambda < 10^{-6}$, where $\mathbf{x}_n$ is the result of the n-th iteration (which measures the reduction in the error since the exact solution is zero). The convergence rate is computed by taking the average of $\|\mathbf{x}_n\|_\Lambda / \|\mathbf{x}_{n-1}\|_\Lambda$.

Table 7-2 reports the convergence rate when the wavenumber $\kappa = 1$. We considered six different coarsest meshsizes h_1, and we used the sparse matrix structure in MATLAB to solve the linear system on the coarsest mesh. For a fixed coarsest level mesh, the convergence rate is nearly constant and clearly independent of the meshsize.

Table 7-2. Backslash-cycle convergence rates: $\kappa = 1$

	h_1					
Level	1	1/2	1/4	1/8	1/16	1/32
2	0.2					
3	0.3	0.3				
4	0.3	0.3	0.3			
5	0.3	0.3	0.3	0.3		
6	0.3	0.3	0.3	0.3	0.3	
7	0.4	0.3	0.3	0.3	0.3	0.3
8	0.4	0.4	0.3	0.3	0.3	0.3
9	0.4	0.4	0.4	0.4	0.3	0.3

Table 7-3. Backslash-cycle convergence rates: $\kappa = 10$

	h_1					
Level	1	1/2	1/4	1/8	1/16	1/32
2	1.8					
3	1478.4	1165.8				
4	736.7	743.8	12			
5	787.6	1176.3	9.7	0.5		
6	926.3	1300.5	9.2	0.3	0.3	
7	948	1323.5	9.1	0.4	0.3	0.2
8	951.2	1327.8	9.1	0.4	0.3	0.3
9	951.9	1328.8	9.1	0.4	0.3	0.3

It appears that when $\kappa = 1$, we have uniform convergence for each coarest meshsize considered. This is no longer the case for higher wavenumbers.

Table 7-3 reports the convergence rate when the wavenumber $\kappa = 10$. In the case when the multigrid diverges, the convergence rate is computed by taking the average of $\|\mathbf{x}_n\|_\Lambda \,/\, \|\mathbf{x}_{n-1}\|_\Lambda$ of the first ten iterations. This example illustrates that, as proved in Theorem 7.2.1, the coarsest meshsize must be smaller than some constant in order to achieve a convergence rate independent of the meshsize for the multigrid backslash cycle.

The next experiment gives us an idea of how the wavenumber and the coarsest meshsize that guarantees multigrid convergence are related. For a fixed meshlevel(level 9), we computed the convergence rate for integer wavenumbers κ ranging from one to

20, and for coarsest meshsizes ranging from $(1/2)^i$ where $0 \leq i \leq 5$. All other settings are the same as the other multigrid experiments above.

In Figure 7.2.3, the coarsest meshsize where multigrid starts to converge for each integer wavenumber were plotted and those dots were connected by straight lines. Roughly speaking, for larger wavenumbers, the coarsest meshsize must be smaller in order to have multigrid convergence. Observe from the graph that, however, this is not always the case. It appears that some wavenumbers behave particularly nicer with multigrid while some behave worse. In fact, while the number of mesh points in one wave ranges from 5 to 10 for most of the wavenumbers considered, for $\kappa = 6$ there were approximately 2 mesh points in one wave, and for $\kappa = 18$ there were approximately 22 meshpoints in one wave when the multigrid started to converge.

The advantage of the multigrid backslash cycle under axial symmetry is that the corresponding matrix system that needs to be solved on the coarsest level mesh for each iteration is still relatively small as we are in two dimension due to axial symmetry.

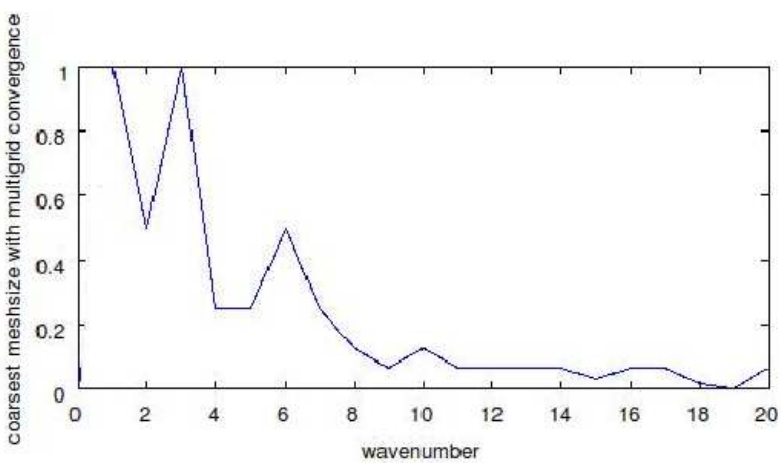

Figure 7-2. Wavenumber vs coarsest meshsize

CHAPTER 8
A BIOMEDICAL APPLICATION OF THE MERIDIAN PROBLEM

In this chapter, we will see a biomedical application of the edge finite element method and the axisymmetric Maxwell equations. The experiment done in this chapter closely follows the information given in [7].

Hepatic Microwave Ablation (MWA) is an alternative treatment to liver cancer. It is an experimental procedure in which a probe is inserted through the skin or during surgery to induce cell necrosis through the heating of deep-seated tumors. An efficient probe for such purpose should be designed so that the electromagnetic power pattern is highly localized near the tip of the probe.

To compute the electromagnetic distribution, we find an approximate solution to the Maxwell equations. Assuming propagation at a single frequency, we can use the finite element method to approximate the time harmonic Maxwell equations. Although a liver is not axisymmetric, we are only interested in the part of the liver that contains the tumor. In other words, since a liver is locally axisymmetric, we can take the computational domain to be a small cylinder containing the tumor minus the probe. Additionally, it is known that the electric field in such a set up has zero θ-component. So we can approximate the meridian problem (1–8) to find the electric field distribution over the part of the liver in our interest. This computation is based on the data and information given in [7].

Let us recall the meridian problem (1–8):

$$\mathbf{curl}_{rz}(\frac{1}{\mu_r}\mathrm{curl}_{rz}\mathbf{E}_{rz}) - \kappa^2\epsilon_r\mathbf{E}_{rz} = \mathbf{F}_{rz}.$$

See Chapter 1 to see the definition of the parameters involved. We find an approximate solution to the meridian problem by using the lowest order Nédélec elements (see Chapter 6):

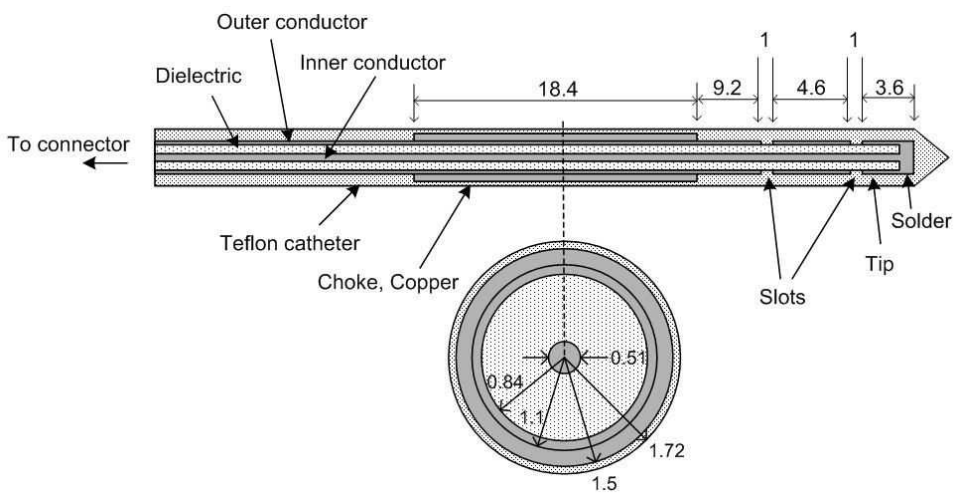

Figure 8-1. Coaxial-based double slot choked probe

Find $\mathbf{u}_h \in \mathbf{W}_{h,\diamond}$ such that

$$(\frac{1}{\mu_r}\text{curl}_{rz}\mathbf{u}_h, \text{curl}_{rz}\mathbf{v}_h)_r - \kappa^2(\epsilon_r\mathbf{u}_h, \mathbf{v}_h)_r = (\tilde{\mathbf{F}}_{rz}, \mathbf{v}_h)_r,$$

for all $\mathbf{v}_h \in \mathbf{W}_{h,\diamond}$.

Figure 8 is the cross section of the axisymmetric probe designed for Hepatic Microwave Ablation (MWA) [7].

$\mathbf{F}_{rz} = \mathbf{0}$, and we put perfectly conducting boundary conditions ($\mathbf{u}_h \cdot \mathbf{t} = 0$) on the part of the boundary that is not on the axis of symmetry except where there are the double slots. As in [7], the electric field inside the probe is calculated by the formula

$$\mathbf{E}(r, z) = \frac{C}{r}e^{-i\kappa z}\mathbf{e}_r,$$

where $C = \frac{264.42P_{in}}{\pi \ln(r_o/r_i)}$, r_o and r_i are the outer and inner radii of the coaxial cable, and P_{in} is the input power. The electric field is in the radial direction only inside the probe and in both radial and axial inside the liver. We compute the boundary values on the double slots by using this formula, and $\tilde{\mathbf{F}}_{rz}$ denotes the source coming from these slots.

We use the commonly used MWA frequency of 2.45 GHz, so the wavenumber $\kappa = 51.31268$. μ_r and ϵ_r depend on the properties of the liver, which is given in [7] as:

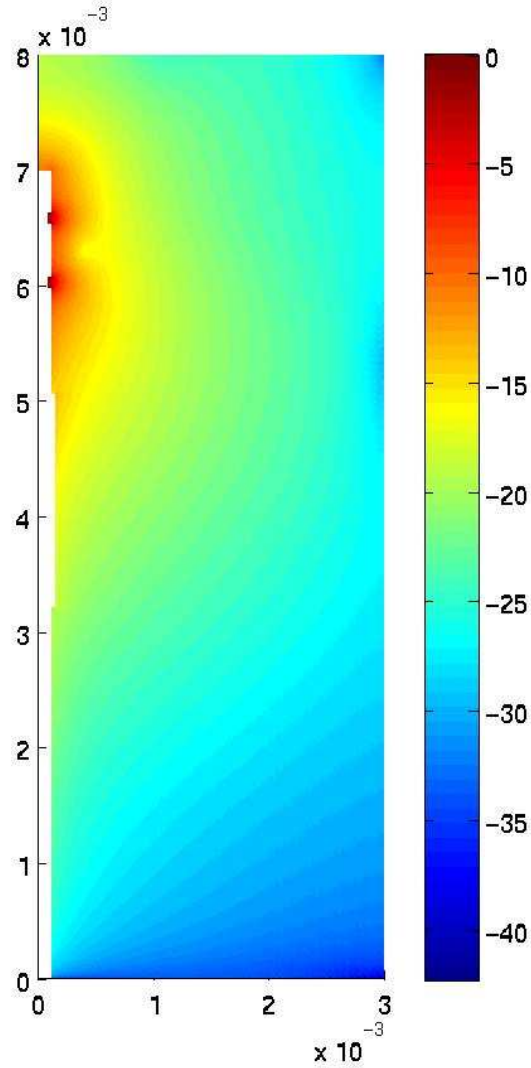

Figure 8-2. Distribution of the electromagnetic power

$\mu_r = \frac{\mu}{\mu_0} = 1$ and $\epsilon_r = \frac{1}{\epsilon_0}(\epsilon + \frac{i\sigma}{\omega}) = 44.4 + 13.95i$. In particular, $\frac{\epsilon}{\epsilon_0} = 44.4$ and the conductivity at the given frequency is $\sigma = 1.9(S/m)$. Figure 8 shows the logarithmic distribution of $|\mathbf{E}|^2$ after scaling.

Note that the domain is not a rectangle, and the missing part of the rectangle near the axis of symmetry corresponds to the probe. The tip of the probe is located at the point $(0, 7 \times 10^{-3})$, and we can see the localization of the electromagnetic power right in front of the tip of the probe. In short, the Maxwell equations under axial symmetry

and the edge finite element method can be used for designing efficient probes for the Hepatic Microwave Ablation (MWA).

APPENDIX A
PROOF OF THE EXACT SEQUENCE PROPERTY

We prove the exactness of the sequence (4–3) under the assumption that Γ_1 is connected and D is simply connected.

The injectivity of $\mathbf{grad}_{rz} : V_{h,\diamond} \mapsto \mathbf{W}_{h,\diamond}$ is trivial, so let us proceed to prove the next item in the exact sequence property, namely $\mathbf{grad}_{rz}(V_{h,\diamond})$ equals the null space of $\mathrm{curl}_{rz} : \mathbf{W}_{h,\diamond} \mapsto S_h$, which is denoted by $\ker(\mathrm{curl}_{rz})$. It is obvious that $\mathbf{grad}_{rz}(V_{h,\diamond}) \subseteq \ker(\mathrm{curl}_{rz})$. Since D is simply connected, any $\mathbf{w}_h \in \mathbf{W}_{h,\diamond}$ satisfying $\mathrm{curl}_{rz}\mathbf{w}_h = 0$ coincides with a gradient, say $\mathbf{grad}_{rz}\phi_h$, and by comparing the polynomial degrees, ϕ_h is in V_h. Moreover, ϕ_h can be chosen to be in $V_{h,\diamond}$, because $\mathbf{t} \cdot \mathbf{grad}_{rz}\phi_h = 0$ on Γ_1 and because Γ_1 is connected.

Thus, it only remains to prove that $\mathrm{curl}_{rz} : \mathbf{W}_{h,\diamond} \mapsto S_h$ is surjective. For this we only need the connectedness of D as we see below.

Lemma A.0.6. *The map* $\mathrm{curl}_{rz} : \mathbf{W}_{h,\diamond} \to S_h$ *is surjective.*

Proof. The collection of indicator functions χ^K, for all mesh elements K, spans S_h. Therefore, to prove the lemma, it suffices to show that there is a $\mathbf{u}_h^K$ in $\mathbf{W}_{h,\diamond}$ such that

$$\mathrm{curl}_{rz}\mathbf{u}_h^K = \chi^K \tag{A–1}$$

for all mesh elements K. To do this we need a commuting projector. We use the projectors $\widehat{\Pi}_h^W$ and $\widehat{\Pi}_h^S$ of [21] which we already introduced earlier (although this proof works equally well, *mutatis mutandis*, with Nédélec's original projector [32]).

To begin, consider all mesh elements K near Γ_0, specifically those in

$$\mathscr{T}_h^0 = \{K \in \mathscr{T}_h : \ \bar{K} \cap \bar{\Gamma}_0 \text{ is non-empty}\}.$$

Let $\alpha_p^K(\mathbf{u}) = (\int_K r^p \ dr\, dz)^{-1} \int_K r^p \,\mathrm{curl}_{rz}\mathbf{u} \ dr\, dz$. Then, for any K in $\mathscr{T}_h^0$, choose a function $\mathbf{u}^K$ in $\mathcal{D}(K)^2$ with nonzero $\alpha_1^K(\mathbf{u}^K)$. By rescaling this function if necessary, we can assume without loss of generality that $\alpha_1^K(\mathbf{u}^K) = 1$. Then consider the interpolant

$\mathbf{u}_h^K \equiv \widehat{\Pi}_h^W \mathbf{u}^K$. Recalling the definition of $\widehat{\Pi}_h^W$ in [21], we find that all the degrees of freedom defining $\widehat{\Pi}_h^W$ applied to $\mathbf{u}^K$ vanish, except the interior degree of freedom on K, namely $\int_K r\,\mathrm{curl}_{rz}\mathbf{u}^K$. Therefore, by the commutativity property (4–1),

$$\mathrm{curl}_{rz}(\mathbf{u}_h^K) = \widehat{\Pi}_h^S \mathrm{curl}_{rz}\mathbf{u}^K = \alpha_1^K(\mathbf{u}^K)\chi^K = \chi^K.$$

Thus, we have proved (A–1) for all K in $\mathscr{T}_h^0$.

To consider the remaining elements, let K' be an element sharing a mesh edge with an element K in $\mathscr{T}_h^0$. Let $\mathbf{u}'$ denote an infinitely differentiable vector function supported in $\bar{K} \cup \bar{K}'$ such that $\alpha_0^{K'}(\mathbf{u}') \neq 0$. Then,

$$\mathrm{curl}_{rz}(\widehat{\Pi}_h^W \mathbf{u}') = \widehat{\Pi}_h^S(\mathrm{curl}_{rz}\mathbf{u}') = \alpha_0^{K'}(\mathbf{u}')\chi^{K'} + \alpha_1^K(\mathbf{u}')\chi^K.$$

Thus, with $\mathbf{u}_h^K$ as set previously, and with $\mathbf{u}_h^{K'} = (\widehat{\Pi}_h^W \mathbf{u}' - \alpha_1^K(\mathbf{u})\,\mathbf{u}_h^K)/\alpha_0^{K'}(\mathbf{u}')$,

$$\mathrm{curl}_{rz}(\mathbf{u}_h^{K'}) = \frac{\mathrm{curl}_{rz}(\widehat{\Pi}_h^W \mathbf{u}') - \alpha_1^K(\mathbf{u}')\,\chi^K}{\alpha_0^{K'}(\mathbf{u}')} = \chi^{K'}$$

so that (A–1) is proved for all elements in $\mathscr{T}_h^1 = \{K^1 \in \mathscr{T}_h \setminus \mathscr{T}_h^0 : \ K^1$ shares an edge with some $K \in \mathscr{T}_h^0\}$ as well.

The proof is completed by generalizing to $\mathscr{T}_h^j = \{K' \in \mathscr{T}_h \setminus \cup_{\ell=0}^{j-1}\mathscr{T}_h^\ell : K'$ shares an edge with some $K \in \mathscr{T}_h^{j-1}\}$, for $j \geq 1$, and formalizing an induction argument. $\square$

APPENDIX B
PROOF OF PROPOSITION 4.2.1

In case 1, $\mathbf{a}$ is a point on the z-axis, and the corresponding semi-disk D_{a} is represented by $r^2 + (z - a_z)^2 < \rho^2$, where $r \geq 0$. Consider the mapping

$$\hat{r} = \frac{r}{\rho} \text{ and } \hat{z} = \frac{z - a_z}{\rho},$$

or

$$r = \hat{r}\rho \text{ and } z = \rho\hat{z} + a_z.$$

Then, it is straightforward to show that this map sends D_{a} in the rz-plane to the semi-disk represented by $\hat{r}^2 + \hat{z}^2 < 1$, where $\hat{r} \geq 0$ in the $\hat{r}\hat{z}$-plane. We call this semi-unit-disk $\hat{D}_1$. Note that the Jacobian arising from change of variables from (r, z) to $(\hat{r}, \hat{z})$ is ρ^2.

Let us define $\hat{\eta}_1 \in \hat{P}_k$ by

$$\int_{\hat{D}_1} \hat{r}\hat{\eta}_1\hat{p}\,d\hat{r}\,d\hat{z} = \hat{p}(\mathbf{0}) \text{ for all } \hat{p} \in \hat{P}_k, \tag{B–1}$$

where $\hat{P}_k$ denotes the space of polynomials of order up to k on $\hat{D}_1$, and define

$$\eta_{\mathrm{a}}(r, z) = \frac{1}{\rho^3}\hat{\eta}_1(\hat{r}, \hat{z}). \tag{B–2}$$

Then, by change of variables,

$$\begin{aligned}
\int_{D_{\mathrm{a}}} r\eta_{\mathrm{a}}(r, z)p(r, z)\,dr\,dz &= \int_{\hat{D}_1} (\hat{r}\rho)\frac{1}{\rho^3}\hat{\eta}_1(\hat{r}, \hat{z})\hat{p}(\hat{r}, \hat{z})\rho^2\,d\hat{r}\,d\hat{z} && \text{by definition (B–2)},\\
&= \int_{\hat{D}_1} \hat{r}\hat{\eta}_1\hat{p}\,d\hat{r}\,d\hat{z},\\
&= \hat{p}(\mathbf{0}) && \text{by definition (B–1)},\\
&= p(\mathbf{a}),
\end{aligned}$$

for all $p \in P_k$, which proves Item 1.

Item 2 follows directly from Item 1:

$$
\begin{aligned}
\|\eta_{\mathrm{a}}\|^2_{r,D_{\mathrm{a}}} &= \int_{D_{\mathrm{a}}} |\eta_{\mathrm{a}}(r,z)|^2 r dr dz, \\
&= \eta_{\mathrm{a}}(\mathbf{a}) && \text{by Item 1 and since } \eta_{\mathrm{a}} \in P_k, \\
&= \hat{\eta}_1(\mathbf{0})\frac{1}{\rho^3} && \text{by definition (B–2)}, \\
&\leq \frac{C}{\rho^3}.
\end{aligned}
$$

The last inequality follows, since $\hat{\eta}_1(\mathbf{0})$ only depends on the reference domain $\hat{D}_1$. This completes the proof in case 1.

Next, we consider case 2 in which $\mathbf{a}$ is a point in $\mathbb{R}^2_+$ that is not on the z-axis, and the corresponding domain D_{a} is the disk represented by $(r-a_r)^2 + (z-a_z)^2 < \rho^2$. Now, consider the mapping

$$\hat{r} = \frac{r-a_r}{\rho} \text{ and } \hat{z} = \frac{z-a_z}{\rho},$$

or

$$r = a_r + \rho\hat{r} \text{ and } z = a_z + \rho\hat{z}.$$

This map transfers D_{a} in the rz-plane to the disk represented by $\hat{r}^2 + \hat{z}^2 < 1$ in the $\hat{r}\hat{z}$-plane. We call this unit disk $\hat{D}_2$. Under this mapping, the Jacobian arising from change of variables from (r,z) to $(\hat{r},\hat{z})$ is ρ^2.

Define $\hat{\eta}_2(\hat{r},\hat{z}) \in \hat{P}_k$ and $\hat{\eta}_{2,\alpha}(\hat{r},\hat{z}) \in \hat{P}_k$ by

$$\int_{\hat{D}_2} \hat{\eta}_2 \hat{p} d\hat{r} d\hat{z} = \hat{p}(\mathbf{0}) \qquad \text{for all } \hat{p} \in \hat{P}_k, \tag{B–3a}$$

$$\int_{\hat{D}_2} \alpha\hat{\eta}_{2,\alpha} \hat{p} d\hat{r} d\hat{z} = \hat{p}(\mathbf{0}) \qquad \text{for all } \hat{p} \in \hat{P}_k, \tag{B–3b}$$

for any positive and bounded function $\alpha(\hat{r},\hat{z})$ on $\hat{D}_2$, where $\hat{P}_k$ is now the space of polynomials of order up to k on $\hat{D}_2$. Define $\eta_{\mathrm{a}} \in P_k$ by

$$\eta_{\mathrm{a}}(r,z) = \frac{1}{\rho^2}\hat{\eta}_{2,\alpha}(\hat{r},\hat{z}) \tag{B–4}$$

with $\alpha = a_r + \rho\hat{r}$ in this case. Note that the function $r(r, z)$ is then mapped to $\alpha(\hat{r}, \hat{z})$.

Then,

$$\begin{aligned}
\int_{D_a} r\eta_a(r,z)p(r,z)drdz &= \int_{\hat{D}_2} (a_r + \rho\hat{r})\frac{1}{\rho^2}\hat{\eta}_{2,\alpha}(\hat{r},\hat{z})\hat{p}(\hat{r},\hat{z})\rho^2 d\hat{r}d\hat{z} && \text{by definition (B–4)},\\
&= \int_{\hat{D}_2} \alpha\hat{\eta}_{2,\alpha}\hat{p}d\hat{r}d\hat{z}, \\
&= \hat{p}(\mathbf{0}) && \text{by definition (B–3b)},\\
&= p(\mathbf{a}),
\end{aligned}$$

for all $p \in P_k$, which completes the proof of Item 1.

To prove Item 2, we first show that

$$\hat{\eta}_{2,\alpha}(\mathbf{0}) \leq \frac{C}{\min_{\hat{\mathbf{y}}\in\hat{D}_2}(\alpha(\hat{\mathbf{y}}))}. \tag{B–5}$$

This is true, since

$$\begin{aligned}
\|\hat{\eta}_{2,\alpha}\|^2_{L^2_\alpha(\hat{D}_2)} &= \hat{\eta}_{2,\alpha}(\mathbf{0}) && \text{by definition (B–3b)},\\
&= \int_{\hat{D}_2} \hat{\eta}_2\hat{\eta}_{2,\alpha}d\hat{r}d\hat{z} && \text{by definition (B–3a)},\\
&\leq \|\hat{\eta}_2\|_{L^2(\hat{D}_2)}\|\hat{\eta}_{2,\alpha}\|_{L^2(\hat{D}_2)}, \\
&\leq \|\hat{\eta}_2\|_{L^2(\hat{D}_2)}\frac{1}{\sqrt{\min_{\hat{\mathbf{y}}\in\hat{D}_2}(\alpha(\hat{\mathbf{y}}))}}\|\hat{\eta}_{2,\alpha}\|_{L^2_\alpha(\hat{D}_2)}.
\end{aligned}$$

Thus,

$$\|\hat{\eta}_{2,\alpha}\|_{L^2_\alpha(\hat{D}_2)} \leq \|\hat{\eta}_2\|_{L^2(\hat{D}_2)}\frac{1}{\sqrt{\min_{\hat{\mathbf{y}}\in\hat{D}_2}(\alpha(\hat{\mathbf{y}}))}},$$

and so

$$\hat{\eta}_{2,\alpha}(\mathbf{0}) = \|\hat{\eta}_{2,\alpha}\|^2_{L^2_\alpha(\hat{D}_2)} \leq \frac{C}{\min_{\hat{\mathbf{y}}\in\hat{D}_2}(\alpha(\hat{\mathbf{y}}))},$$

where $C = \|\hat{\eta}_2\|^2_{L^2(\hat{D}_2)}$ only depends on the fixed reference domain. Hence,

$$\begin{aligned}
\|\eta_{\mathsf{a}}\|^2_{L^2_r(D_{\mathsf{a}})} &= \eta_{\mathsf{a}}(\mathbf{a}) && \text{by Item 1 and since } \eta_{\mathsf{a}} \in P_k, \\
&= \frac{1}{\rho^2}\hat{\eta}_{2,\alpha}(\mathbf{0}) && \text{by definition (B–4)}, \\
&\leq \frac{C}{\rho^2 \min_{\hat{\mathsf{y}}\in\hat{D}_2}(\alpha(\hat{\mathbf{y}}))} && \text{by (B–5)}, \\
&= \frac{C}{\rho^2 \min_{\mathsf{y}\in D_{\mathsf{a}}}(r(\mathbf{y}))}.
\end{aligned}$$

The last equality holds, since $r(r, z)$ is mapped to $\alpha(\hat{r}, \hat{z})$. This completes the proof of Item 2 for case 2.

Lastly, we prove the proposition for case 3. In this case, as in case 2, $\mathbf{a}$ is a point in $\mathbb{R}^2_+$ that is not on the z-axis, but the corresponding domain D_{a} is the open disk with center $\tilde{\mathbf{a}}$ and radius ρ, where $\tilde{\mathbf{a}} = (\tilde{a}_r, \tilde{a}_z)$ is obtained by

$$\begin{pmatrix} \tilde{a}_r \\ \tilde{a}_z \end{pmatrix} = \begin{pmatrix} a_r \\ a_z \end{pmatrix} + \begin{pmatrix} \cos\theta & -\sin\theta \\ \sin\theta & \cos\theta \end{pmatrix} \begin{pmatrix} 2\rho \\ 0 \end{pmatrix},$$

for some fixed angle $\theta \geq 0$. Consider the mapping

$$\begin{pmatrix} \hat{r} \\ \hat{z} \end{pmatrix} = \frac{1}{\rho} \begin{pmatrix} \cos\theta & \sin\theta \\ -\sin\theta & \cos\theta \end{pmatrix} \begin{pmatrix} r - a_r \\ z - a_z \end{pmatrix},$$

or

$$\begin{pmatrix} r \\ z \end{pmatrix} = \begin{pmatrix} a_r \\ a_z \end{pmatrix} + \rho \begin{pmatrix} \cos\theta & -\sin\theta \\ \sin\theta & \cos\theta \end{pmatrix} \begin{pmatrix} \hat{r} \\ \hat{z} \end{pmatrix}.$$

Then, it is straight forward to show that, this map sends the disk D_{a} in the rz-plane to the disk $(\hat{r} - 2)^2 + \hat{z}^2 < 1$ in the $\hat{r}\hat{z}$-plane. We call this disk $\hat{D}_3$. Furthermore, the Jacobian arising from change of variables from (r, z) to $(\hat{r}, \hat{z})$ is ρ^2.

Let us define $\hat{\eta}_3 \in \hat{P}_k$ and $\hat{\eta}_{3,\alpha} \in \hat{P}_k$ by

$$\int_{\hat{D}_3} \hat{\eta}_3 \hat{p} d\hat{r} d\hat{z} = \hat{p}(2,0) \qquad \text{for all } \hat{p} \in \hat{P}_k, \tag{B–6a}$$

$$\int_{\hat{D}_3} \alpha \hat{\eta}_{3,\alpha} \hat{p} d\hat{r} d\hat{z} = \hat{p}(2,0) \qquad \text{for all } \hat{p} \in \hat{P}_k, \tag{B–6b}$$

for any positive and bounded function $\alpha(\hat{r}, \hat{z})$ on $\hat{D}_3$, where $\hat{P}_k$ is now the space of polynomials of order up to k on $\hat{D}_3$. We then define $\eta_{\mathrm{a}} \in P_k$ by

$$\eta_{\mathrm{a}}(r,z) = \frac{1}{\rho^2} \hat{\eta}_{3,\alpha}(\hat{r}, \hat{z}). \tag{B–7}$$

Then, by defining $\alpha(\hat{r}, \hat{z}) = a_r + \rho((\cos\theta)\hat{r} - (\sin\theta)\hat{z}))$, we have that

$$\begin{aligned}
\int_{D_{\mathrm{a}}} r\eta_{\mathrm{a}}(r,z)p(r,z)drdz &= \int_{\hat{D}_3} \alpha(\hat{r},\hat{z}) \frac{1}{\rho^2} \hat{\eta}_{3,\alpha}(\hat{r},\hat{z}) \hat{p}(\hat{r},\hat{z}) \rho^2 d\hat{r} d\hat{z} && \text{by definition (B–7)}, \\
&= \hat{p}(2,0) && \text{by definition (B–6b)}, \\
&= p(\mathbf{a}).
\end{aligned}$$

This completes the proof of Item 1.

Next, by the same way as in case 2, it follows that

$$\hat{\eta}_{3,\alpha}(2,0) \leq \frac{C}{\min_{\hat{\mathrm{y}} \in \hat{D}_3} \alpha(\hat{\mathbf{y}})}, \tag{B–8}$$

and so,

$$\|\eta_{\mathrm{a}}\|^2_{L^2_r(D_{\mathrm{a}})} = \eta_{\mathrm{a}}(\mathbf{a}) = \frac{1}{\rho^2} \hat{\eta}_{3,\alpha}(2,0) \leq \frac{C}{\rho^2 \min_{\hat{\mathrm{y}} \in \hat{D}_3} \alpha(\hat{\mathbf{y}})} = \frac{C}{\rho^2 \min_{\mathrm{y} \in D_{\mathrm{a}}} r(\mathbf{y})},$$

which completes the proof of Item 2. The proposition holds for all three cases 1, 2, and 3, and thus we are done.

REFERENCES

[1] D. N. Arnold, R. S. Falk, and R. Winther, *Multigrid in* $\mathbf{H}(\mathrm{div})$ *and* $\mathbf{H}(\mathbf{curl})$, Numer. Math. **85** (2000), 197–217. MR 1754719 (2001d:65161)

[2] F. Assous, P. Ciarlet, Jr., and S. Labrunie, *Theoretical tools to solve the axisymmetric Maxwell equations*, Math. Methods Appl. Sci. **25** (2002), 49–78. MR 1874449 (2002j:78008)

[3] Z. Belhachmi, C. Bernardi, and S. Deparis, *Weighted Clément operator and application to the finite element discretization of the axisymmetric Stokes problem*, Numer. Math. **105** (2006), 217–247. MR 2262757 (2008c:65310)

[4] Jöran Bergh and Jörgen Löfström, *Interpolation spaces. An introduction*, Springer-Verlag, Berlin, 1976, Grundlehren der Mathematischen Wissenschaften, No. 223. MR 0482275 (58 #2349)

[5] A. Bermúdez, C. Reales, R. Rodríguez, and P. Salgado, *Numerical analysis of a finite element methods for the axisymmetric eddy current model of an induction furnace*, IMA J Numer Anal (Submitted).

[6] C. Bernardi, M. Dauge, and Y. Maday, *Spectral methods for axisymmetric domains*, Series in Applied Mathematics (Paris), vol. 3, Gauthier-Villars, Éditions Scientifiques et Médicales Elsevier, Paris, 1999, Numerical algorithms and tests due to Mejdi Azaïez. MR 1693480 (2000h:65002)

[7] J. M. Bertram, D. Yang, M. C. Converse, J. G. Webster, and D. M. Mahvi, *Antenna design for microwave hepatic ablation using an axisymmetric electromagnetic model*, Biomedical Engineering Online (2006).

[8] D. Boffi, P. Fernandes, L. Gastaldi, and I. Perugia, *Computational models of electromagnetic resonators: analysis of edge element approximation*, SIAM J. Numer. Anal. **36** (1999), 1264–1290 (electronic). MR 1701792 (2000g:65112)

[9] S. Börm and R. Hiptmair, *Multigrid computation of axisymmetric electromagnetic fields*, Adv. Comput. Math. **16** (2002), 331–356. MR 1894928 (2003d:78042)

[10] D. Braess and W. Hackbusch, *A new convergence proof for the multigrid method including the* V*-cycle*, SIAM J. Numer. Anal. **20** (1983), 967–975. MR 714691 (85h:65233)

[11] J. H. Bramble, *Multigrid methods*, Pitman Research Notes in Mathematics Series, vol. 294, Longman Scientific & Technical, Harlow, 1993. MR 1247694 (95b:65002)

[12] J. H. Bramble, D. Y. Kwak, and J. E. Pasciak, *Uniform convergence of multigrid* V*-cycle iterations for indefinite and nonsymmetric problems*, SIAM J. Numer. Anal. **31** (1994), 1746–1763. MR 1302683 (95i:65170)

[13] J. H. Bramble and J. Xu, *Some estimates for a weighted L^2 projection*, Math. Comp. **56** (1991), 463–476. MR 1066830 (91k:65140)

[14] J. H. Bramble and X. Zhang, *The analysis of multigrid methods*, Handbook of numerical analysis, Vol. VII, North-Holland, Amsterdam, 2000, pp. 173–415. MR 1804746 (2001m:65183)

[15] _____, *Uniform convergence of the multigrid V-cycle for an anisotropic problem*, Math. Comp. **70** (2001), 453–470. MR 1709148 (2001g:65134)

[16] F. Brezzi and M. Fortin, *Mixed and hybrid finite element methods*, Springer Series in Computational Mathematics, vol. 15, Springer-Verlag, New York, 1991. MR 1115205 (92d:65187)

[17] Snorre H. Christiansen and Ragnar Winther, *Smoothed projections in finite element exterior calculus*, Math. Comp. **77** (2008), 813–829. MR 2373181 (2009a:65310)

[18] P. G. Ciarlet, *The Finite Element Method for Elliptic Problems*, North-Holland Publishing Company, Amsterdam, 1978.

[19] B. Cockburn and J. Gopalakrishnan, *Error analysis of variable degree mixed methods for elliptic problems via hybridization*, Math. Comp. **74** (2005), 1653–1677 (electronic). MR 2164091 (2006e:65215)

[20] D. M. Copeland, J. Gopalakrishnan, and M. Oh, *Multigrid in a weighted space arising from axisymmetric electromagnetics*, Math. Comp. (To appear).

[21] D. M. Copeland, J. Gopalakrishnan, and J. E. Pasciak, *A mixed method for axisymmetric div-curl systems*, Math. Comp. **77** (2008), 1941–1965. MR 2429870 (2009e:65171)

[22] Martin Costabel, *A remark on the regularity of solutions of Maxwell's equations on Lipschitz domains*, Math. Methods Appl. Sci. **12** (1990), 365–368. MR 1048563 (91c:35028)

[23] R. S. Falk and J. E. Osborn, *Error estimates for mixed methods*, RAIRO Anal. Numér. **14** (1980), 249–277. MR 592753 (82j:65076)

[24] V. Girault and P.-A. Raviart, *Finite element methods for Navier-Stokes equations*, Springer Series in Computational Mathematics, vol. 5, Springer-Verlag, Berlin, 1986. MR 851383 (88b:65129)

[25] J. Gopalakrishnan and J. E. Pasciak, *The convergence of V-cycle multigrid algorithms for axisymmetric Laplace and Maxwell equations*, Math. Comp. **75** (2006), 1697–1719 (electronic). MR 2240631 (2007g:65116)

[26] J. Gopalakrishnan, J. E. Pasciak, and L. F. Demkowicz, *Analysis of a multigrid algorithm for time harmonic Maxwell equations*, SIAM J. Numer. Anal. **42** (2004), 90–108 (electronic). MR 2051058 (2005c:65115)

[27] R. Hiptmair, *Multigrid method for Maxwell's equations*, SIAM J. Numer. Anal. **36** (1999), 204–225 (electronic). MR 1654571 (99j:65229)

[28] A. Kufner, O. John, and S. Fučík, *Function Spaces*, Monographs and textbooks on mechanics of solids and fluids, Noordhoff International Publishing, Leyden, The Netherlands, 1977.

[29] R. Leis, *Exterior boundary-value problems in mathematical physics*, Trends in applications of pure mathematics to mechanics, Vol. II (Second Sympos., Kozubnik, 1977), Monographs Stud. Math., vol. 5, Pitman, Boston, Mass., 1979, pp. 187–203. MR 566529 (81d:78016)

[30] P. Monk, *A finite element method for approximating the time-harmonic Maxwell equations*, Numer. Math. **63** (1992), 243–261. MR 1182977 (94b:65134)

[31] _____, *Finite element methods for Maxwell's equations*, Numerical Mathematics and Scientific Computation, Oxford University Press, New York, 2003. MR 2059447 (2005d:65003)

[32] J.-C. Nédélec, *Mixed finite elements in* $\mathbf{R}^3$, Numer. Math. **35** (1980), 315–341. MR 592160 (81k:65125)

[33] J. Nitsche, *Ein Kriterium für die Quasi-Optimalität des Ritzschen Verfahrens*, Numer. Math. **11** (1968), 346–348. MR 0233502 (38 #1823)

[34] P.-A. Raviart and J. M. Thomas, *Primal hybrid finite element methods for* 2*nd order elliptic equations*, Math. Comp. **31** (1977), 391–413. MR 0431752 (55 #4747)

[35] Joachim Schöberl, *A posteriori error estimates for Maxwell equations*, Math. Comp. **77** (2008), 633–649. MR 2373173 (2008m:78017)

[36] J. Wloka, *Partial differential equations*, Cambridge University Press, Cambridge, 1987, Translated from the German by C. B. Thomas and M. J. Thomas. MR 895589 (88d:35004)

BIOGRAPHICAL SKETCH

Minah Oh was born in Seoul, Korea in 1981. She grew up in both Seoul and Seattle, WA, and got her B.S. degree in Aug. 2005 from Yonsei Univeristy, Seoul, Korea, where she also got a middle/high school teacher's license in mathematics. During her undergraduate studies, she spent a year in St. Olaf College, Northfield, MN as an exchange student, and that is when she decided to pursue mathematics. She went to University of Florida for graduate studies in Aug. 2005 and got her M.S. degree in mathematics in May 2007. She continued to study numerical analysis at the University of Florida, finite element methods and multigrid in particular, and got her Ph.D. in mathematics in May 2010.